THE UNIVERSITY OF CALGARY

QUANTIFICATION OF RISK IN FORECASTED RESERVOIR PERFORMANCE

by

Christos Tomos

A THESIS

SUBMITTED TO THE FACULTY OF GRADUATE STUDIES

IN PARTIAL FULFILMENT OF THE REQUIREMENTS FOR THE

DEGREE OF

MASTER OF SCIENCE

DEPARTMENT OF CHEMICAL AND PETROLEUM ENGINEERING

CALGARY, ALBERTA

APRIL, 1995

THE UNIVERSITY OF CALGARY

FACULTY OF GRADUATE STUDIES

The undersigned certify that they have read, and recommend to the Faculty of Graduate Studies for Acceptance, a thesis entitled, " Quantification Of Risk In Forecasted Reservoir Performance ", submitted by Christos Tomos in partial fulfilment of the requirements for the degree of Master of Science.

Dr. N.E. Kalogerakis (Supervisor)
Department of Chemical & Petroleum Engineering

Dr. J.D.M Belgrave
Department of Chemical & Petroleum Engineering

Dr. R.G. Moore
Department of Chemical & Petroleum Engineering

Dr. R.C.K. Wong
Department of Civil Engineering

Date: APR 17 1995

ABSTRACT

This study addresses the problem of the quantification of the risk involved in predicting future production of hydrocarbon reservoirs, using numerical simulation techniques. Automatic History Matching (based on nonlinear regression), has been employed in order to arrive at the best reservoir parameters estimates for a given reservoir structure.

By using typical techniques from statistical analysis (and statistical properties of multi-variable nonlinear regression estimates), the error bounds (95% confidence intervals) of the predicted production rates of a given reservoir are readily determined. These confidence intervals incorporate the uncertainty of all reservoir parameters, used in the automatic history matching and hence, a realistic measure of the uncertainty in the model predictions of the future reservoir performance is obtained.

The proposed extrapolation method was incorporated into a Black Oil Simulator. The resulting simulator has been tested in numerous reservoir models. A comprehensive set of simulator runs are reported in this thesis, namely a typical five spot pattern, where the effect of the space discretization error and the degree of implicitness is investigated, the reliability of horizontal well performance on a field scale and the effect of impermeable barriers like shales and faults is examined.

ACKNOWLEDGEMENTS

This research has been made possible, by the assistance, advice and support of the professors and students of the department of Chemical and Petroleum Engineering of the University of Calgary. Special thanks to Richard Baker for many stimulating discussions.

I wish to express my gratitude to my supervisor Dr. Nicolas Kalogerakis for providing continuous guidance, help and encouragement whenever needed and the financial means during the course of this work.

I would also like to thank the National Science and Engineering Research Council (NSERC) of Canada, for the financial support for this project. Special thanks to Dr. Tony Settari and Ms. Alda Behie of SIMTECH Consulting Services Ltd. (Calgary, AB, Canada) for their help in implementing the automatic history matching on DRS (Dynamic Reservoir Simulator).

Dedicated to my parents

TABLE OF CONTENTS

APPROVAL PAGE ii

ABSTRACT iii

ACKNOWLEDGEMENTS iv

TABLE OF CONTENTS vi

LIST OF TABLES ix

LIST OF FIGURES x

LIST OF SYMBOLS xiv

1.0 INTRODUCTION 1

1.1 Reservoir Simulation 1

1.2 Incentives for Reservoir Simulation 3

1.3 Steps in a Typical Simulation Study 4

1.4 History Matching 5

1.4.1 Current Approach 5

1.4.2 Motivation for Automatic History Matching 6

1.5 Problem Statement 6

1.6 Outline of Thesis 8

2.0 MATHEMATICAL FORMULATION OF RESERVOIR SIMULATION MODELS 10

2.1 Introduction 10

2.2 Governing Equations 10

2.2.1 Equation of Continuity 10

2.2.2 Additional Equations 13

2.3 Black Oil Models 14
2.4 Discretization of Flow Equations 15
2.5 Well Models 16
2.6 Solution Methods 18
2.6.1 IMPES Solution 18
2.6.2 Semi-Implicit Method 19
2.6.3 Fully Implicit Method 19
2.6.4 Adaptive Implicit Method 19
2.7 Comparison Between the Solution Method 20

3.0 LITERATURE REVIEW 21
3.1 Methods Used for Automatic History Matching 21
3.1.1 Nonlinear Regression Analysis 21
3.1.2 Optimal Control Methods 24
3.1.3 Regularization Procedures 25
3.1.4 Simulated Annealing Method 26
3.1.5 Other Methods 27
3.2 Identifiability of Parameters 30
3.3 Incorporation of Prior Information and Constraints 31

4.0 PARAMETER ESTIMATION TECHNIQUES 32
4.1 Model Forms for Parameter Estimation 33
4.1.1 Least Squares Estimation 33
4.2 Gauss-Newton Method 34
4.3 Incorporating Prior Information and Penalty Function 37
4.4 Parameter Covariance Matrix 38

5.0 PREDICTION OF FUTURE PERFORMANCE WITHIN CERTAIN CONFIDENCE INTERVALS 41
5.1 Inferences on Well Production Rates 41
5.2 Overall Reservoir Production 43
5.3 Implementation Considerations 44

5.4 Multiple Reservoir Descriptions 44
5.5 Convergence Testing of the Proposed Algorithm in Chemical Kinetic Models. 46
5.5.1 Example 1 46
5.5.2 Example 2 51
5.5.3 Summary 55

6.0 APPLICATION TO A 5-SPOT SYSTEM 57
6.1 Introduction 57
6.2 Overview of the Actual Model 57
6.3 Overview of the Postulated Models A & B. 61
6.4 Varying the Degree of Implicitness 70
6.5 Varying the Grid Block Dimensions 70

7.0 APPLICATION TO HETEROGENEOUS RESERVOIRS 77
7.1 Reliability of horizontal well performance 75
7.1.1 Overview of the Actual Model 77
7.1.2 Postulated Models A, B and C 82
7.2 Case Study - Horizontal Shale Barriers 96
7.2.1 Overview of the Actual Model 96
7.2.2 Postulated Models A & B 100
7.3 Application to a reservoir with a sealing fault. 110
7.3.1 Overview of the Actual Model 110
7.3.2 Postulated Models A, B and C 113

CONCLUSIONS 130

REFERENCE 132

APPENDIX A' 140
A.1 Detailed Description of the Dual Porosity Model Used. 140

LIST OF TABLES

Table 5.1: Region of Convergence of the Gauss-Newton Method - Example #2 55

Table 6.1: PVT Data of the Actual Model. 59

Table 6.2: Converged Values of the Parameters for the Postulated Models. 64

Table 7.1: Porosity and Permeability Distribution of the Actual Model from Top to Bottom. 80

Table 7.2: Estimated Porosities and Permeabilities for Model A 83

Table 7.3: Estimated Porosities and Permeabilities for Model B 91

Table 7.4: Estimated Porosities and Permeabilities for the Fractured System and Matrix System 94

Table 7.5: Geometrical Attributes of the Fracture System for the Actual Model. 95

Table 7.6: Comparison of Recovery Estimates Between the Actual and the Three Postulated Models 95

Table 7.7: Porosity and Permeability Distribution of the Actual Model - Horizontal shale barriers (from Top to Bottom). 100

Table 7.8: Converged Values of the Parameters of the Postulated Model A. 103

Table 7.9: Converged Values of the Parameters of the Postulated Model B. 103

Table 7.10: Estimated Porosities and Permeabilities for Postulated Model A. 115

Table 7.11: Estimated Porosities and Permeabilities for Postulated Model B. 118

Table 7.12: Estimated Porosities and Permeabilities for Postulated Model C. 118

LIST OF FIGURES

Figure 1.1	Major Components of a Reservoir Simulator Adopted from SPE Reprint Series 1986.	2
Figure 2.1	Differential Elements of Volume. (A)One-dimensional Flow. (B) Two-dimensional flow. (C) Three-dimensional flow. (Peaceman D. W. 1977)	11
Figure 3.1	Schematic diagram of the Simulating Annealing method. (After Ownes, 1992 A)	28
Figure 4.1	Schematic diagram of the Gauss-Newton Method	39
Figure 5.1	Chemical Kinetic Models - Example 1. 95% Confidence Intervals of the Model Variables	48
Figure 5.2	Approximate Region of Convergence of the Parameters, by Annealing method.	49
Figure 5.3	Surface Plot of the Objection Function, by Annealing Method.	50
Figure 5.4	Simulated Measurements of the Model Variables Example 2	53
Figure 5.5	95% Confidence Intervals of the Model Variables for Example 2	54
Figure 6.1	Grid Block Representation and the Zonation Used for the Actual Model.	58
Figure 6.2	Relative Permeability Curves of the Actual model	60
Figure 6.3	Grid Block Representation and the Zonation used in the Postulated Model A.	62
Figure 6.4	Grid Block Representation and Zonation used in the Postulated Model B.	63
Figure 6.5	Quality of the Obtained Match for the Model A.	65
Figure 6.6	95% Confidence Intervals for the Cumulative Oil and Gas Production of Model A.	66
Figure 6.7	95% Confidence Intervals of the Cumulative Production Rate of Water of the Model A.	67

Figure 6.8 95% Confidence Intervals for the Cumulative Oil and Gas Production of the Model B. 68
Figure 6.9 95% Confidence Intervals of the Cumulative Production Rate of Water of the Model B. 69
Figure 6.10 Quality of the Obtained Match of the Oil Production Rate Run Model B, Fully Implicit, Adaptive Implicit and IMPES. 71
Figure 6.11 Maximum Confidence Intervals for the Cumulative Oil Production of Model B, running Adaptive Implicit, Fully Implicit and IMPES. 72
Figure 6.12 Minimum Confidence Intervals of the Cumulative Oil Production of Model B, running Adaptive Implicit, Fully Implicit and IMPES. 73
Figure 6.13 Comparison of the Production Rates for Different Grid Block Representations of Model A. 74
Figure 6.14 95% Confidence Intervals of the Cumulative Oil Production for Different Grid Block Representations of Model A 76
Figure 7.1 Grid Block Representation of the Actual Reservoir: (a)Producer Layer (b) Cross Section 78
Figure 7.2 Permeability and Porosity Distribution of the Actual Reservoir: (a) Layer 4 and (b) Layer 7 79
Figure 7.3 Relative Permeability Curves of the Actual Model 81
Figure 7.5 95% Confidence Intervals of Cumulative Oil and Gas Production Based on Model A 84
Figure 7.6 95% Confidence Intervals of Cumulative Water Production Based on Model A 85
Figure 7.7 95% Confidence Intervals of Cumulative Oil and Gas Production Based on Model B. 86
Figure 7.8 95% Confidence Intervals of Cumulative Water Production Based on Model B. 87
Figure 7.9 95% Confidence Intervals of Cumulative Oil and Gas Production Based on Model C 88

Figure 7.10 95% Confidence Intervals of the Cumulative Water Production Based on Model C 89
Figure 7.11 Comparison of 95% Confidence Intervals for Cumulative Oil Production Based on Model B with Good and Poor Prior Estimates. 90
Figure 7.12 Comparison Between Gas (□) and Water (O) Production Rates of the Actual Reservoir and Postulated Models B, C. 92
Figure 7.13 Comparison Between Oil (⊙) Production Rates of the Actual Reservoir and Postulated Models B, C. 93
Figure 7.14 Grid Block Representation of the Actual Model: (a) First Layer and (b) Cross Section 97
Figure 7.15 Schematic Representation of the Porosity and the Permeability Distribution of the Second and Forth Layer of the Actual Model. 98
Figure 7.16 Relative Permeability Curves of the Actual Model. 99
Figure 7.17 Frequency of the Shale Barriers for the First Two Layers of the Actual Reservoir - Plan View 101
Figure 7.18 Grid Block Representation of the Postulated Models A (a) & B (b), Along with the Assumed Porosity and Permeability Zonation. 102
Figure 7.19 Quality of the Obtained Match of the Postulated Model A. 104
Figure 7.20 Quality of the Obtained Match of the Postulated Model B. 105
Figure 7.21 95% Confidence Intervals of the Cumulative Oil and Gas Production for the Postulated Model A. 106
Figure 7.22 95% Confidence Intervals of the Cumulative Water Production of the Postulated Model A. 107
Figure 7.23 95% Confidence Intervals of the Cumulative Oil and Gas Production for the Postulated Model B. 108
Figure 7.24 95% Confidence Intervals of the Cumulative Water Production of the Postulated Model B. 109
Figure 7.25 Grid block representation of the Actual model. 111
Figure 7.26 Porosity and Permeability Distribution of the Actual Model. . . . 112

Figure 7.27 Production Performance of Prod #1 & #2 - Actual Model. 114
Figure 7.28 Comparison of the Postulated Model A with the Actual Reservoir, where the First is Superimposed on the Second. 116
Figure 7.29 Comparison of the Postulated Model B with the Actual Model, Where the First is Superimposed on the Second. The Arrows Indicate the Path of the Injected Water. 117
Figure 7.30 Comparison of the Postulated Model C Superimposed on the Actual Model. The Arrows Indicated the Flow Path of the Injected Water. 119
Figure 7.31 Quality of the Obtained Match for the Model A - (a) Producer #1, (b) Producer #2 121
Figure 7.32 Quality of the Obtained Match for the Model B - (a) Producer #1, (b) Producer #2 122
Figure 7.33 Quality of the Obtained match for the Model C - (a) Producer #1, (b) Producer #2 123
Figure 7.34 95% Confidence Intervals of the Cumulative Field Oil Production of Models A, B and C. 124
Figure 7.35 95% Confidence Intervals of the Cumulative Field Gas Production of Models A, B and C. 125
Figure 7.36 95% Confidence Intervals of the Cumulative Field Water Production of Models A, B and C. 126
Figure 7.37 Predictions of the Oil Production Rates of the Postulated Models 127
Figure 7.38 Predictions of the Gas Production Rates of the Postulated Models 128
Figure 7.39 Predictions of the Water ProductionRates of the Postulated Models 129
Figure A.1 Schematic Representation of the Matrix and the Fracture Continuum. 142

LIST OF SYMBOLS

B = Formation Volume Factors (bbl/stb or ft^3/scf)

Cov(**k**) = Covariance matrix of the parameters

$E(\bullet)$ = Expectation operator

f = Fractional Flow Function

G(t) = Sensitivity Coefficient Matrix at time t

GOR = Gas oil ratio (scf/stb)

H = Hydrostatic pressure (psi)

k = Absolute permeability (mD)

k = Parameter vector

m = Number of observations at each time

M = mobility (mD/cp)

n_0 = Number of observation times

P = Pressure (psia)

Pb(•) = Prior Probability

Pc = Capillary pressure (psia)

P_{wb} = Flowing bottom hole pressure (psia)

Q_i = Injection/Production of the component i

Q_p = Flow rate of phase p

R_s = Cumulative produced gas oil ratio (scf/stb)

r_w = Wellbore radius

S(k) = Objective function

S_p = Saturation of phase p

t = Time

u = Vector of user specified variables (e.g., injection rates)

W = Weighting matrix

W_{pi} = Well productivity index

x = State variable vector

x_{Ip} = Mole fraction of the component I in the phase p

y = Calculated variable vector

$\hat{\mathbf{y}}$ = Measured variable vector

Greek Characters

α = Normalized distance of the initial guess from the optimum

Δ = Difference operator

λ = Step length

$_P$ = Viscosity of the phase p (cp)

ρ_P = Density of the phase (lb/ft^3)

σ_ε = Standard deviation of the measurement errors

Φ = Porosity (%)

ν =total number of measurements minus the number of the parameters (degrees of freedom)

T = Transmissibility

Subscripts

c = Hydrocarbon phase (oil, gas, water)

g = Gas

i = Observation time index

LS = Least squares

max = Maximum value

min = Minimum value

o = Oil

p = Phase (oil, gas, water)

rp = Relative permeability of the phase p

tot = Total

w = water

Superscripts

* = Value of the variable at the optimum

j = Iteration level for Gauss-Newton Method

n = Last time step taken

n+1 = Next time step to be taken

T = Transpose

CHAPTER 1

INTRODUCTION

1.1 Reservoir Simulation

Reservoir Simulation is a highly specialized blend of engineering , physics, mathematics, numerical analysis, chemistry, and systems programming. Reservoir simulation is the implementation of the above sciences, where a computer model transforms the measured data into a computed reservoir performance. The basic components of a reservoir simulation are presented in Fig 1.1 adopted by SPE Reprint Series 1986, where the dashed line separates the data (above the line) from the model (below the line).

The mathematical model consists of a set of partial differential equations with initial and boundary conditions. These equations describe the fluid flow inside porous media, the mass transfer between the phases, the gravity, capillary and viscous forces, that are present in a reservoir. The boundary conditions result from the assumption that the reservoir is an isolated region and there is no flow at the external boundary. Typical initial conditions originate from the assumption that initially the reservoir is at the state of equilibrium, with each phase having a zero velocity.

In general these equations can not be solved analytically. They can only be solved numerically, by replacing, for example, the differential equations with finite difference equations. This can be done by assuming that the reservoir is composed by a number of discrete volume element (grid blocks) and the computations are made to determine any changes of the state variables in each volume elements, over many

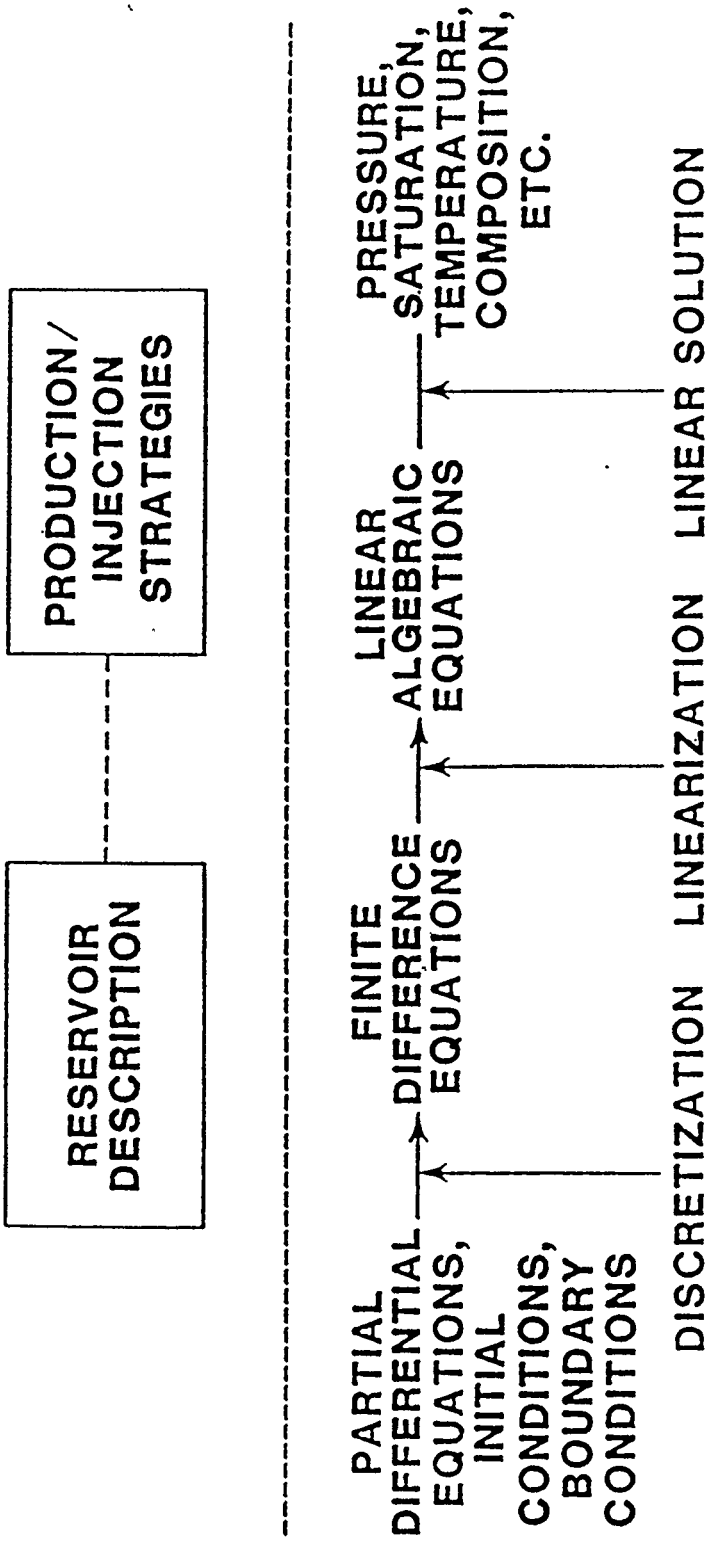

Figure 1.1 Major Components of a Reservoir Simulator Adopted from SPE Reprint Series 1986.

discrete time intervals (timesteps). The above assumption, *discretization*, is an approximation of the real reservoir, and it is subject not only to truncation errors, that are proportional to the order of the grid spacing and timesteping (*numerical dispersion*), but to loss of information, since we are able to assign only one value of porosity or permeability to each of the volume element. The result of discretization is a set of nonlinear algebraic equations. These equations are still intractable. Linearization is always required to produce a set of linear algebraic equations which can be solved by a variety of direct and iterative methods for the primary variables, such as pressures, fluid saturations, temperature and composition.

1.2 Incentives for Reservoir Simulation

According to Mattax and Dalton (1990) the main motivation for reservoir simulation is *the increase of oil and gas recovery, through better reservoir management*. The knowledge obtained by reservoir simulation can be used for optimizing the production strategy of the reservoir.

The major benefits of a reservoir simulation study are:

- Improving our understanding of the reservoir. Obtaining vital information about the major flow mechanisms, the degree of heterogeneity, the external boundaries of the reservoir, the existence and strength of an aquifer, is crucial to the reservoir management.
- The engineer has the ability of comparing the reservoir performance under alternative depletion strategies, without any expensive pilot tests.
- The reservoir simulator can be used for prediction of the future reservoir performance. This is very important especially for Enhanced Oil Recovery (EOR) procedures.
- Modelling of critical well rates can help us to avoid water conning or gas cusping.

- Reservoir simulation can be a very powerful tool for decision-making, performance monitoring, and timing of the reservoir management.

It is obvious that the quality of a reservoir simulation study, will always depend on the availability and quality of past production data. The more accurate the data the more confidence can be placed on the resulting match. The need of good reservoir data becomes even more pronounced in EOR procedures (Elasyed *et al* Oct. 1993, Baker 1993).

1.3 Steps in a Typical Simulation Study

A complete reservoir simulation study may take considerable time to conclude. All studies, of this nature, follow simple steps in order to incorporate all the necessary information of the given reservoir. These steps are summarized below:

- **Definition of the problem.** In this stage the objectives and the scope of the study should be determined.
- **Data Review.** Screening and organization of the gathered data is necessary, since they have often been collected for a number of loosely related reasons. Usually these data have been obtained by seismic tests, pressure transient analysis, well log analysis, core displacement and PVT tests, production history e.t.c.
- **Construction of the model.** The data that have been congregated so far, have to take the form of an input file for the specific simulator. Time or cost constraints frequently impose compromises on the type of simulator to use and on the design of the model. The level of sophistication of the model should be the result of an optimized trade off.
- **History Matching.** This is the most time consuming step. The objective is to replicate the reservoir performance, with the simulation model as closely as possible. Simulation of pressure transient tests can be beneficial especially when there are insufficient data about the reservoir.

- **Prediction the future performance and analysis.** Once an acceptable history match has been achieved one uses the simulator to predict the future production of oil, gas and water, the total recovery, the position of the displacing fronts, the breakthrough times and the pressure profiles of the reservoir.
- **Conclusions and report.**

1.4 History Matching

History matching can be a time-consuming, expensive and frustrating procedure, since the reservoir performance results from numerous interactions, which usually are difficult to comprehend. The difficulty increases as the degree of heterogeneity of the reservoir increases.

The purpose of history matching is to improve the accuracy or confidence of the predicted reservoir performance. To do so effectively, one needs to know which parameters to adjust, how to adjust them and the influence of the parameter on the predicted performance. Nevertheless having obtained a set of reservoir parameters that match the past reservoir performance does not in itself mean that those parameters will provide an accurate prediction of reservoir performance. Thus the confidence in the prediction of the future reservoir performance, following a history match, will depend on the confidence that one has in the values of the reservoir parameters.

1.4.1 Current Approach

In general, the data that are history matched are bottom hole and well head pressures, WOR, GOR, gas and water arrival times, fluid contact movement and fluid saturations measured in cores.

Currently the engineer should use his own experience and judgement to obtain a history match. It is therefore a trial and error procedure to ascertain the optimum value of the reservoir parameters.

1.4.2 Motivation for Automatic History Matching

Currently, as it has been stated above, extensive experience and erudition of the important parameters is required from the engineer, for a successful simulation study. At the same time, the computer advances have led to the reduction of the computer costs, while the manpower costs are becoming increasingly high. The objective, therefore, is to make history matching more facile to the engineer, by letting the computer do all the trial and error runs. This will allow the engineer to spend more time on the interpretation of the results, rather trying to obtain an acceptable match. Attempts to accomplish an automated version of history matching, have produced numerous algorithms, many of which will be discussed briefly in a later chapter.

It should be noted, though, that having a systematic parameter estimation scheme does not mean that history matching should be automatic with nothing left to the discretion of the engineer. The engineer should establish which parameters are to be adjusted to match a given variable and determine the constraints on the value of the parameters (Parish *et al.*, 1993).

1.5 Problem Statement

Generally, all the algorithms adjust the reservoir parameters according to predetermined guidelines. The quality of the obtained match is quantified in terms of an objective function, a relationship that reflects the difference between the observed and calculated values of the matching variables. The goal is to find the reservoir model that minimizes the value of the objective function. This process is generally referred to as "*automatic history matching*" , or "*inverse simulation*".

Using least squares (LS) estimation, the objective function is defined as:

$$S_{LS}(k) = \sum_{i=1}^{n_o} [\hat{y}(t_i) - y(t_i,k)]^T \; W_i \; [\hat{y}(t_i) - y(t_i,k)] \qquad (1.1)$$

where $\hat{y}(t_i)$ represents a vector of m measurements at observation time t_i, n_o is the number of observation times, $y(t_i,k)$ represents the vector of corresponding model predictions and W_i is an mxm, user supplied, positive definite, symmetric weighting matrix.

Tan and Kalogerakis (1991), have pointed out that the role of the weighting matrix is essentially to normalize the data, so that all the measurements are of the same order of magnitude. On statistical grounds, this is the correct choice if the error in the measurements is proportional to the magnitude of the variable, that is, if we have a constant percentage error.

Any spatially discretized reservoir model, can be represented by a set of ordinary differential equations which are of the form:

$$\frac{dx}{dt} = f\,(x(t),u(t),k)\,, \qquad x(0)=x_0 \qquad (1.2)$$

where x is an n-dimensional vector of state variables (e.g. pressure and saturations at all grid points), x_o is the initial state and u represents all user specified variables (e.g. injection flow rates, production rates, etc.). The m-dimensional output vector, y, is related to state vector x through a relationship of the form:

$$y(t) = C\; x(t) \qquad (1.3)$$

where C is a constant mxm matrix.

1.6 Outline of Thesis

This thesis begins with an introduction (Chapter 1) to the objectives of reservoir simulation, the steps required for a complete reservoir simulation study and the "inverse simulation" problem.

The mathematical structure of the reservoir simulation models is presented in chapter 2. A brief insight of the governing equations of reservoir simulation models, the discretization techniques, the boundary conditions, the well models and finally the methods of solution according to the degree of implicitness is provided.

Chapter 3 presents a review of the literature. Methods that have been used in the past for automatic history matching, are introduced. Previous works on algorithm development, identifiability of parameters, incorporation of prior information and the employment of constraints are cited and analyzed.

The parameter estimation techniques are introduced in chapter 4. The advantages and disadvantages of each method are analyzed. A detailed description of the method that has been used throughout this project, is also provided.

Chapter 5 provides the methodology for determining the error bounds of forecasted well and field performance. Also a comparison between Gauss-Newton method and Simulating Annealing in chemical kinetic models is presented.

In chapter 6 a simple 5-spot homogeneous system is examined. The performance of the algorithm to history match and predict the future production of a reservoir is investigated. The effect of the degree of implicitness and the dimensions of the grid block dimensions on the forecast of the performance of the reservoir is explored.

In chapter 7 the simulator was tested on heterogeneous reservoirs. The degree of heterogeneity was varied, employing models which are naturally fractured, have randomly placed discontinuous shales and sealing faults, or impermeable barriers.

Chapter 8 summarizes the conclusions of this project. Advantages and disadvantages of the Gauss-Newton method, the benefits of employing the Automatic History Matching in field development and the key parameters that ensure a successful implementation are listed.

CHAPTER 2

MATHEMATICAL FORMULATION OF RESERVOIR SIMULATION MODELS

2.1 Introduction

The reservoir simulation models can be categorized into four distinct classes; namely, the black oil models, the compositional models, the miscible displacement models and the thermal models. Although the governing equations in the above models, appear to be different, they are all based on the equation of continuity, using different simplifying assumptions.

In this chapter the theoretical and practical aspects of mathematical models that are in use, will be discussed.

2.2 Governing Equations

2.2.1 Equation of Continuity

The basic equations, that govern the fluid flow inside the porous media are obtained, by combining several physical principles, namely:

- Conservation of mass
- Conservation of momentum
- Conservation of energy (first law of thermodynamics)
- Equations of State

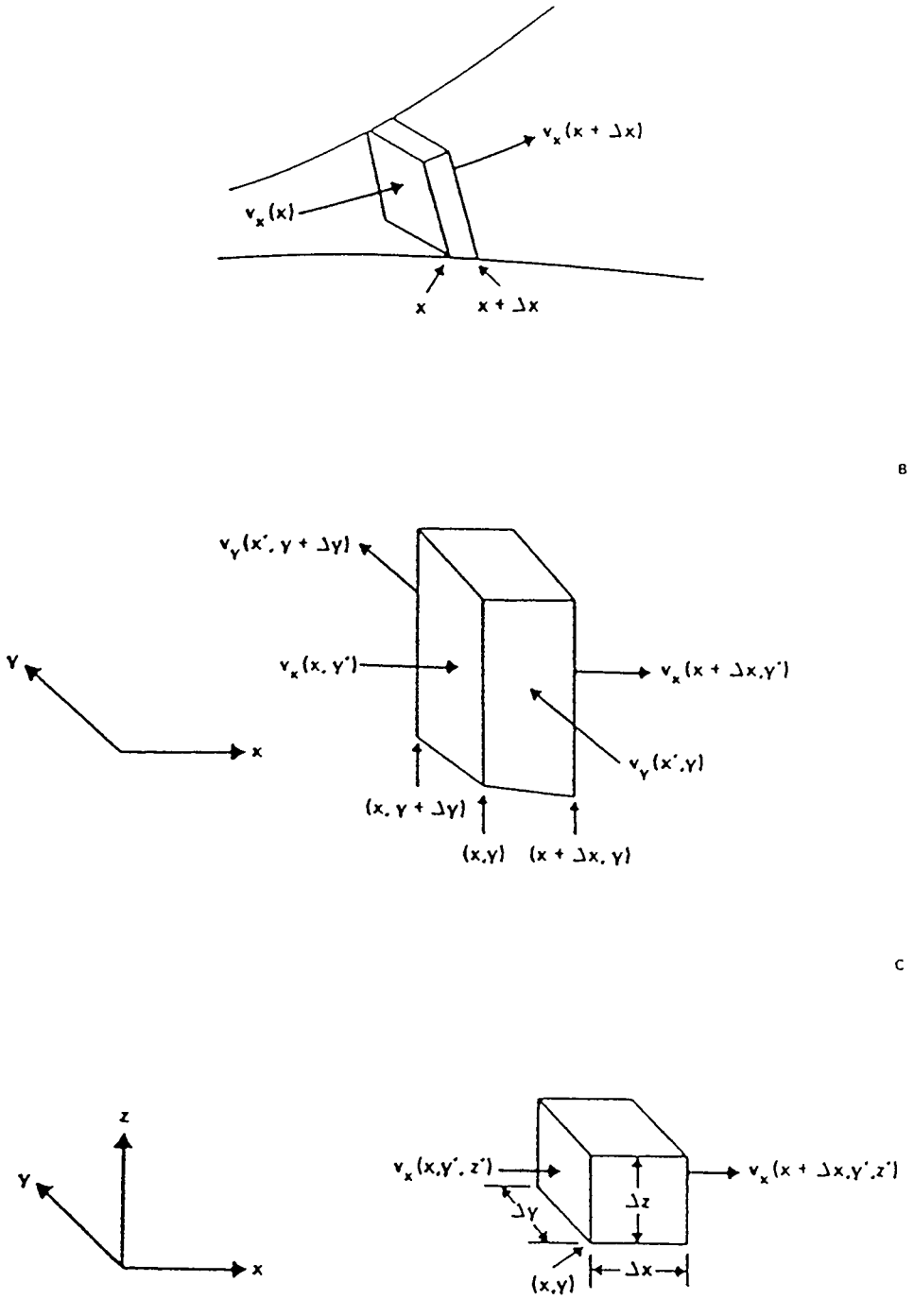

Figure 2.1 Differential Elements of Volume. (A)One-dimensional Flow. (B) Two-dimensional flow. (C) Three-dimensional flow. (Peaceman D. W. 1977)

The conservation of mass is considered to be the basis of all the reservoir flow equations. It states that the rate of mass accumulation in a grid-block is equal to the mass rate entering the grid-block, minus the mass rate at which if flows out of the grid-block, as it is shown at Fig. 2.1.

$$(\text{Rate of Mass In}) - (\text{Rate of Mass Out}) = (\text{Rate of Mass Accumulation}) \qquad (2.1)$$

For the three dimensional flow case the mass balance for a volume element would be:

$$\left((\rho u_x)|_x - (\rho u_x)|_{x+\Delta x}\right)\Delta y\ \Delta z = \frac{\partial}{\partial t}(\rho \Phi)\ \Delta x\ \Delta y\ \Delta z \qquad (2.2)$$

Adding similar terms for the y and z direction, dividing by $\Delta x \Delta y \Delta z$ and taking the limit as the dimensions of the volume element approach to zero results:

$$-\frac{\partial}{\partial x}(\rho u_x) - \frac{\partial}{\partial y}(\rho u_y) - \frac{\partial}{\partial z}(\rho u_z) = \frac{\partial}{\partial t}(\rho \Phi) \qquad (2.3)$$

or simply by using vector notation:

$$-\nabla \cdot (\rho \mathbf{u}) = \frac{\partial}{\partial t}(\rho \Phi) \qquad (2.4)$$

The left hand side of the above equation is simply the net rate of influx per unit volume. Therefore one can say that the increase of density in a small volume is equal to the rate of mass influx divided by the volume.

If we consider a **multiphase** system, (oil and gas), then the above equation becomes:

$$-\nabla\cdot(\rho_o \mathbf{u}_o + \rho_g \mathbf{u}_g) = \frac{\partial}{\partial t}\left(\Phi(\rho_o S_o + \rho_g S_g)\right) \tag{2.5}$$

For a **multi-component** system the equation of continuity must hold separately for each component. In order to do so we have to introduce the concept of mass fraction of each component in each phase in the equation. If ω_{oi} and ω_{gi} are the mass fractions of the component i in the oil and gas phase the equation of continuity will become:

$$-\nabla\cdot(\rho_o \omega_{oi}\mathbf{u}_{oi} + \rho_g \omega_{gi}\mathbf{u}_{gi}) = \frac{\partial}{\partial t}\left(\Phi(\rho_o \omega_{oi} S_o + \rho_g \omega_{gi} S_g)\right) \tag{2.6}$$

If we consider a **multi-mechanism** system, where the flow occurs, due to different mass transport mechanisms, like convection and dispersion the continuity equation becomes:

$$\begin{aligned} -\nabla\cdot(\rho_o \omega_{oi}\mathbf{u}_o^c + \rho_g \omega_{gi}\mathbf{u}_g^c) - \nabla\cdot(\rho_o \omega_{oi}\mathbf{u}_{oi}^d + \rho_g \omega_{gi}\mathbf{u}_{gi}^d) = \\ \frac{\partial}{\partial t}\left(\Phi(\rho_o \omega_{oi} S_o + \rho_g \omega_{gi} S_g)\right) \end{aligned} \tag{2.7}$$

where the superscripts c and d denote the velocity due to convection and dispersion respectively.

2.2.2 Additional Equations

Auxiliary equations are required in order to solve the system of mass balance equations for each element volume, at each time-step. These are the conditions that make sure that the sum of saturations of each phase, and the sum of the mole fractions of any component for all the phases is equal to unit. Also, density and viscosity of any fluid should be a function of the phase pressure and composition. Relative permeability curves are the main source of nonlinearities, in the solution procedure. They are considered as functions of phase saturation. The capillary pressure couples

the phase pressures and it is always equal to the difference, between the non-wetting phase pressure and wetting phase pressure. Reservoir parameters, such as permeability and porosity, are functions of reservoir pressure and direction. Finally the equilibrium values (k-values) are functions of pressure and composition for a given temperature.

The convective velocity is given by the Darcy's law, while the dispersion velocity by the Fick's law as shown:

$$u_l^c = - \frac{k k_{rl}}{u_l} (\nabla p_l - \gamma_l \nabla h) \tag{2.8}$$

and

$$\rho \omega_{li} u_{li}^d = - K_{li} \nabla (\rho_l \omega_{li}) \tag{2.9}$$

where K_{li} is the ratio of the moles of a component in the gas and in the oil phase.

2.3 Black Oil Models

Black oil models are the most commonly used models in reservoir simulation studies. Black oil simulators are based on the following assumptions:

- Up to three phases are considered to be present in the system (oil, gas and water).
- Up to three components are considered, namely, oil, gas and water.
- The dispersion is negligible.
- The oil component is assumed to be only in the oil phase, the gas component could be present in the gas phase, as free gas and in the oil phase, as dissolved gas. Finally water component is only present in the water phase.

- The formation volume factor and the solution gas oil ratio are functions of the reservoir pressure only. Also functions of pressure are the oil and gas compressibility and the viscosity.

The implementation of the above assumptions is represented in the following equations for the liquid and the vapour hydrocarbon phase:

$$-\nabla\cdot\left(\frac{kk_{rL}}{\mu_L B_l}\left(\nabla p_L - \gamma_L \nabla h\right)\right) = \frac{\partial}{\partial t}\left(\frac{\Phi S_L}{B_L}\right) \tag{2.10}$$

$$\begin{aligned}-\nabla\cdot\left(\frac{kk_{rV}}{\mu_V B_V}\left(\nabla p_V - \gamma_V \nabla h\right)\right) - \nabla\cdot\left(\frac{kk_{rL}}{\mu_L B_L} R_s \left(\nabla p_L - \gamma_L \nabla h\right)\right) \\ = \frac{\partial}{\partial t}\left(\frac{\Phi S_V}{B_V}\right) + \frac{\partial}{\partial t}\left(\frac{\Phi S_L}{B_L} R_s\right)\end{aligned} \tag{2.11}$$

with additional equations:

$$S_L + S_v = 1 - S_W \qquad \text{and} \qquad p_V - p_L = P_C \tag{2.12}$$

The subscripts L and V refer to the liquid and vapour phase.

The simulator (DRS, SIMTECH Consulting Services Ltd.) used, throughout the course of this project, belongs in this category of models. DRS is a three phase, three dimensional, black oil reservoir simulator.

2.4 Discretization of Flow Equations

The partial differential equations, that describe the fluid flow, must be solved, according to the appropriate boundary conditions. The numerical solution is obtained by replacing the partial differential equations with finite difference approximations, that are amenable to solution by digital computers. The error involved by the above

approximation is called *truncation error*, because of using truncated Taylor's series. The impact of the truncation error on the solution of the equations is called *numerical dispersion* or *diffusion*. The model is divided into a discrete number of grid blocks and the time domain is divided into discrete time intervals. The form of the discretized flow equations has been presented in numerous textbooks (Crichlow 1977, Settari and Aziz 1979, Peaceman 1977, SPE Monograph 1990). The final form of the finite difference equation, if one considers the well injection and production rates, of a black oil simulator, for oil is :

$$\Delta T \cdot M_o[\Delta(p_o)_{i,j} - g\rho_o \Delta D_{i,j}] + (q_o)_{i,j} = \left(\frac{V_{i,j}}{\Delta t}\right) \Delta_t \left(\frac{\Phi S_o}{B_o}\right)_{i,j} \tag{2.13}$$

similarly, the water and gas equation is:

$$\Delta T \cdot M_w[\Delta(p_w)_{i,j} - g\rho_w \Delta D_{i,j}] + (q_w)_{i,j} = \left(\frac{V_{i,j}}{\Delta t}\right) \Delta_t \left(\frac{\Phi S_w}{B_w}\right)_{i,j} \tag{2.14}$$

$$\Delta T \cdot M_g[\Delta(p_g)_{i,j} - g\rho_g \Delta D_{i,j}] + \Delta T\, R_s \cdot M_o[\Delta(p_o)_{i,j} - g\rho_o \Delta D_{i,j}] + (q_w)_{i,j} = \left(\frac{V_{i,j}}{\Delta t}\right) \Delta_t \left(\left(\frac{\Phi S_g}{B_g}\right)_{i,j} + \left(\frac{\Phi S_o R_s}{B_o}\right)_{i,j} \right) \tag{2.15}$$

where ΔT is the difference of physical transmissibility between adjacent grid blocks, B_i, i=o, w, g formation volume factor of oil, water and gas respectively, R_s solution GOR, ΔP pressure drop, ΔD depth difference, ρ density, g acceleration of gravity, q volumetric flow rate, Δt length of time-step, S_i, i=o, w, g saturation fraction of oil, water and gas respectively.

2.5 Well Models

The well which penetrates the petroleum reservoir is our only window into the vast unknown to which we most diligently attribute rock and fluid properties,

make predictions, and perform all the other engineering calculations that comprise the scope of reservoir engineering (Crackle 1977) .

Analytical solutions for single phase radial flow of a cylindrical region around the well of radius r_w have been discussed thoroughly by Aziz and Settari (1979). Peaceman (1978) presented the expression for the well production rate, under the assumption of the fluid is incompressible, with influx on the external boundary r_e:

$$Q = -\frac{P_{wf} - P_{av}}{\mu \left(\ln \frac{r_o}{r_w} \right)} (2\pi k \Delta z) \qquad (2.16)$$

where r_o is the effective (equivalent) radius, which is the radius at which the steady state flowing pressure for the actual well is equal to the numerically calculated pressure of the well block. Peaceman (1978) proved that the equivalent radius is equal to $0.2\Delta x$ for a square grid block, and for a non-square grid block is given by:

$$r_o = 0.14 \, (\Delta x^2 + \Delta y^2) \qquad (2.17)$$

Peaceman (1983) has also extended the analysis to include anisotropic permeability and an expression for the effective well-block radius in terms of Δx, Δy, k_x and k_y. Williamson and Chappelear (1981) further developed the source representation for a variety of circumstances. According to Settari (1993), the ultimate solution to the problem of modelling a well would be to eliminate the use of well index, by using griding techniques that represent the boundaries directly, or to use grid refinement to the point where the difference between the well flowing pressure and the block pressure is insignificant. Special griding techniques is a recent area of research. Pedrosa-type grids have been used in modelling vertical and horizontal wells, while, Voronoi-type (Heinemann *et al.*, 1991) grids have been used in reservoir simulation because of their ability to represent complex geological patterns and well boundaries.

Finally for multiphase production well, the source/sink representation must be modified to calculate the production of each phase properly.

2.6 Solution Methods

The most common methods of solution of the mass balance equations are:

- IMPES solution
- Semi-Implicit method
- Adaptive Implicit method and
- Fully Implicit method

2.6.1 IMPES Solution

In this method the phase pressures and saturations are calculated sequentially. This is done, by combining all the single phase equations into a single multiphase equation based on pressure. Initially the pressure equation is solved implicitly and then the model calculates saturations in an explicit mode. This procedure was introduced by Stone et al (1961).

One main limitation of the IMPES solution, is that it is conditionally stable. Such limitations result from the explicit treatment of capillary pressures and the transmissibilities, which are the strongest nonlinearities involved. Aziz and Settari (1979) developed expressions for the maximum time-step, that can be used in order to avoid any instabilities. For example the method is stable with respect to transmissibilities only when:

$$\Delta t \prec \frac{\text{Pore Volume}}{\frac{df_w}{dS_w} Q_T} \tag{2.18}$$

where f_w is the fractional flow of water and Q_T is the total flow rate of water.

2.6.2 Semi-Implicit Method

This method exhibits increased stability, which results from estimating mobility factors at the new time step by extrapolation simply by using the knowledge of the shape of the fractional flow function[1]. A common method that is used is the linear extrapolation, even if the fractional flow curve is not linear:

$$f_o^{n+1} = f_o^n + \frac{df_o^n}{dS_o} (S_o^{n+1} - S_o^n) \tag{2.19}$$

2.6.3 Fully Implicit Method

This procedure involves the simultaneous solution of the partial differential equations for flow of oil, water, and gas to obtain the pressures in each phase. The saturations of each phase are calculated implicitly using capillary pressure relations. All the state variables in the equations are in the *n+1* time level.

This method is very complex, computationally intense, but unconditionally stable. It has, also, extensive computer storage requirements.

2.6.4 Adaptive Implicit Method

This method is considered as a variant of the fully implicit method. Rather than providing a fixed degree of implicitness in every grid-block at every time-step or iteration, the adaptive implicit method operates with different levels of implicitness in adjacent grid-blocks. Each variable is therefore treated explicitly, or implicitly according to the magnitude of it's gradient with respect to space and time.

---

[1]Fractional flow of a phase is the ratio of the production rate of that phase over the summation of the production rates of all the phases present in the reservoir

2.7 Comparison Between the Solution Method

In general, many areal problems, can be handled with IMPES-type formulation, especially in systems where the capillary pressures are smaller compared to the viscous forces. If that's not the case, then a more stable solution should be more appropriate.

The modelling of undersaturated oil reservoirs needs a certain degree of implicitness in order to handle rapid gas movements, when the pressure drops below the bubble point.

The adaptive-implicit method invokes only the necessary level of implicitness an a cell by cell basis. For black oil reservoir simulation problems, the method provides substantial reduction in computer processing costs, yet provides the stability characteristics of the fully implicit method. Also the method can reduce computer storage requirements to approximately those levels associated with the IMPES method (Thomas *et al*; 1983).

Modelling of thermal processes, naturally fractured reservoirs, or even gas conning problems, requires more stability, and therefore the fully implicit method is more suitable. It is, very important though, to remember that the fully implicit method produces the highest numerical dispersion than any other method. On the other hand, IMPES method adds less numerical dispersion to the solution compared to semi-implicit, fully-implicit or adaptive-implicit, method.

CHAPTER 3

LITERATURE REVIEW

With the continuous development of powerful workstations and desktop personal computers, a renewed interest in automatic history matching procedures can be observed in the past few years. Nevertheless, the literature available in this area is considerably limited, because of the intricacy that the automatic history matching problem exhibits.

For the minimization of the objective function two different approaches have been widely used, nonlinear regression and optimal control methods. Recently the simulated annealing has also been proven to be a reliable procedure. In practical applications always some form of regularization, is required to overcome the very serious problem of ill-conditioning, particularly as the number of parameter increases to more than ten or so. A problem is called ill-conditioned when, significant changes in the reservoir parameters, does not cause a significant change of the objective function.

3.1 Methods Used for Automatic History Matching

3.1.1 Nonlinear Regression Analysis

In a nonlinear regression method, the derivatives of the objective function with respect to each variable are analyzed concurrently to determine the optimum direction for the parameters. The effects of all variables on each residual are included

simultaneously. These methods include the method of Steepest Descent, the Gauss-Newton method, the Quasilinearization method and the Newton's method.

One common characteristic of all the above methods is the calculation of the sensitivity coefficients. These are the partial derivatives of the reservoir variables (pressures, saturations, temperature) with respect to the unknown parameters. These coefficients are usually obtained by numerical differentiation. Each parameter is perturbed independently and a full simulation run is made to evaluate the sensitivity of the reservoir variables to the parameter. This procedure must be repeated for all the parameters for each iteration. Therefore if there are k parameters to be estimated, the simulator should perform (k+1) runs to determine the sensitivity coefficient for each iteration. Gavalas et al (1976) discusses briefly the computational trade-offs in the various ways of calculating sensitivity coefficients.

All the above methods are iterative procedures. A typical iterative sequence is as follows: given an initial value of $\mathbf{k}^{(o)}$ of the parameters and the objective function $S(\mathbf{k}^{(0)})$, we seek a new value of $\mathbf{k}^{(1)}$ which is closer the minimum, in the sense that $S(\mathbf{k}^{(1)}) < S(\mathbf{k}^{(0)})$. Once $\mathbf{k}^{(1)}$ has been obtained, we proceed to find, $\mathbf{k}^{(2)}$, $\mathbf{k}^{(3)}$, $\mathbf{k}^{(4)}$,..., each, in turn, having the property of being closer to the minimum. In the class of methods which have proved to be successful for parameter estimation, the formula used for finding the new value of the parameter is:

$$\mathbf{k}^{(1)} = \mathbf{k}^{(0)} - \lambda \mathbf{R} g \tag{3.1}$$

where λ is a scalar, R is a matrix and g the gradient vector of the S ($\bar{d}S/\bar{d}k$). The matrix R pre-multiplies the vector g, twists g in vector space to produce a new vector. Therefore matrix R determines the direction to go from $\mathbf{k}^{(0)}$. λ, on the other hand, being a scalar defines how far along this direction to go and determines the length of the step.

The choice of R = I constitutes the *method of steepest descent*. It converges slowly in most practical problems. The choice of R, as the inverse of the Hessian matrix, G, constitutes

$$\mathbf{R} = \left[\frac{\partial^2 S}{\partial k^2} \right]^{-1} = \mathbf{G}^{-1} \tag{3.2}$$

the *Newton-Raphson* method. It performs well when one is near the minimum, but suffers from two major difficulties:

- Except near the minimum, a step taken along the Newton-Raphson direction is not guaranteed to reduce S, no matter what value is chosen for λ
- the method requires the computation of second derivatives of S, which usually is a laborious procedure

Finally if :

$$\mathbf{R} = \mathbf{G}^{-1} \tag{3.3}$$

and G is given by:

$$\mathbf{G}_{i,l} \cong 2 \sum_{j=1}^{M} \frac{\partial f_j}{\partial k_i} \frac{\partial f_j}{\partial k_l} \tag{3.4}$$

the method is called *Gauss-Newton method.* It can be seen from equation (3.4) that the Gauss-Newton method uses an approximation of the second derivatives.

Quasilinearization method is very similar to Gauss-Newton method. Both are best known for their quadratic convergence to the optimum. The major problem, of quasilinearization, according to Seinfeld *et al;* (1970), Seinfeld *et al;* (1974), and Kalogerakis (1983) is its small region of convergence.

Jacquard and Jain (1965) were among the first researchers to develop a system of automatic interpretation of the pressure measurements. They proposed a method, in which, starting from the relation which exists between a local perturbation of permeability and its effect on the velocity potentials in the wells, they determined by

successive approximation the modification to be made to the permeability map by fitting the least squares between the measured pressures and the pressures indicated by the mathematical model.

Slater and Dutter (1971), Thomas *et al.* (1972), Kalogerakis and Luus (1983 A), Kalogerakis (1983B) have also developed variants of gradient and Gauss-Newton method. Specifically Slater and Dutter proposed a modification of Jacquard and Jain's method that reduces the time required to obtain the solution.

Dogru *et al* (1977) used nonlinear regression theory to determine the effect of erroneous parameter estimates in the future prediction of reservoir pressures.

Smith *et al.* (1993) and Watson et al. (1990) used nonlinear regression theory to improve reservoir characterization of a fractured reservoir. Savioly et al. (1991) has also applied nonlinear regression analysis in automatic history matching of well test data.

3.1.2 Optimal Control Methods

The second type of parameter estimation technique, that has been applied to automatic history matching problem, is the optimal control methods. Chen et al (1974) and Chavent et al (1975) published algorithms that use this approach.

The optimal control methods require the solution of a set of adjoint ordinary differential equations together with the ordinary differential equations of the model. It therefore requires two simulation runs per iteration for each parameter. These methods exhibit linear convergence properties. It is therefore obvious that when the number of parameters exceeds a certain level, or when the model is highly nonlinear, then these kind of methods are very computationally demanding.

Watson *et al* (1980) modified an automatic history matching algorithm, which was based on optimal control approach, to account for joint estimation of spatially varying permeability and porosity and coefficients of relative permeability functions in two phase reservoirs.

Dogru *et al* (1981) used second order optimal control method to investigate the computational effort that it is required to determine the sensitivity coefficients in a two dimensional, single fluid model. Dogru, found that the nonlinear regression methods should be preferred over the optimal control methods when the number of parameters is less than the number of ordinary differential equations that have to be solved. This is usually the case, especially when a zonation approach is used. As the number of parameter increases optimal control methods become more economical than the nonlinear regression methods.

Wasserman et al (1975) modified the standard optimal control technique to treat multiphase problems.

Yang et al (1987) applied optimal control methods to two-phase, one and two dimensional models. He increased the rate of convergence by using metric methods.

3.1.3 Regularization Procedures

The process of estimating unknown properties, such as porosities and permeabilities, in a mathematical reservoir model, to give the best fit to measured pressure or other production data, is mathematically ill posed. This ill-posed nature coupled with the large number of unknown parameters cause numerous difficulties in its solution. The principal approach that has been used to alleviate the ill-conditioning in the parameter estimates is to decrease the number of unknown parameters and, if possible to utilize any available prior information to constrain the values of the unknown parameters.

The regularization of an ill-posed problem consists of modulating the original problem to a well-posed one, whose solution approximates the solution of the original problem. Lee *et al.*, (1986) used as the regularization formulation of parameter estimation the norm of the parameter in an appropriate Hilbert space. This is measure of the "non-smoothness" of the estimated parameter. The customary history matching least squares objective function is augmented with an weighted function. The augmenting term exerts a penalty action against anomalous oscillations in the parameter estimates. Eventually the objective function looks like:

$$J_{SM} = J_{LS} + \beta_{\alpha} J_{ST} \tag{3.5}$$

where J_{LS} is the sum of the least squares term, J_{ST} is the stabilizing function and β_{α} is a weighting coefficient to reflect the degree of importance given to J_{ST}. The theoretical details of regularization are described by Kravaris et al (1985; 1986).

Palatnik *et al* (1990) proposed a form of regularization in complex geological models (history matching problems in filtration theory).

Other authors proposed simpler forms of regularization. Kalogerakis and Rein (1983) used Marquardt's modification to increase the region of convergence of the algorithm.

3.1.4 Simulated Annealing Method

The simulated annealing method has been applied, as a parameter estimation procedure, to automatic history matching. The idea of annealing came from the observation of how nature optimizes the placement of atoms in a lattice when a material sample is slowly cooled. When this happens the atoms find the lowest energy configuration possible, yielding a very regular structure. On the other hand when the temperature is reduced rapidly (*quenching*) the atoms settle down in places far away from the optimum, yielding a very irregular structure. A slow reduction of temperature, corresponds to permitting non-improving moves to be selected with a certain

probability, which diminishes as the objective function diminishes. Thus the *simulated annealing method* is *an uphill climbing method*, because it allows the objective function, at some point, to take higher values and eventually permits the system to "climb out" of local minima. Eventually the algorithm converges to the global minimum. A schematic diagram of the simulating annealing is shown in Fig. 3.1

Ouens *et al* (1992A; 1992B; 1992C; 1992D; 1993), have used simulated annealing method to improve reservoir characterization, by determining reservoir parameters, like porosity and permeability. Ouens *et al* (1992E) applied the algorithm to a simplified reservoir-plus-aquifer model where more than 50 subsurface properties have been estimated by inverse modelling. Other applications of simulating annealing methods include the simultaneous estimation of relative permeability and capillary pressure curves from two phase laboratory corefloods by Quens et al (1992 E) and the development of the inverse modelling procedure on the CO_2-foam pilot area of the East Vacuum Grayburg/San Andres Unit (EVGSAU) by Sultan A.J. et al (1993).

Ghori et al (1992) has compared the simulated annealing method with three other geostatistical methods (source point method, fast fourier transform method and the turning band method) for generation of property distribution. The comparison of the four methods has shown that the simulated annealing method produces the best fit of the experimental variograms regardless of the type of variogram. However, one fact was certain - simulated annealing methods were slower than any other stochastic model.

3.1.5 Other Methods

A special category of methods, known as global optimization methods, has also been developed. This category is comprised by the following approaches:

- The *neural network* modelling is based on the early work of McCulloch and Pitts (1943) and Rosenblatt (1962)

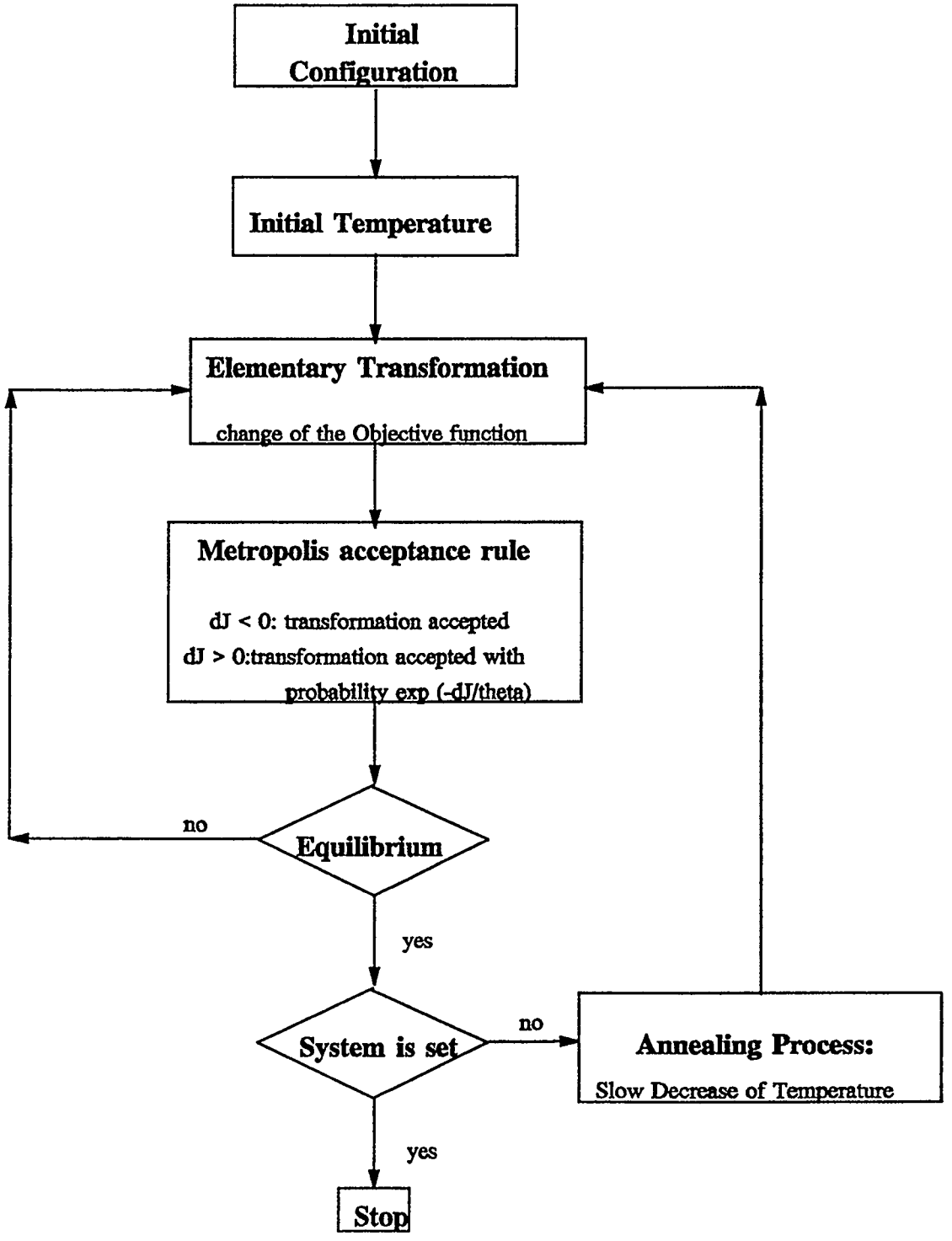

Figure 3.1 Schematic diagram of the Simulating Annealing method. (After Ownes, 1992 A)

- *Genetic algorithms* introduced by Holland (1975), Liepins (1992), Walbridge (1989) and Hajela (1992). These algorithms are based on the process of mating, mutating and selecting. They are, essentially random search algorithms, with the ability to accumulate all the knowledge gained from the previous iterations
- *Tabu search* introduced by Glover (1977, 1986). In this method when a local minimum is reached the algorithm structures the operation of its embedded heuristic in a manner that permits it to continue. This is accomplished by forbidding moves with certain attributes (making them tabu) and choosing moves, from the remaining ones that are mostly appealing in some optimal fashion.
- *Random Walk Method.* This approach is based on generating a sequence of improved approximations to the minimum. The search pattern is totally random and each step is accepted only if the objective function is less then the one in the previous iteration.

Hirasaki (1975) provided tools to influence coefficients for adjusting reservoir properties of simple models. As the degree of complexity of a model increases, more sophisticated history matching methods are required.

Coats *et al.* (1970) presented a method that employs the least squares and linear programming techniques to determine a reservoir description from given performance data. The reservoir properties were supplied by a random number generator.

Hird K.B. *et al.* (1992) used a conditional simulation technique to constrain areal permeability fields to typical statistical information (i.e., permeability histogram, spational correlation and well data) and indirectly to waterflood well performance (i.e., oil and water producing rates, water injection rates and water-oil ratios).

3.2 Identifiability of Parameters

The estimation of reservoir properties is inherently an ill-conditioned problem (one not having a unique solution), because of the large number of unknowns relative to the available data. In order to demonstrate the importance of estimating correctly the reservoir properties the following general rules of thumb in reservoir engineering are summarized below:

- The parameters that have a significant effect on depletion by solution gas drive are: the extent of the reservoir, the bubble point pressure, the gas-oil relative permeability, the porosity and the absolute permeability. The gas-oil relative permeability has a strong impact on the produced GOR. The absolute permeability will influence the well productivity and the production rates. Porosity estimates will determine the original oil in place and the distribution of the latter will influence both the individual well GOR and the pressure.
- The parameters that have a significant effect on waterflood performance include the initial waterflood movable oil in place, initial gas saturation, water-oil relative permeability, water-oil capillary pressure, stratification, permeability anisotropy, porosity and permeability distribution.

The above examples demonstrate how closely the reservoir properties are related and the impact that each one has on the final production rates of a hydrocarbon reservoir. Shah et al. (1978) investigated the accuracy of the estimated porosity and permeability obtained in reservoir history matching using covariance analysis. Dogru et al (1977) used nonlinear regression the determine the effect of erroneous parameter estimates obtained from well testing on the future prediction of reservoir pressures.

3.3 Incorporation of Prior Information and Constraints

Farouq Ali et al. (1988) pointed out that:" *the most serious problem in automatic history matching is the tendency to construct ill-conditioned systems of equations Ax=b. By the very nature of the history-matching problem, inherent uncertainties exist in both A and b, because they are based on a measured performance history. This problem therefore can only be treated by incorporating some a priori information about the solution vector x*".

Any information available from geology studies, core tests, seismic and pressure transient analysis, or log interpretation, can be used to set bounds in the estimated parameters. This way the engineer may prevent the parameter estimates to attain unrealistic values.

Carter *et al.*, (1974) and Coats *et al.*, (1970) used inequality constraints in order to restrict the parameter estimates. The latter found out that quite often the parameter values were very close to the upper or lower bound. Farouq Ali et al. (1988) asserted that this is caused because the bounds are not symmetrical about the true values of the estimated parameters.

Yang *et al.*, (1991) used a Bayesian approach to estimate relative permeability curves, in a two dimensional two phase model. A relative weight was considered, which was given to the production data and prior estimates so that the final estimates are least different from the prior estimates without compromising the match of reservoir production data. The optimum weighting factor was estimated in an algorithm based on observation of slope changes of the minimum objective function obtained from many regression run using various weighting factors. The same author (Yang *et al.*, 1987) incorporated inequality constraints with variable metric methods, in a two dimensional, two phase model.

Finally Neuman et al (1979) and Cooley (1992) incorporated prior information about the estimated parameters, in the objective function, in the field of underground hydrology.

CHAPTER 4

PARAMETER ESTIMATION TECHNIQUES

The problem of parameter estimation to find the unknown model parameters of a given model, by matching the model predictions with the actual measured data, in some optimal fashion. Therefore the parameter estimation techniques could be viewed as optimization procedures, whereby the unknown parameters are obtained by minimizing the chosen objective function.

In general any mathematical model can be described by a set of algebraic equations, or by a set of differential equations. Depending on whether the parameters are linearly or non-linearly related to the output vector the models are characterized as linear or non-linear models.

The algebraic equation models are of the form:

$$y = f(x, k) \tag{4.1}$$

where y is the output vector of the model (measured data), x is the vector of the state variables and k is the vector of the unknown parameters.

The differential equation models are more complicated and computationally demanding. If the state variables are functions of time, then the model is characterized as *dynamic*. The general form of these models is:

$$\frac{dx}{dt} = f(x(t),u(t),k) \ , \quad x(0)=x_0 \tag{4.2}$$

where **x** is the n-dimensional state vector, $\mathbf{x}_0$ is the given initial state, **k** is a p-dimensional vector of unknown parameters and **u** represents all user specified variables. The m-dimensional output vector **y** is related to the state vector by:

$$\mathbf{y}(t) = \mathbf{C}\ \mathbf{x}(t) \tag{4.3}$$

where **C** is a constant mxn matrix.

The automatic history matching of a hydrocarbon reservoir is a typical non-linear parameter estimation model. The model is described by a set of partial differential equations (continuity equations as described in chapter 2), the output vector **y** is comprised of production rates, the state variable vector **x** consists of values of pressures and phase saturations and finally the parameter vector **k** contains values of porosity and permeability. Automatic history matching procedures have also been used for estimating relative permeability curves and rock and fluid parameters from core flood tests.

4.1 Model Forms for Parameter Estimation

4.1.1 Least Squares Estimation

The unknown parameters are estimated by matching the measured data and the output of the model, in some optimal manner. If $\hat{\mathbf{y}}(t_i)$ are the measurements of the output vector for different times t_i and $\mathbf{y}(t_i)$ is the output vector of the model the error involved in each phase of the parameter estimation procedure is:

$$\boldsymbol{\varepsilon}(t_i) = \hat{\mathbf{y}}(t_i) - \mathbf{y}(t_i, \mathbf{k}) \tag{4.4}$$

Using the least squares technique, an objective function $S_{LS}(\mathbf{k})$ is defined as the sum of the squares of errors as shown:

$$S_{LS}(k) = \sum_{i=1}^{n_o} [\hat{y}(t_i) - y(t_i,k)]^T \; W_i \; [\hat{y}(t_i) - y(t_i,k)] \qquad (4.5)$$

where n_0 is the number of the observation times, and W_i is an mxm positive definite, symmetric matrix of weighting factors which may vary with time.

Depending on the selection of W we have:

- *Simple Least Square Estimation* if W=I (minimization of the sum of squares of errors).
- *Weighted Least Square Estimation* if W_i=W (using constant weights) and
- *Generalized Least Square Estimation* if W_i=W_i (using non-constant weights)

Usually the choice of W_i depends on the distribution of the errors. Namely one should select W_i such that:

$$W_i = COV^{-1}[\varepsilon(t_i)] \qquad (4.6)$$

where COV is the covariance matrix of the errors.

4.2 Gauss-Newton Method

One of the most efficient methods in parameter estimation is the Gauss-Newton method.

In general any reservoir model can be represented by a set of differential equations which have the form:

$$\frac{dx}{dt} = f\,(x(t),u(t),k)\,, \quad x(0)=x_0 \qquad (4.7)$$

where x is the n-dimensional state vector (e.g. pressures or saturations), x_0 is the given initial state, k is a p-dimensional vector of unknown parameters and u repre-

sents all user specified variables (e.g. flow rates, pressures, etc). The m-dimensional output vector y is related to the state vector by:

$$y(t) = C\ x(t) \tag{4.8}$$

where **C** is a constant mxn matrix.

If we suppose that the estimate $\mathbf{k}^{(j)}$ of the unknown parameter vector is available at the j^{th} iteration, using the Taylor's series expansion we can obtain $y^{(j+1)}$, at the $(j+1)^{th}$ iteration as a linear function of $\mathbf{k}^{(j+1)}$:

$$y^{(j+1)}(t) = y^{(j)}(t) + \left(\frac{\partial y^T}{\partial x}\right)^T \left(\frac{\partial x^T}{\partial k}\right)^T (k^{(j+1)} - k^{(j)}) \tag{4.9}$$

Substitution of eq. (4.9) into eq. (4.8) yields:

$$y^{(j+1)}(t) = C\ x^{(i)}(t) + CG(t)\Delta k^{(j+1)} \tag{4.10}$$

where G(t) is the nxp sensitivity matrix. Substituting $y^{(j+1)}(t)$ into the performance index in eq (4.5) and setting $s/k^{(j+1)} = 0$ we obtain a set of linear algebraic equations which have the form:

$$A\ \Delta k^{(j+1)} = b \tag{4.11}$$

where:

$$A = \sum_{i=1}^{N} G^T(t_i)\ C^T\ W_i\ C\ G(t_i) \tag{4.12}$$

and

$$b = \sum_{i=1}^{N} G^T(t_i) C^T W_i \left[\hat{y}(t_i) - y(t_i, k^{(j)})\right] \tag{4.13}$$

The new parameter estimate is obtained from:

$$k^{(j+1)} = k^{(j)} + \lambda \, \Delta k^{(i+1)} \tag{4.14}$$

where λ is the step-size with $0 \leq \lambda \leq 1$. The step size in chosen either by the bisection rule or through a cautious step-size policy.

The sensitivity coefficient matrix G is obtained by differentiating both sides of the model equation (4.10) with respect to the parameter vector k to yield:

$$\frac{dG(t)}{dt} = \left(\frac{\partial f^T}{\partial x}\right)^T G(t) + \left(\frac{\partial f^T}{\partial k}\right)^T \tag{4.15}$$

with initial conditions:

$$G(t_o) = 0 \tag{4.16}$$

The method computes an approximation of the Hessian matrix without calculating any second derivatives of the model equations. A schematic diagram of the Gauss-Newton method is shown in Fig. 4.1

The advantages of the Gauss-Newton method are:

- Exhibits quadratic convergence
- Does not require calculation of any second derivatives.
- One can compute statistical information from the Gauss-Newton matrix, at convergence in order to provide reliability estimates of the final values of the parameter .

The solution of the eq. (4.11), strongly depends on the how close the initial guesses of the parameters are to the optimum. The problems associated with the quality of the initial estimates are:

- The $\Delta k^{(j+1)}$ may correspond to a wrong direction
- The change of $\Delta k^{(j+1)}$ may be in the right direction, but large in magnitude (excessive over-stepping) and
- The state equations may be numerically unstable at $k^{(j)} + \Delta k(j+1)$.

4.3 Incorporating Prior Information and Penalty Function

If additional information is available for certain parameter values from core data analysis, well tests, geological studies or any drilling information, then we can incorporate this information into the objective function, in order to bias the parameter search in favour of parameter values and condition the problem. The impact of this a priori information is decreasing as the number of observations increases (Tan and Kalogerakis 1992). The objective function is augmented to:

$$S(k) = S_{LS}(k) + S_{prior}(k) \tag{4.17}$$

where $S_{prior}(k)$ is:

$$S_{prior}(k) = (k - k_p)^T W_p (k - k_p) \tag{4.18}$$

where W_p is the covariance matrix of the probability distribution of the unknown parameter. Equation (4.14) is derived under the assumption that our prior knowledge of the parameter vector **k** can be summarized in the form of a multivariable normal distribution with mean $\mathbf{k}_p$ and covariance matrix $\mathbf{W}_p^{-1}$. The latter is often a diagonal matrix with elements σ_{kj}^2, j=1, ...,p.

In addition hard constraints on the parameters can be incorporated in the form of a penalty function if required (Tan 1991). For instance the porosity can take values between 0 and 1. There is no guarantee that the final estimates of the parameters will be within logical boundaries. In order to make sure that the estimated parameters will not reach extremal values a penalty function can be incorporated into the objective function as shown:

$$S(k) = S_{ls}(k) + S_{prior}(k) + S_{penalty}(k) \tag{4.19}$$

where:

$$S_{penalty}(k)=\sum_{i=1}^{npar}\left[\frac{1}{k_i - k_{min}} + \frac{1}{k_{max} - k_i}\right] \qquad (4.20)$$

The penalty function is responsible for increasing the value of the objective function when the parameters are close to their physical boundaries. Inside the feasible region of convergence the effect of the penalty function is minor.

Both the prior information and the penalty function affect the elements of the main diagonal of the matrix A in eq. 4.11. resulting in a numerically superior matrix, since the condition matrix is decreased.

Core analysis can give us useful information regarding the reservoir, namely porosity and permeability distribution around the wells and even relative permeability curves. Among the preceding parameters, porosity values are considered to be the most reliable information. On the other hand, relative permeability curves, since they depend on numerous factors, like wettability, direction of saturation changes and rock properties, are the least reliable. In this work we concentrate on searching suitable values for porosities and permeabilities. The adjustment of relative permeabilities from history matching data will be the focus of a subsequent thesis. Here we assume that the relative permeability curves obtained from the lab are sufficiently accurate. One of the first priorities in any reservoir engineering study, is to determine the relationship between porosity and permeability using the results from the core analysis. Such prior information can only be used in automatic history matching to provide reasonable initial guesses for the parameters. The converged values represent the effective porosity and permeability which depend strongly on the chosen reservoir zonation, structure and reservoir complexity. Typically one prefers to have a few parameters in order to maintain rather simple reservoir descriptions.

4.4 Parameter Covariance Matrix

Once the series $k^{(1)}$, $k^{(2)}$, $k^{(3)}$, ...$k^{(j)}$, have converged to k^*, under the hypothesis that the model is adequate and the measurement errors, e_i, taken at time $t=t_i$ are

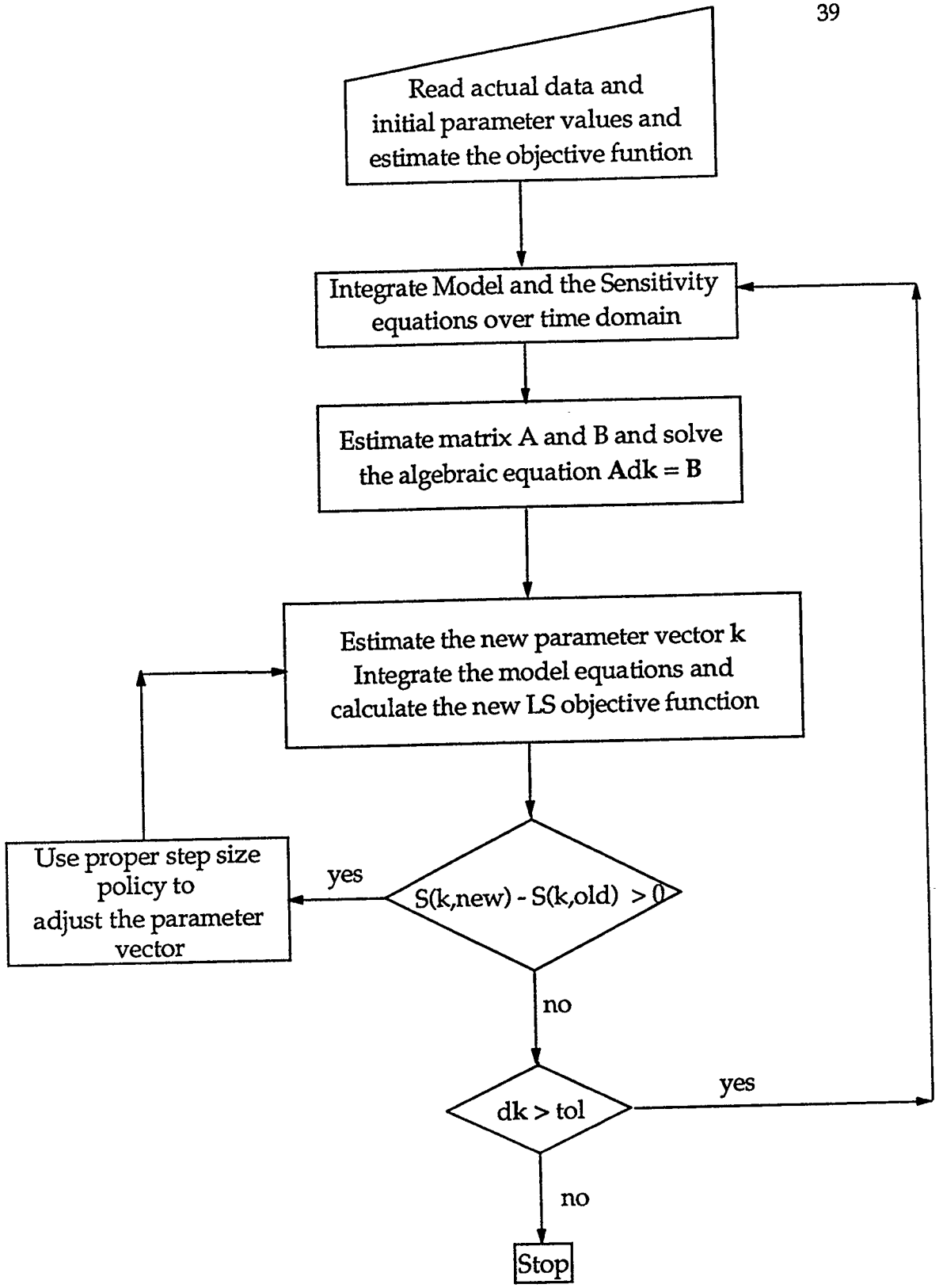

Figure 4.1 Schematic diagram of the Gauss-Newton Method

independently distributed with zero mean and covariance $Cov(e_i)= \sigma^2_e W^{-1}$, the covariance matrix of the parameters is given by:

$$Cov(k) = \sigma_e^2 A^{-1} \tag{4.21}$$

where the matrix A is evaluated at k^* and an estimate of the σ_e^2 is obtained from:

$$\sigma_e^2 = \frac{S_{LS}(k^*)}{\nu} \tag{4.22}$$

where ν are the degrees of freedom (Nm-p).

CHAPTER 5

PREDICTION OF FUTURE PERFORMANCE WITHIN CERTAIN CONFIDENCE INTERVALS

5.1 Inferences on Well Production Rates

Let as consider one well that is producing from different layers. The production rate from the i^{th} layer is given by the following equations:

$$Q_{oi} = WP\ M_o \frac{\left(P_{BH} + H - P_{block}\right)}{B_o} \tag{5.1}$$

$$Q_{gi} = WP M_g \left(P_{BH} + H - P_{block}\right) E_g + R_s Q_o \tag{5.2}$$

$$Q_{wi} = WP\ M_w \frac{\left(P_{BH} + H - P_{block}\right)}{B_w} \tag{5.3}$$

where H is the wellbore head pressure, M_i, $i=_{o,q,w}$ is the mobility of oil, gas and water and the well productivity index (WP) is given by :

$$WP_i = \frac{2\pi Kh}{\ln\left(\frac{R_o}{R_w}\right) + F_{skin}} \tag{5.4}$$

Therefore the total production rate from the well can written as:

$$Q_i \equiv Q_i(x,k) = \sum_{i=1}^{N_L} Q_{i'} \qquad i=o,g,w \tag{5.5}$$

where N_L is the number of the layers that the well is completed at.

At any point in time, t, where the state variables, x(t), and the sensitivity coefficients, G(t), are available, the sensitivity of the cumulative production rate can be readily obtained from solving the following equation:

$$\frac{dQ_c}{dk} = \left[\frac{\partial Q_c}{\partial x}\right]^T G(t) + \left[\frac{\partial Q_c}{\partial k}\right] \tag{5.6}$$

and the behaviour of the well production around the k^* is simply:

$$Q_c(k,t) = Q_c(k^*,t) + \left[\frac{dQ_c}{dk}\right]^T (k-k^*) \tag{5.7}$$

where the derivatives have been evaluated at $k=k^*$ and at time t. Taking variances from both sides we obtain:

$$\sigma^2_{Qc} = \left[\frac{\partial Q_c}{\partial k}\right]^T COV(k) \left[\frac{\partial Q_c}{\partial k}\right] \tag{5.8}$$

Having the standard error of estimate, we can readily obtain the (1-a)% confidence intervals of Q_c at time t as:

$$Q_{c,mim}(t) \le Q_c(k,t) \le Q_{c,max}(t) \tag{5.9}$$

where:

$$Q_{c,min}(t) = Q_c(k^*,t) - t^v_{a/2}\, \sigma_{Q_c} \tag{5.10}$$

$$Q_{c,max}(t) = Q_c(K^*,t) + t^{\nu}_{a/2}\ \sigma_{Qc} \tag{5.11}$$

and $t_{a/2}^{\nu}$ is obtained from the t-distribution tables for ν=Nm-p degrees of freedom. If ν is greater than 30, we can simply use 1,96 for $t_{0.025}^{\nu}$ corresponding to the 95% confidence intervals.

5.2 Overall Reservoir Production

While evaluating alternative depletion strategies, the reservoir engineer is often interested in the total production rate from all wells rather than individual well production. Hence it is often of interest to develop confidence intervals for the total production rate.

Due to the correlation of the individual well production rates through the governing reservoir equation of mass flow, we cannot simply sum up the variance calculated for each well to obtain the variance of the overall reservoir production rate. Instead, we must first compute the total production rate as:

$$Q_{c,tot} = \sum_{l=1}^{N_w} Q_{c,l} \tag{5.12}$$

where N_w is the number of wells and $Q_{c,l}$ is the production from the l^{th} well. Using the equation (22) the total production rate becomes:

$$Q_{c,tot}(k,t) = Q_{c,tot}(k^*,t) + \left[\sum_{l=1}^{N_w}\left[\frac{dQ_{c,l}}{dk}\right]^T\right](k-k^*) \tag{5.13}$$

where:

$$Q_{c,tot}(k^*,t) = \sum_{l=1}^{N_w} Q_{c,l}(k^*,t) \tag{5.14}$$

Again taking variances from both sizes of the equation 27 we obtain the variance of the total reservoir production rate as:

$$\sigma^2_{Q_c,tot} = \left[\sum_{l=1}^{N_w}\left[\frac{dQ_{c,l}}{dk}\right]^T\right] COV(k) \left[\sum_{l=1}^{N_w}\left[\frac{dQ_{c,l}}{dk}\right]\right] \tag{5.15}$$

and the (1-a)% confidence interval of $Q_{c,\,tot}$ at time t are as follows:

$$Q_{c,tot,min}(t) \leq Q_{c,tot,}(k,t) \leq Q_{c,tot,max}(t) \tag{5.16}$$

where:

$$Q_{c,tot,max}(t) = Q_{c,tot}(k^*,t) + t^v_{a/2}\ \sigma_{Qc,tot} \tag{5.17}$$

$$Q_{c,tot,mim}(t) = Q_{c,tot}(k^*,t)\ t^v_{a/2}\ \sigma_{Qc,tot} \tag{5.18}$$

where c = o, g, w

5.3 Implementation Considerations

It should be noted that the partial derivatives used in the calculation of the above noted variances depend on time t and hence, these variances should be computed simultaneously with the state variables and sensitivity coefficients by the simulator. The confidence intervals of the cumulative production of each well and the total reservoir are calculated by integrating $Q_{c,\,min,\,l}$, $Q_{c,\,max,\,l}$, for l = 1, Nw, $Q_{c,\,tot,\,min}$ and $Q_{c,\,tot,\,max}$, c = o, g, w, with respect to time.

5.4 Multiple Reservoir Descriptions

With the help of automatic history matching procedure the reservoir engineer can arrive at several plausible history matched descriptions of the reservoir. These

descriptions may differ in the grid block representation of the reservoir, existence of sealing or non-sealing faults, or simply different zonation of constant porosity and permeability.

For each of these reservoir characterizations, we can compute as described previously, the expected, the minimum and the maximum total production rates. In addition, to each one of these models we could assign a probability of being the correct one. This probability should be the result of other geological information available at hand as well as the plausibility of the values of the estimated parameters.

In a nutshell, given the expected, minimum and maximum total oil production rates, $Q_{o,\,tot}^{(r)}$, $Q_{o,\,tot,\,min}^{(r)}$, $Q_{o,\,tot,\,max}^{(r)}$ and the prior probability, $P_b(r)$ for the r^{th} model to be the correct one, we can estimate the expected overall field production rate from:

$$E[Q_{o,tot}(t)] = \sum_{r=1}^{N_m} P_b(r)\, Q_{o,tot}^{(r)} \tag{5.19}$$

$$E[Q_{o,tot,min}(t)] = \sum_{r=1}^{N_m} P_b(r)\, Q_{o,tot,min}^{(r)} \tag{5.20}$$

$$E[Q_{o,tot,max}(t)] = \sum_{r=1}^{N_m} P_b(r)\, Q_{o,tot,max}^{(r)} \tag{5.21}$$

where N_m is the number of the alternate models. The above computed min/ max limits represent the (1-a)% confidence intervals when all plausible reservoir descriptions are taken into account. As described previously, one can compute the risk level α to meet a certain to meet a certain desired production level.

5.5 Convergence Testing of the Proposed Algorithm in Chemical Kinetic Models.

A more thorough investigation was attempted in order to ascertain the convergence behaviour of the Gauss-Newton method, using chemical kinetic models. It was also of great interest to compare the Gauss-Newton method (Gradient technique), with the Annealing method, which can be categorized under the Direct search methods.

The problems that have been employed were based on typical chemical engineering processes, used by Kalogerakis and Luus (1983).

5.5.1 Example 1

This example addresses the pyrolytic dehydrogenation of benzene to diphenyl and triphenyl:

$$2C_6H_6 \rightarrow C_{12}H_{10} + H_2$$

$$C_6H_6 + C_{12}H_{10} \rightarrow C_{18}H_{14} + H_2$$

The two parameter model,initially proposed by Hougen and Watson (1948) is described by the following equations:

$$\frac{dx_1}{dt} = -r_1 - r_2 , \qquad x_1(0) = 1 \tag{5.22}$$

$$\frac{dx_2}{dt} = \frac{r_1}{2} - r_2 , \qquad x_2(0) = 0 \tag{5.23}$$

where:

$$r_1 = k_1 \left[x_1^2 - x_2 \frac{2 - 2x_1 - x_2}{3k_1} \right] \tag{5.24}$$

$$r_2 = k_2 \left[x_1 x_2 - (1 - x_1 - 2x_2) \frac{2 - 2x_1 - x_2}{9k_2} \right] \tag{5.25}$$

with x_1 and x_2 being the pound moles of benzene and diphenyl per pound-mole of pure benzene feed. The parameters k_1 and k_2 are to be obtained by minimizing the deviation of the simulated estimates of the system variables, from the experimental measurements. The optimum values of parameters k_1 and k_2 are found to be 355 and 401 respectively, in only four iterations. Figure 5.1 presents the confidence intervals of the simulated variables x_1 and x_2 for the converged values of the parameters k_1 and k_2. From the graph it is apparent that the upper and the lower boundary of the simulated variables approach asymptotically the experimental data curve, as time progresses. This kind of behaviour is an indication that the model has reached the steady state. It can be also seen that the match between the experimental measurements and the simulated variables is perfect.

The same problem was solved by using a Simulated Annealing Method. The algorithm converged to almost the same values of the parameters k_1 and k_2 (355.1 and 402), but it was significantly demanding in computation time. Figure 5.2 shows a scatter plot of the parameter values estimated by the Annealing method. It also illustrates the approximate region of convergence in the k_1 - k_2 plane. Figure 5.3 shows the surface plot of the objective function (sum of square of errors) for approximately the same region of convergence of the parameters. The local minima of the objective function could potentially be regions of convergence. In order to overcome such problems different initial values of the parameters were examined when the Gauss-Newton method was used. The latter method converged to the optimum values of the parameters from different initial guesses, but the further the starting values were from the optimum the more iterations were required, until the convergence criteria were met.

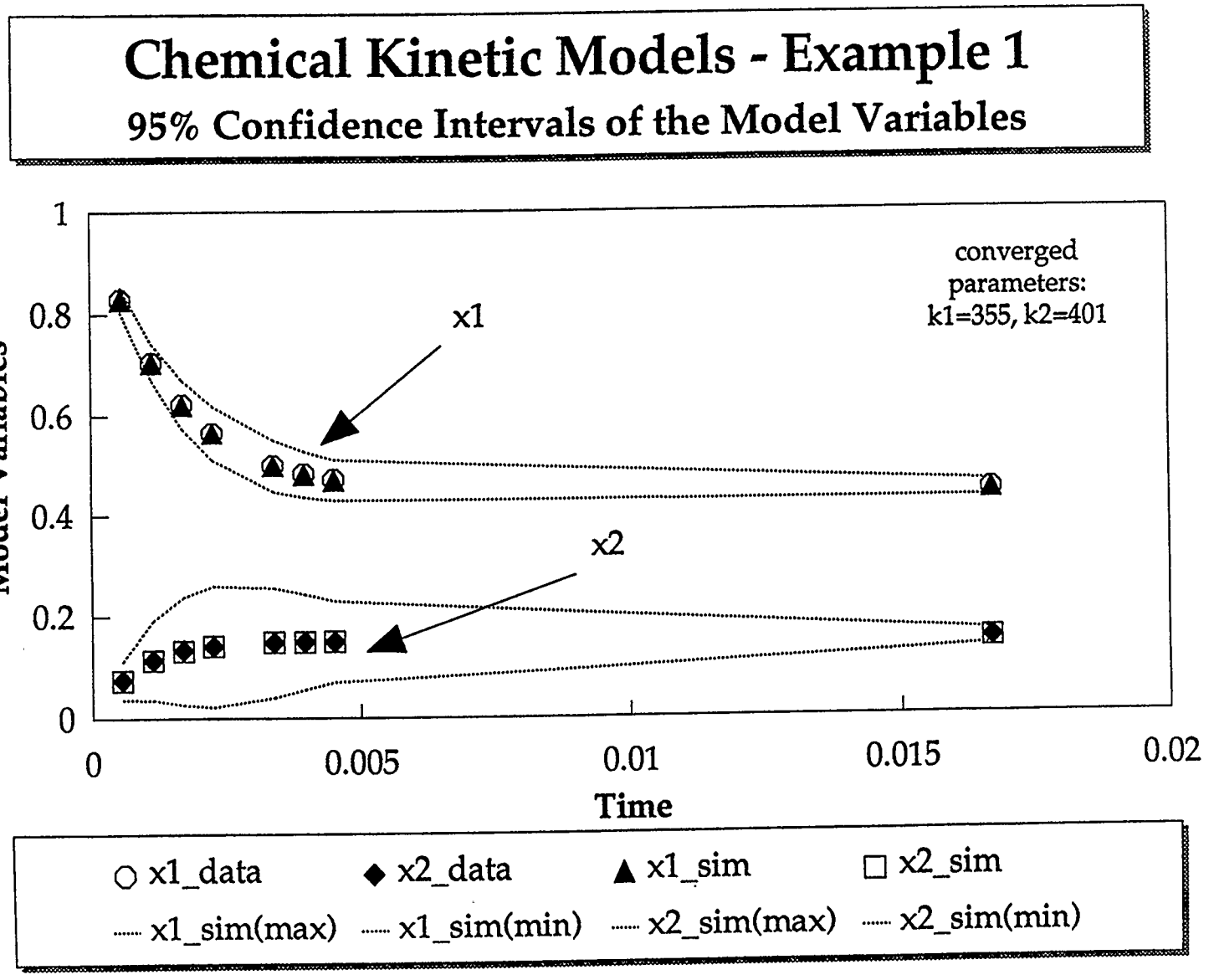

Figure 5.1 Chemical Kinetic Models - Example 1.
95% Confidence Intervals of the Model Variables

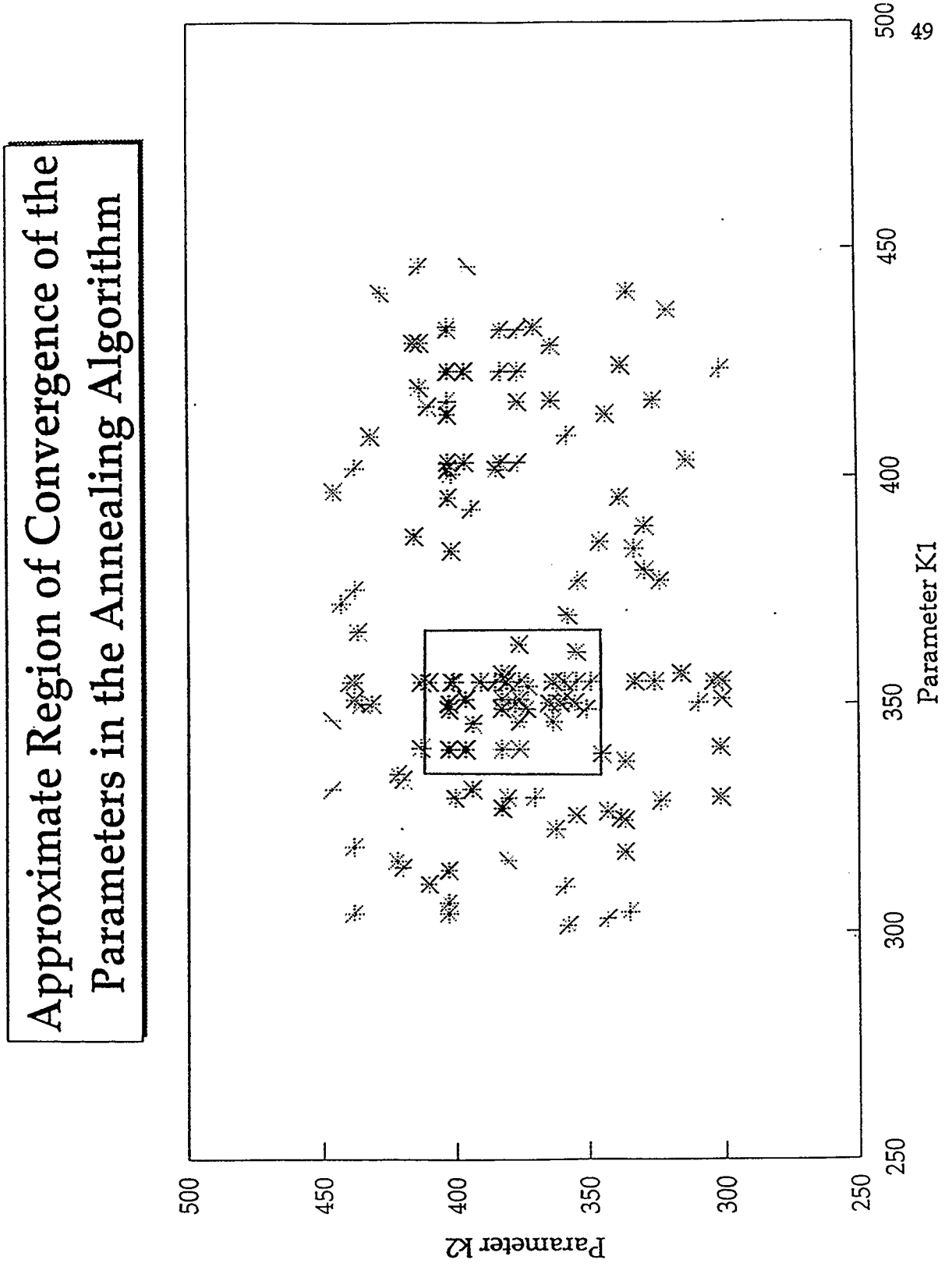

Figure 5.2 Approximate Region of Convergence of the Parameters, by Annealing method.

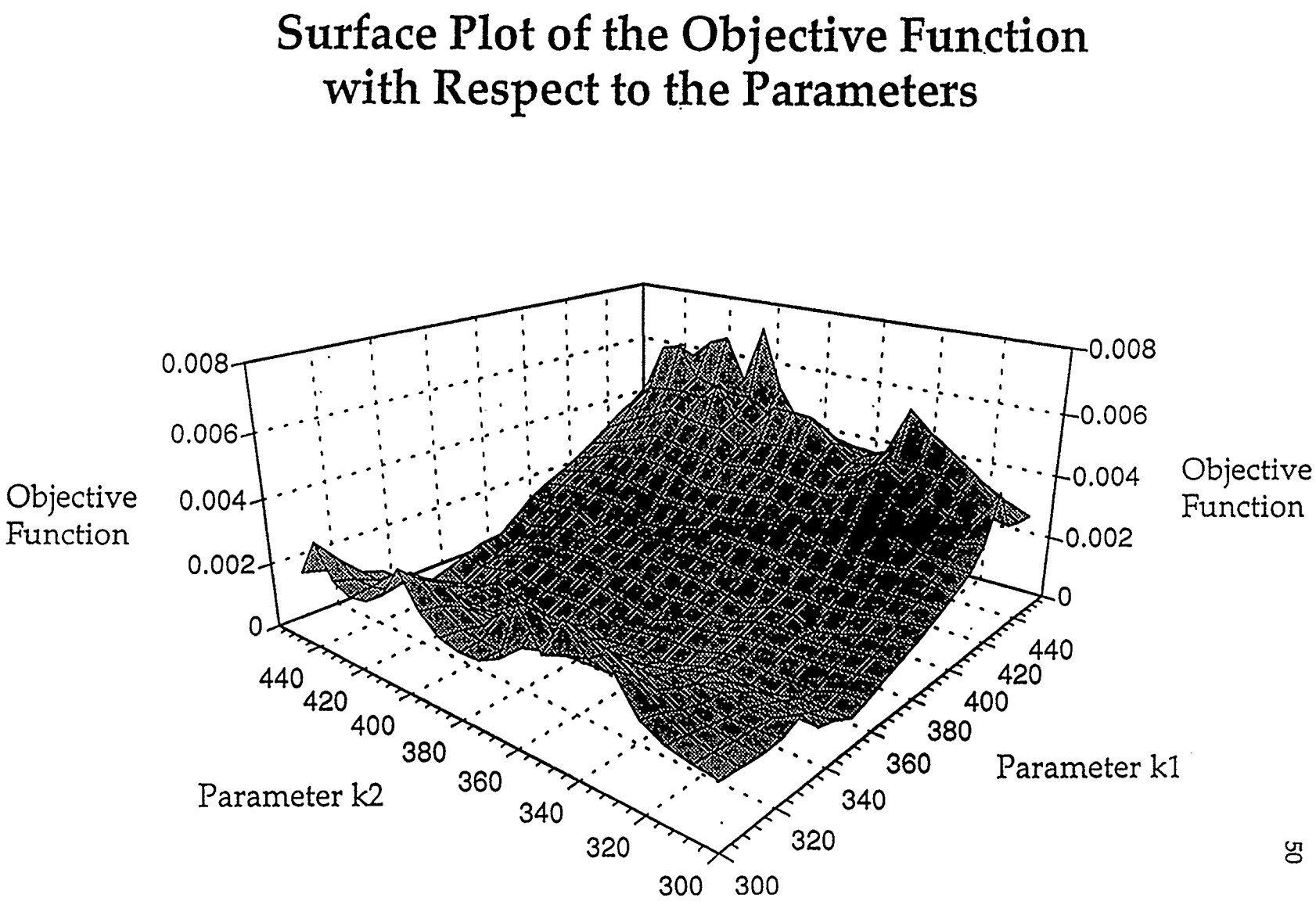

Figure 5.3 Surface Plot of the Objection Function, by Annealing Method.

5.5.2 Example 2

An isothermal CSTR with complex reactions used by Lapidus and Luus (1967) and Rao and Luus (1972) for optimal control studies is the second example. The five parameter model is described by the following equations:

$$\frac{dx_1}{dt} = k_5 - qx_1 - k_1x_1x_2 - k_4x_1x_6\sqrt{0.9}\,, \qquad x_1(0) = 0.1883 \tag{5.26}$$

$$\frac{dx_2}{dt} = 7.0 - qx_2 - k_1x_1x_2 - 2k_2x_2x_3\,, \qquad x_2(0) = 0.2507 \tag{5.27}$$

$$\frac{dx_3}{dt} = 1.75 - qx_3 - k_2x_2x_3\,, \qquad x_3(0) = 0.0476 \tag{5.28}$$

$$\frac{dx_4}{dt} = -qx_4 + 2k_1x_1x_2 - k_3x_4x_5\,, \qquad x_4(0) = 0.0899 \tag{5.29}$$

$$\frac{dx_5}{dt} = -qx_5 - 3k_2x_2x_3 - k_3x_4x_5\,, \qquad x_5(0) = 0.1804 \tag{5.30}$$

$$\frac{dx_6}{dt} = -qx_6 + 2k_3x_4x_5 - k_4x_1x_6\sqrt{0.9}\,, \qquad x_6(0) = 0.1394 \tag{5.31}$$

$$\frac{dx_7}{dt} = -qx_7 - 2k_4x_1x_6\sqrt{0.9}\,, \qquad x_7(0) = 0.1046 \tag{5.32}$$

where:

$$q = 8.75 + k_5 \tag{5.33}$$

The values of the parameters, initially assumed are, k_1=17.6, k_2=73.0, k_3=51.3, k_4=23.0 and k_5=6.0. Using these values, synthetic measurements of the observed variables were obtained by integrating the above equations. Two study cases were examined. In the first all the model variables were matched, while in the second we pretended that only four variables were observed (y_1 , y_4 , y_5 , y_6). In the last case the variables are presented in Fig. 5.4.

In the first case the Gauss_Newton converged after 15 iterations to the correct values of the parameters. Due to the increased number of the unknown parameters the method was more computationally demanding than in the first example. Also the more the variables one attempts to match the better the solution he gets, but the solution is harder to find. In all the study cases the initial values of the parameters where generated by:

$$k^{(o)} = \left[I + \alpha E_i\right] k^*, \qquad (i = 1,2,...,6) \tag{5.34}$$

where E_1=diag(1,1,1,1,1), E_2=diag(1,1,1,1,1), E_3=diag(1,1,1,1,1), E_4=diag(1,1,1,1,1), E_5=diag(1,1,1,1,1), E_6=diag(1,1,1,1,1) and the maximum value of α denotes the region of convergence along the chosen direction (given by the E_i terms). Figure 5.5 presents the 95% confidence intervals of the matched variables for the first study case. The convergence behaviour of the Gauss-Newton method, in the second case study, along six different directions is presented in Table 5.1. The results in Table 5.1 are identical with the ones presented by Kalogerakis and Luus (1983). Finally the annealing algorithm has also converged to the optimum values of the parameters. All the methods reduced the objective function (sum of squares of errors) to values close to $0.79x10^{-09}$.

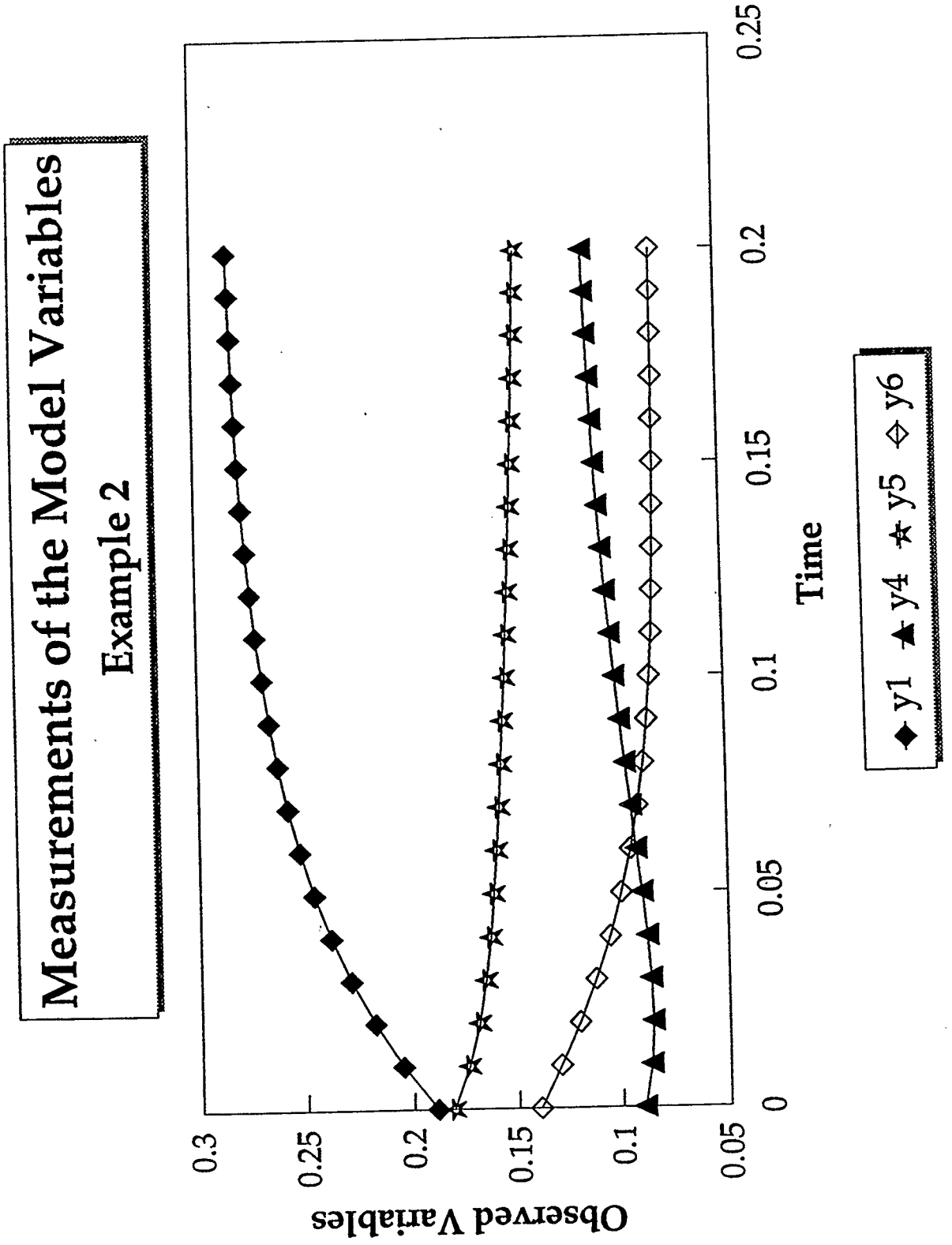

Figure 5.4 Simulated Measurements of the Model Variables Example 2

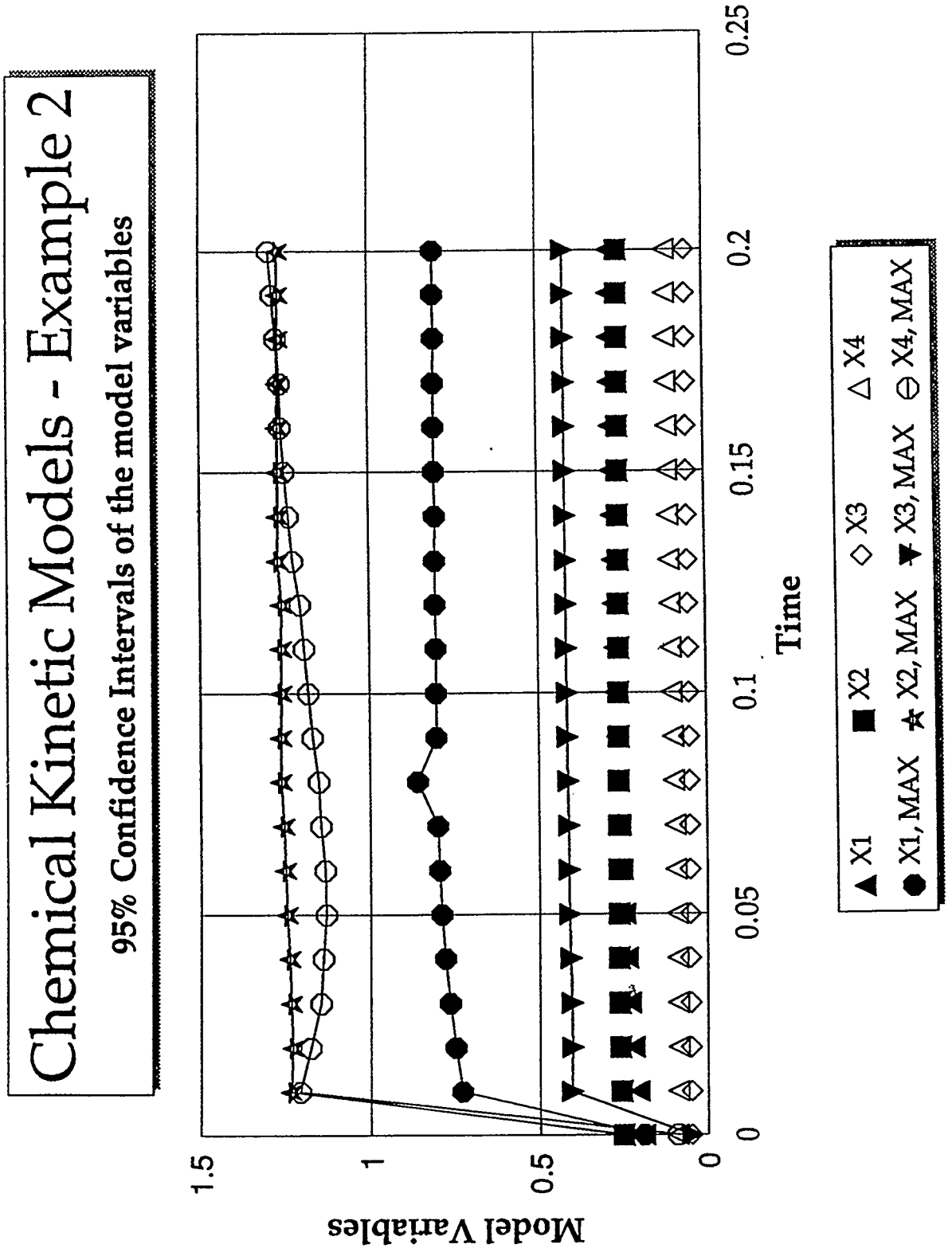

Figure 5.5 95% Confidence Intervals of the Model Variables for Example 2

Table 5.1: Region of Convergence of the Gauss-Newton Method - Example # 2

Direction	α	Number of iterations
(1., 1., 1., 1., 1)	15	10
(1., .1, .1, .1, .1)	160	11
(.1, 1., .1, .1, .1)	290	16
(.1, .1, 1., .1, .1)	310	18
(.1, .1, .1, 1., .1)	70	9
(.1, .1, .1, .1, 1)	10	9

5.5.3 Summary

Two methods of optimization were compared, using simple chemical kinetic models. Both methods converged to the optimum values of the parameters for the problems tested. The Gauss-Newton method exhibits quadratic convergence and the region of convergence appears to be the same as the one found by Kalogerakis and Luus (1983). Also the 95% of the confidence intervals of the model variables were estimated, using statistical information obtain by the Gauss-Newton method.

The Simulated Annealing method, as a global optimization method, overcomes the limitations of the gradient methods (when the initial guesses of the parameters are far from the optimum and regarding the maximum number of the parameters to be estimated). Nevertheless the CPU requirements were found to be one order of magnitude greater from the one of the Gauss Newton method, even though the Simulated Annealing method does not require the computation of the sensitivity coefficients. This was expected since the Simulated Annealing searches the whole parameter space and the search method is random. Using annealing for providing initial estimates of the parameters for the Gauss-Newton method seems to combine the advantages of both worlds. Such an approach would be numerically stable and computationally efficient. Development of computers with parallel computing capa-

bilities will make methods, like Simulated Annealing, genetic algorithms, neural network and tabu search more attractable

The confidence on the predicted model variables depends on the number of the unknown parameters. The bigger the number the greater the uncertainty of the model predictions.

CHAPTER 6

APPLICATION TO A 5-SPOT SYSTEM

6.1 Introduction

In an attempt to formulate a more realistic matching problem, a finer grid block representation of the reservoir (actual model) is used in order to produce synthetic data, assuming a certain permeability and porosity distribution. These measurements are used by the Automatic History Matching Program to determine porosity and permeability distribution of a simplified model of the reservoir (postulated model). This approach enables us to examine the effect of approximating porosity and permeability distributions, encountered in an actual reservoir with much simpler reservoir models. After determining the values of the parameters, the 95% confidence intervals are estimated, using the parameter covariance matrix, Cov(k).

6.2 Overview of the Actual Model

This example is similar to the problem described by Jahns (1966). The actual model is comprised by a 11 x 11 x 2 grid block system, which is shown schematically in Fig. 6.1. As seen the actual model, is a typical 5-spot pattern and has three zones of constant permeability and porosity. The shadowed area represents the quarter element of symmetry. This was done in an effort to decrease the computational time.

The PVT data were taken from a typical Alberta heavy oil. Table 6.1 presents the formation volume factors (Bo, Bg, Rs) and the oil and gas viscosity with respect

to pressure. The relative permeability curves of the actual model are shown in Figure 6.2.

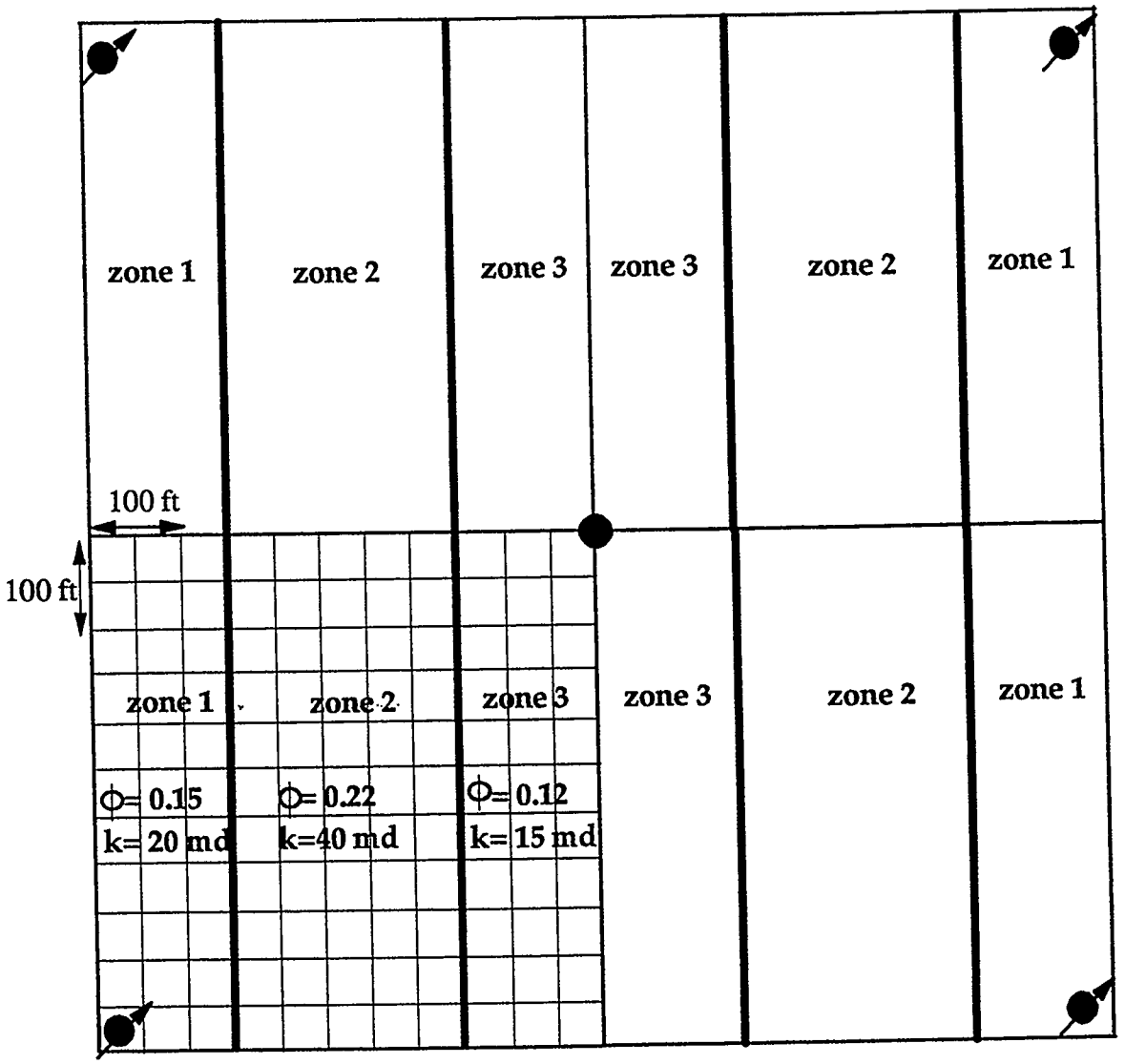

Figure 6.1 Grid Block Representation and the Zonation Used for the Actual Model.

Table 6.1 : PVT Data of the Actual Model.

Pressure psia	Rs scf/bbl	Bo bbl/bbl	1/Bg scf/bbl	Oil viscosity cp	Gas viscosity cp
14.70	1.4678	1.01867	5.22	79.037	0.00816
300.00	39.7366	1.03585	114.45	48.627	0.00947
400.00	54.4297	1.04245	156.57	41.750	0.00996
500.00	69.4747	1.04921	200.94	36.235	0.01045
600.00	84.8061	1.05609	247.70	31.762	0.01097
800.00	116.1640	1.07017	348.93	25.053	0.01203
1000.0	148.2730	1.08459	460.88	20.349	0.01315
1200.0	180.9937	1.09929	582.95	16.927	0.01432
1400.0	214.2314	1.11421	712.48	14.359	0.01553
1600.0	247.9185	1.12934	844.51	12.380	0.01679
1800.0	282.0035	1.14465	972.69	10.820	0.01807
2200.0	351.2130	1.17573	1197.4	8.544	0.02074

The wells are operated under different operating constraints, like maximum bottom hole pressure, minimum oil production rate and maximum injection pressure. The injector is completed in the lower layer while the producer in the upper one. This completion strategy was adopted in order to maximize the total oil recovery.

For history matching purposes we assumed that production data were available for the first 1096 days (about three years). The actual model was used to generate artificial observations (monthly) which were subsequently corrupted by Gaussian noise, simply by adding random generated numbers of small magnitude to the model variables. All the assumed models were simulated by employing quarter

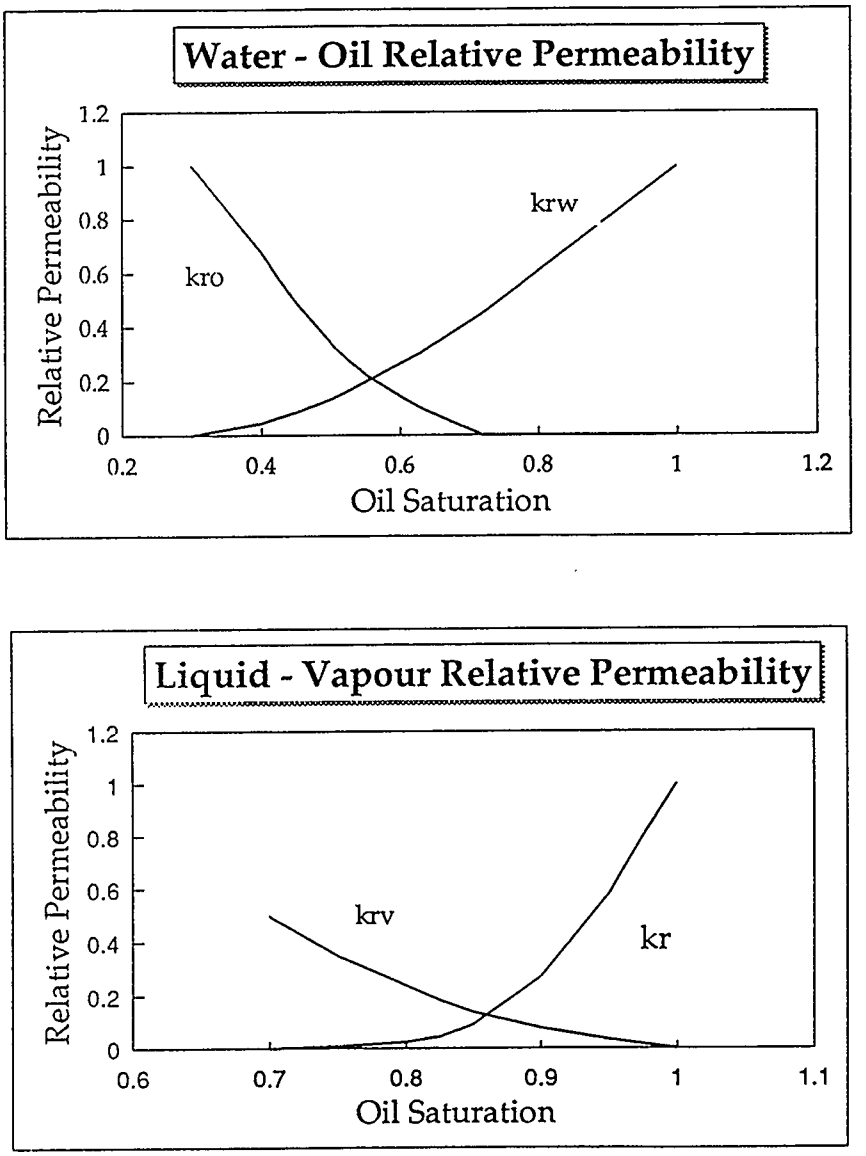

Figure 6.2 Relative Permeability Curves of the Actual model

element of symmetry.

In reservoir simulation, one of the most difficult numerical problems associated with the displacements under unfavourable mobility ratios[2], is the grid orientation effect. The grid orientation effect results from one of the common assumptions in a reservoir simulator, that the flow does not occur diagonally between grid blocks. Such a supposition has severe repercussions, since the shape of the displacement front is distorted and no longer radial. Several methods have been reported in the literature for reducing the grid orientation effect (Settari 1993). In all models considered in this project the grid orientation effect was assumpted negligible.

6.3 Overview of the Postulated Models A & B.

As postulated models we consider a $11x11x1$ reservoir, which is shown in Figures 6.3 and 6.4. As seen both models have the same grid block dimensions, but different zonation of porosity and permeability distribution. Model A has two zones, thus the number of the unknown parameters is four. Model B has three zones and therefore six parameters. Both models have only one layer and the PVT data are exactly the same as the ones in the actual model. The wells are operated under pressure and production constraints and a skin factor has been introduced to the producer due to partial penetration .

By employing the Automatic History Matching for each of the postulated models, we were able to estimate the values of the unknown parameters. The converged values of the porosity and the permeability of each zone, for both models, are presented in Table 6.2.

[2]Mobility ratio is defined as the mobility of the displacing phase divided by that of the displaced phase

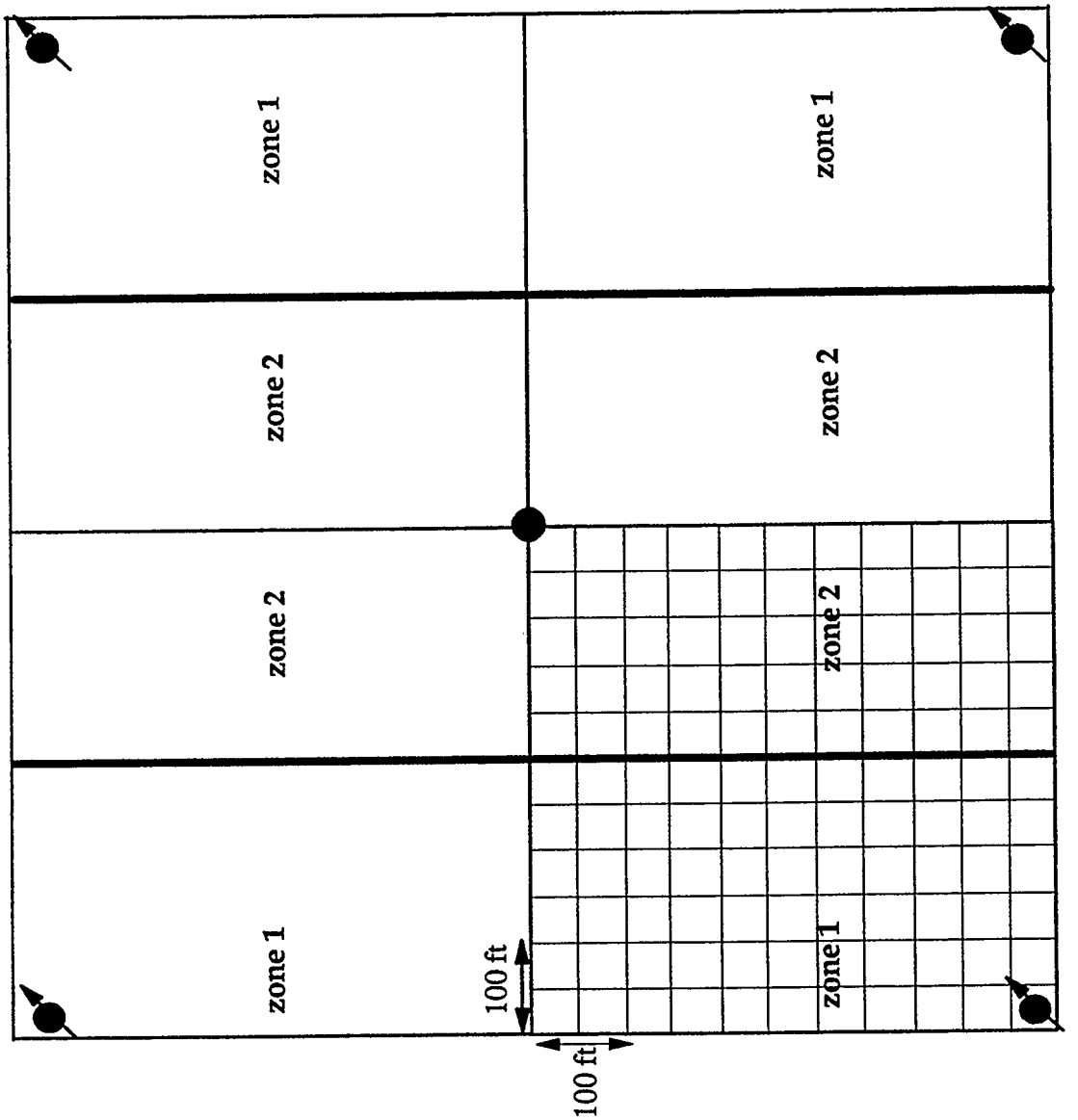

Figure 6.3 Grid Block Representation and the Zonation used in the Postulated Model A.

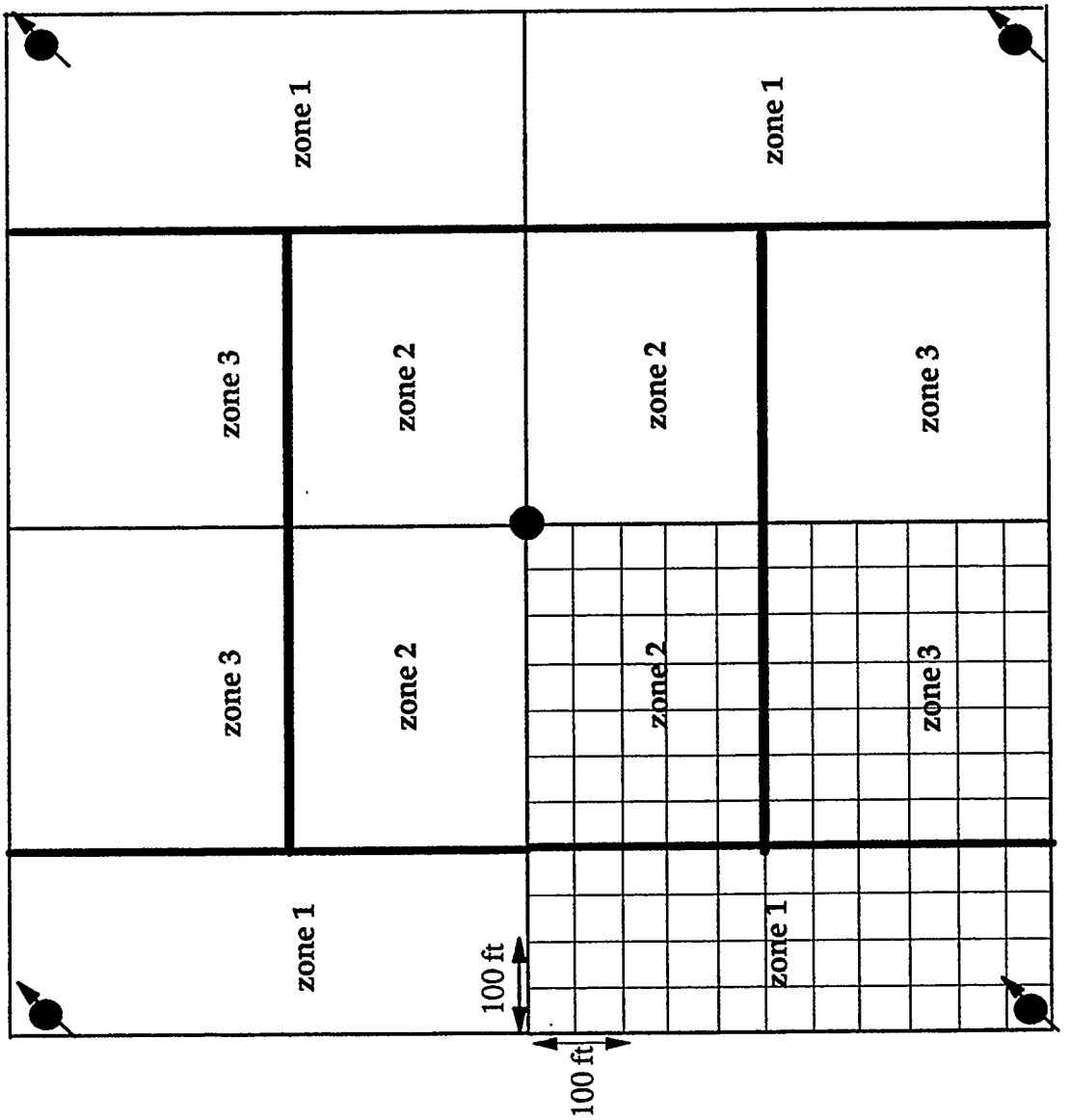

Figure 6.4 Grid Block Representation and Zonation used in the Postulated Model B.

Table 6.2 Converged Values of the Parameters for the Postulated Models.

Postulated Model A			Postulated Model B	
Zone	Porosity	Permeability (md)	Porosity	Permeability (md)
#1	0.23	16.0	0.24	16.6
#2	0.13	22.1	0.31	28.8
#3	-	-	0.07	16.3

The quality of the obtained match for the oil, gas and water production rates of the model A is presented in Figure 6.5.

Once the parameter covariance Cov(k) has been calculated, we can perform one pass with the simulator to determine the 95% confidence intervals. The 95% confidence intervals of the Model A for the cumulative oil, gas and water production are presented in Figures 6.6 and 6.7 and for the Model B in Figures 6.8 and 6.9. From the preceding figures it is evident that the error boundaries of the forecast, for both models, deviate considerably from the forecasted cumulative production. These confidence intervals incorporate the uncertainty of all the estimated parameters of the postulated models. It was not in our intentions to improve the reservoir characterization. In order to reduce the deviation of the minimum and maximum forecasted performance, one has to incorporate all the available information about the actual model. Data from core analysis, log interpretation, seismic and outcrop studies are crucial, not only to suggest good initial estimates of the parameters to be evaluated, but to better condition the matrix A in Equation 4.11. One can say, as a rule of thumb, that the greater the number of the parameters to be estimated, the wider the bounds between the minimum and maximum of the forecasted production, however we can compensate this effect, by using all the available prior information.

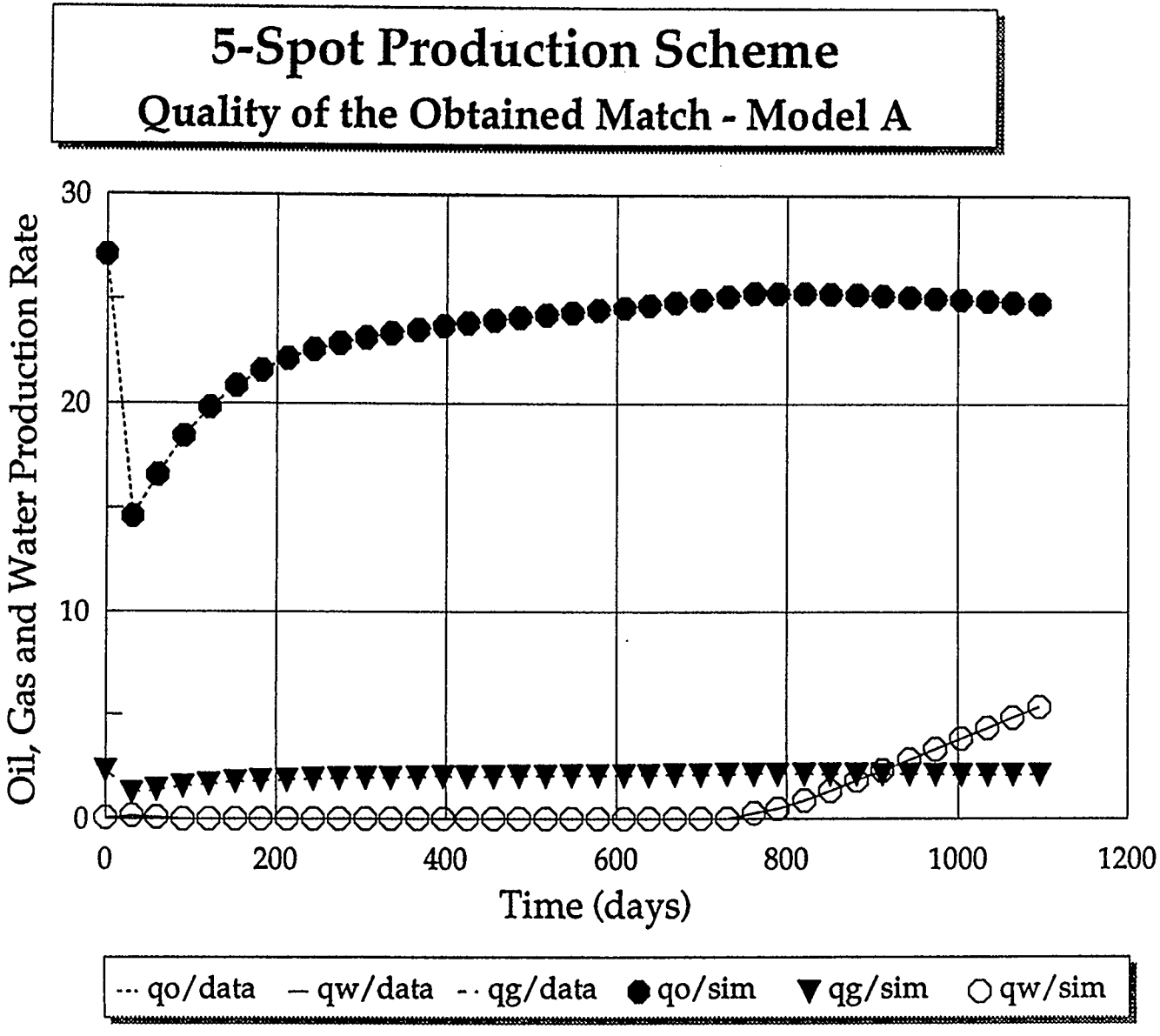

Figure 6.5 Quality of the Obtained Match for the Model A.

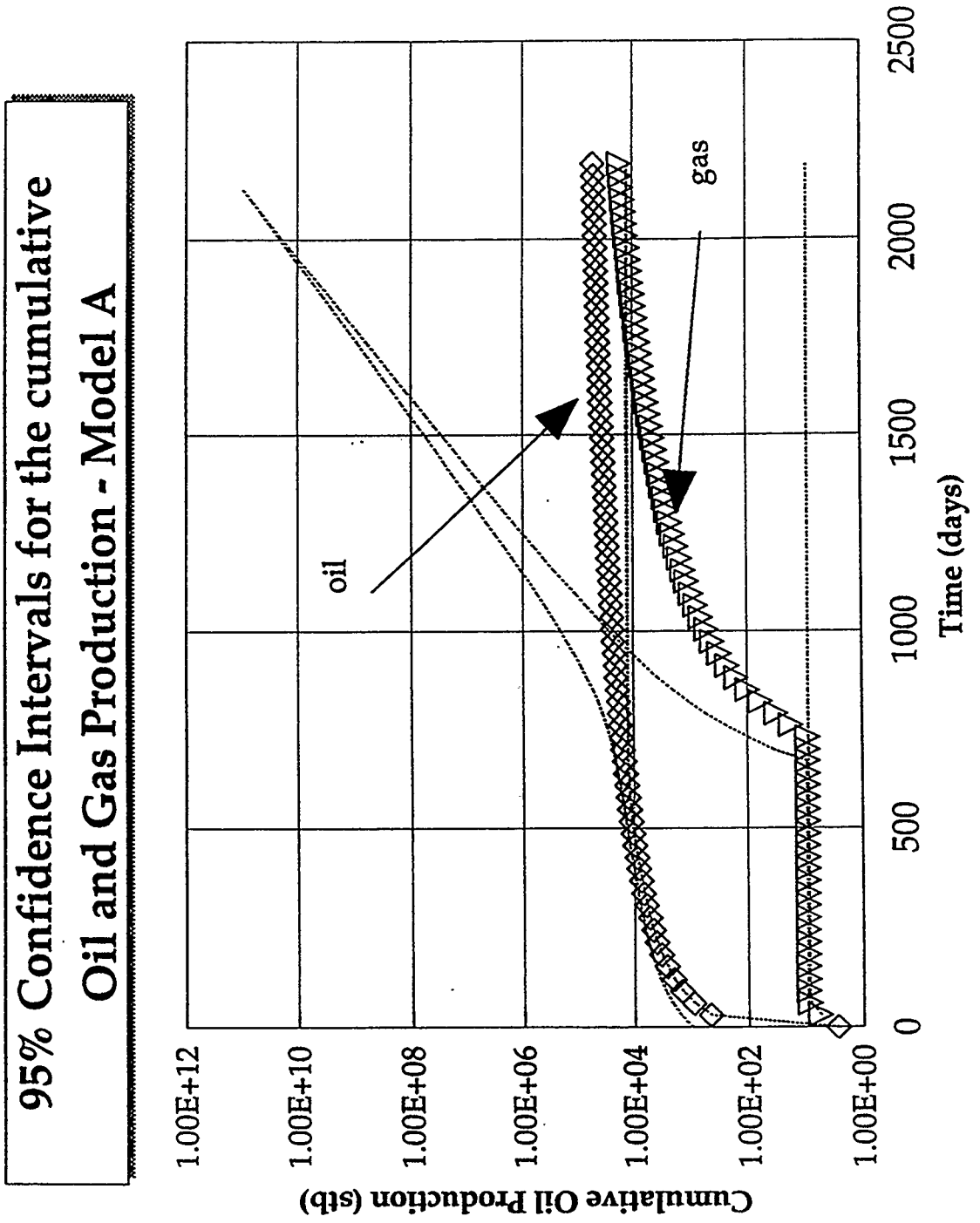

Figure 6.6 95% Confidence Intervals for the Cumulative Oil and Gas Production of Model A.

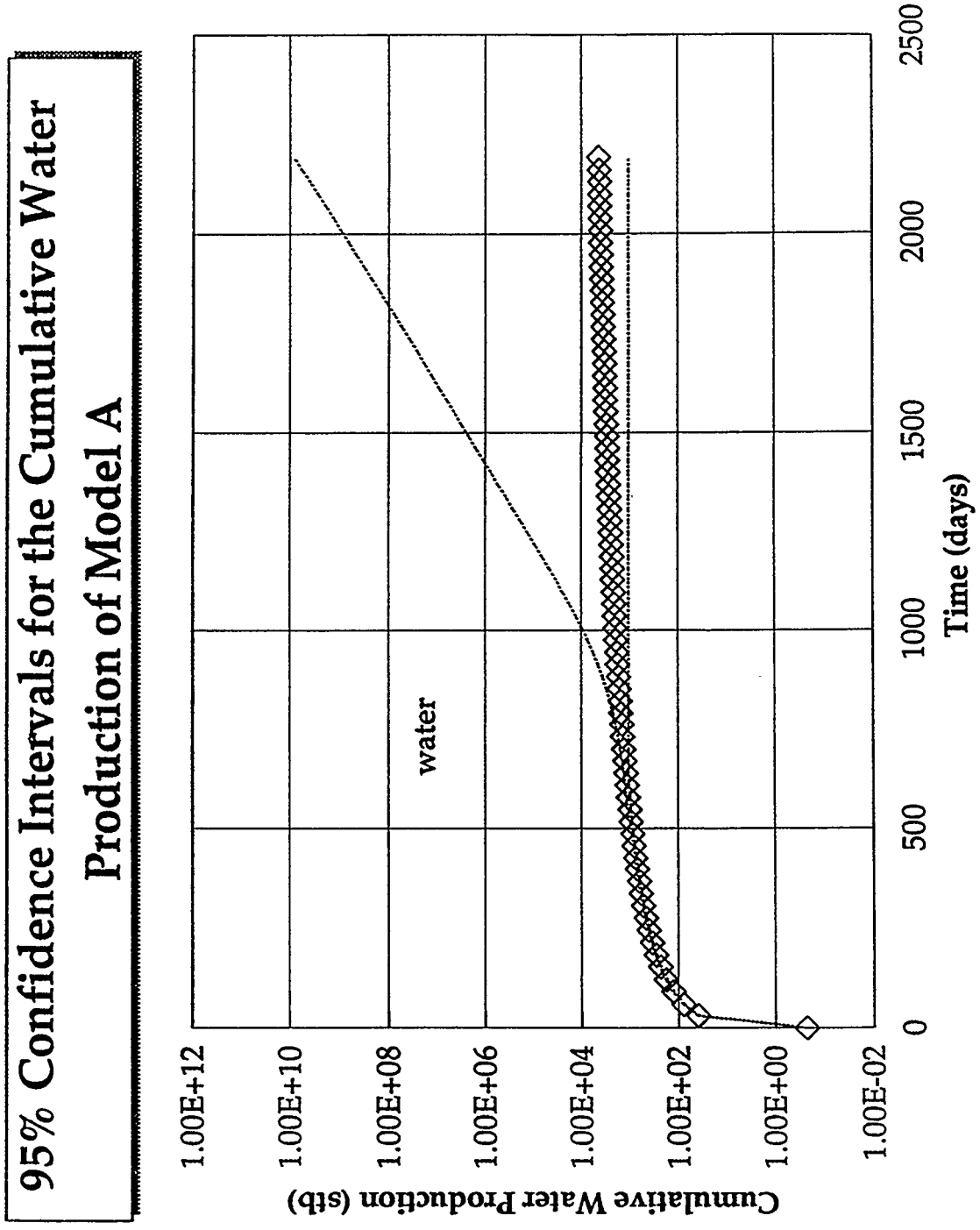

Figure 6.7 95% Confidence Intervals of the Cumulative Production Rate of Water of the Model A.

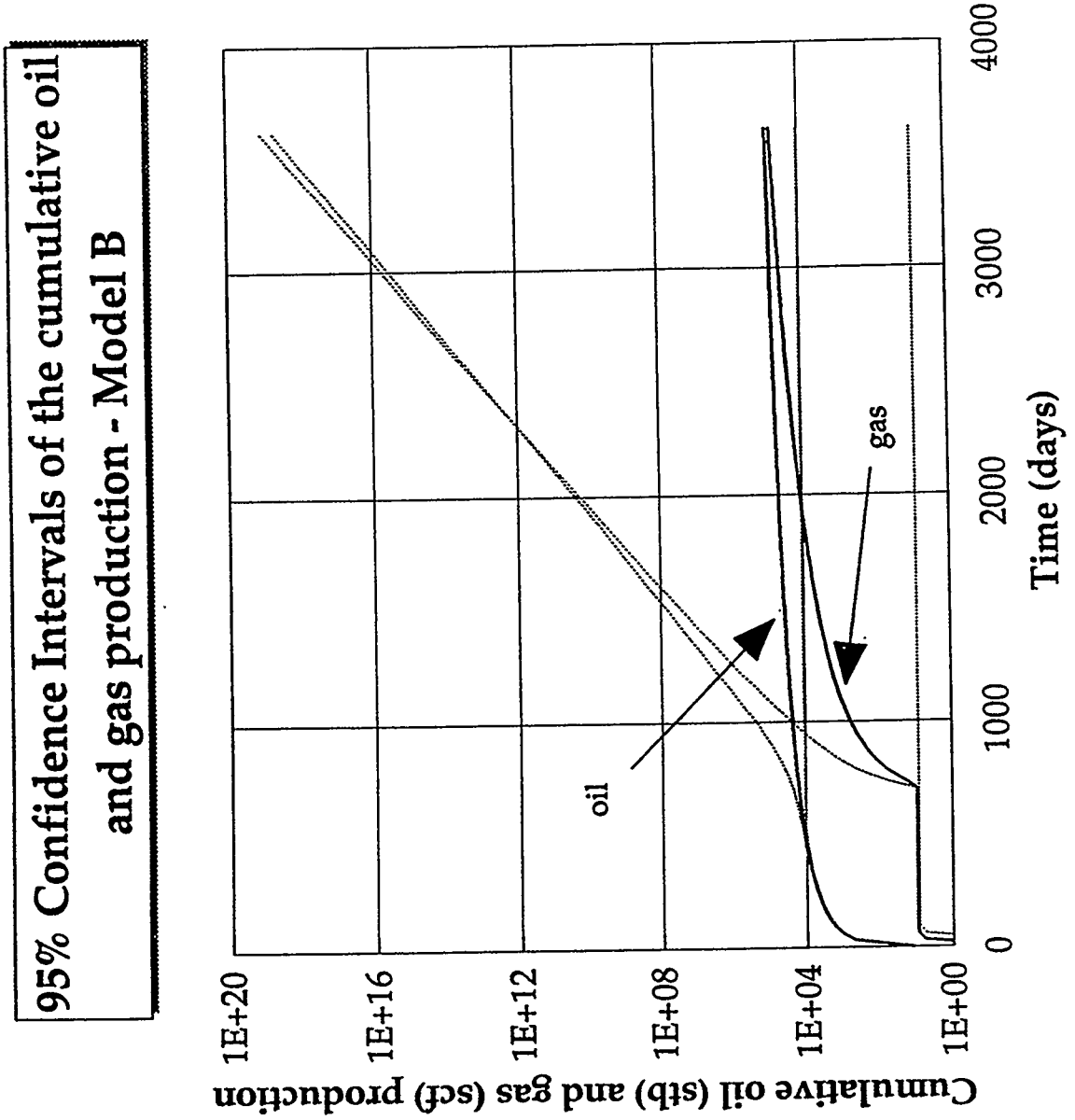

Figure 6.8 95% Confidence Intervals for the Cumulative Oil and Gas Production of the Model B.

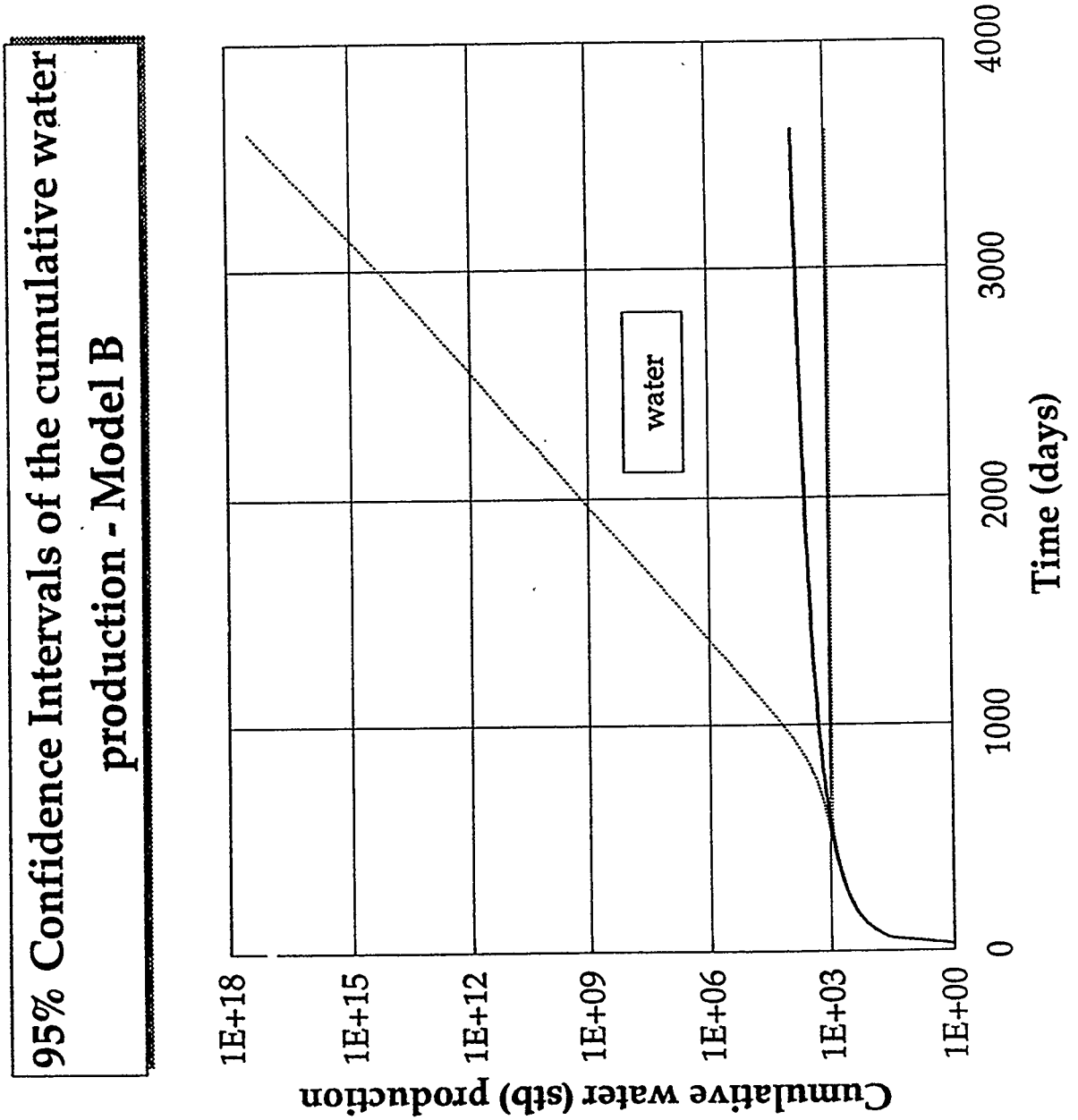

Figure 6.9 95% Confidence Intervals of the Cumulative Production Rate of Water of the Model B.

6.4 Varying the Degree of Implicitness

An attempt was made to determine the effect of the degree of implicitness on the quality of the obtained match and the prediction of the future performance. In order to do so, we ran model B, employing the same converged values of the porosities and the permeabilities, and then we ran the model using the fully implicit and the IMPES formulation. Since IMPES method is unstable for large timesteps, a stability time was calculated using eq. 2.18. The results of the obtained match for the oil production rate are presented in Figure 6.10, varying the degree of implicitness. As seen the obtained match is adequate regardless the discretization method used. Minor improvements in the performance of the preceding models could have been achieved, if the automatic history matching parameters had been changed. However, it was our intention to examine the effect of the degree of implicitness on the same model. Figure 6.11 presents the maximum boundary of the cumulative oil production, using the three methods. It can be seen that the maximum cumulative oil production for the fully implicit and the adaptive implicit model are fairly close together, while the IMPES model exhibits a big deviation after the first one third of the production. On the other hand the minimum oil cumulative production, for all the model, presented in Figure 6.12 doesn't exhibit such deviation. Such behaviour using the IMPES formulation can be attributed to instabilities regarding the calculation of the sensitivity coefficients and not the estimation of the pressures and saturations of each grid block. It should be noted that the model, which is run using the IMPES formulation does not exhibit any instabilities as it is shown in Figure 6.10.

6.5 Varying the Grid Block Dimensions

The effect of the grid block dimensions on the prediction of the future production was also investigated. Figures 6.13 and 6.14 present a comparison of the oil, gas, and water production rates and the 95% confidence intervals of the cumulative oil production for a $4x4$, $6x6$ and $11x11$ grid block system. The converged values porosity and permeability were kept constant. The increase of the grid block dimension was

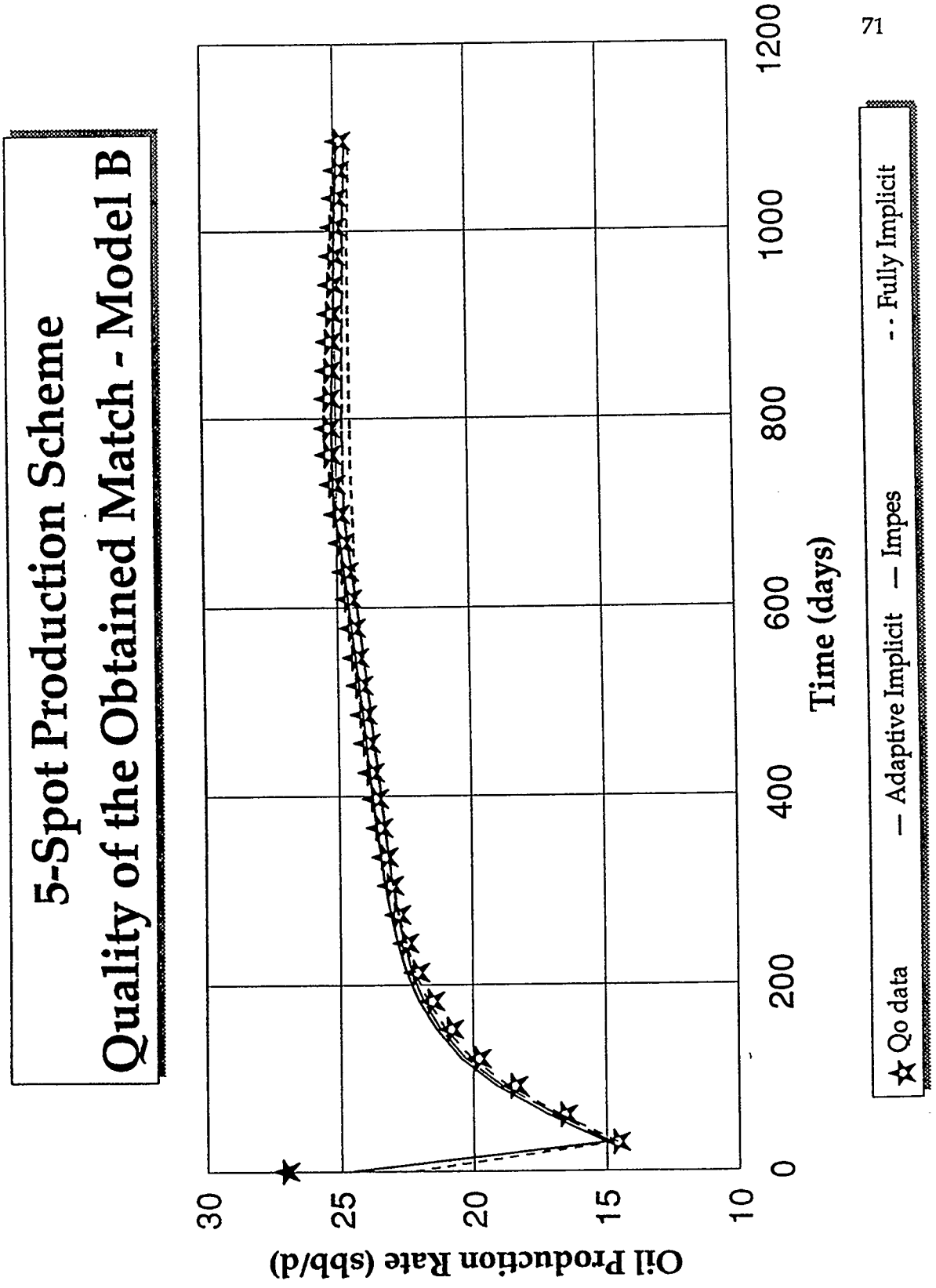

Figure 6.10 Quality of the Obtained Match of the Oil Production Rate Run Model B, Fully Implicit, Adaptive Implicit and IMPES.

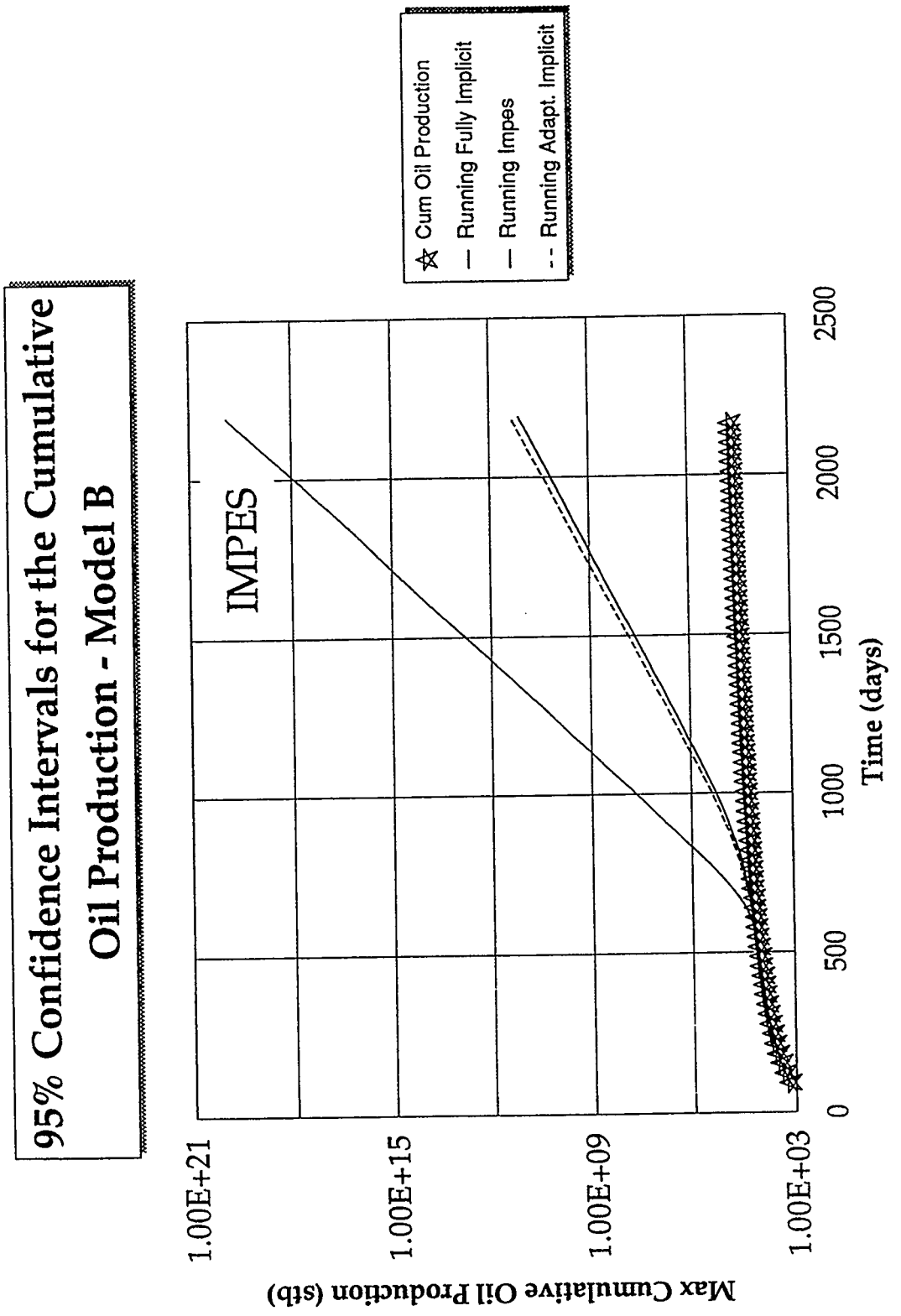

Figure 6.11 Maximum Confidence Intervals for the Cumulative Oil Production of Model B, running Adaptive Implicit, Fully Implicit and IMPES.

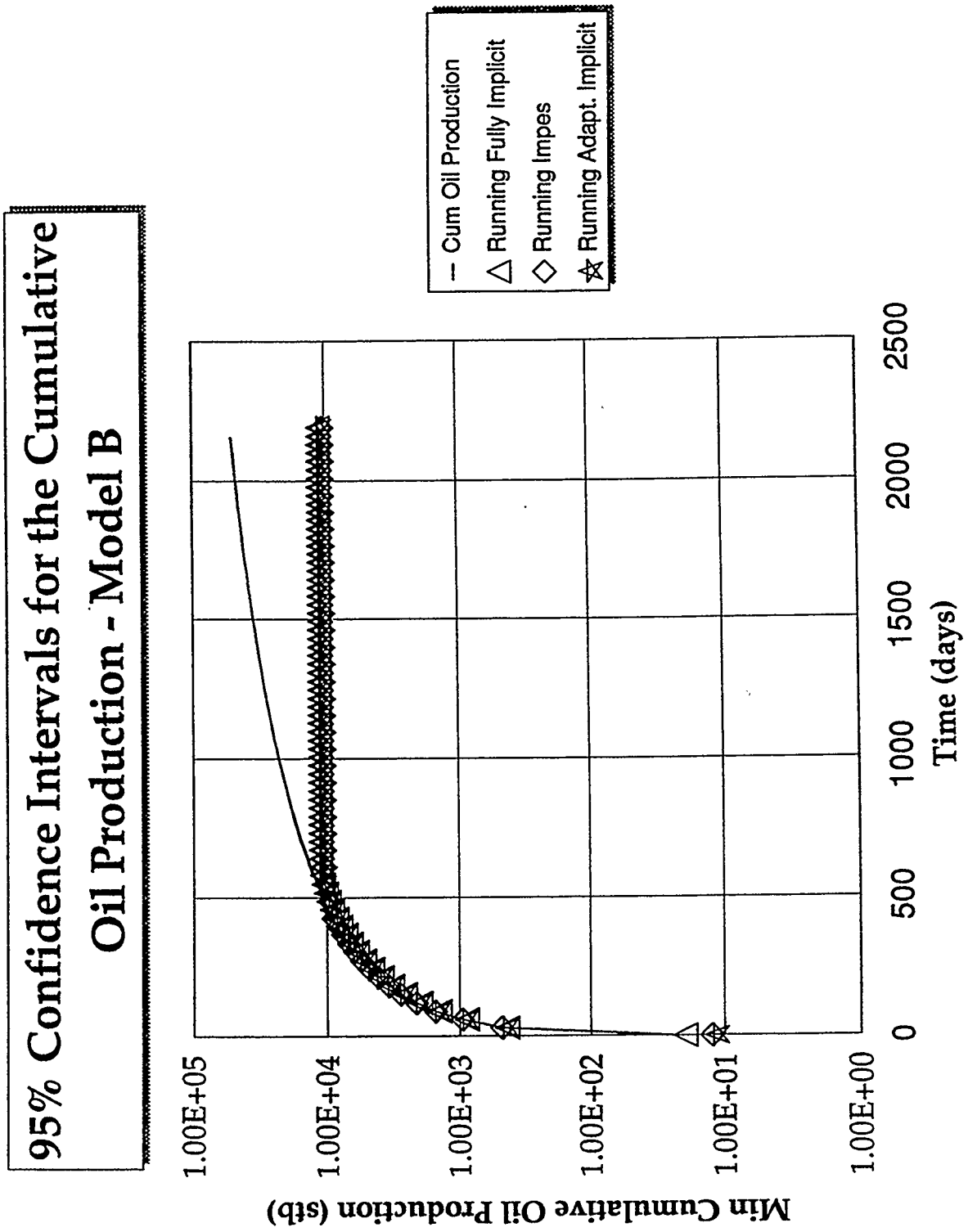

Figure 6.12 Minimum Confidence Intervals of the Cumulative Oil Production of Model B, running Adaptive Implicit, Fully Implicit and IMPES.

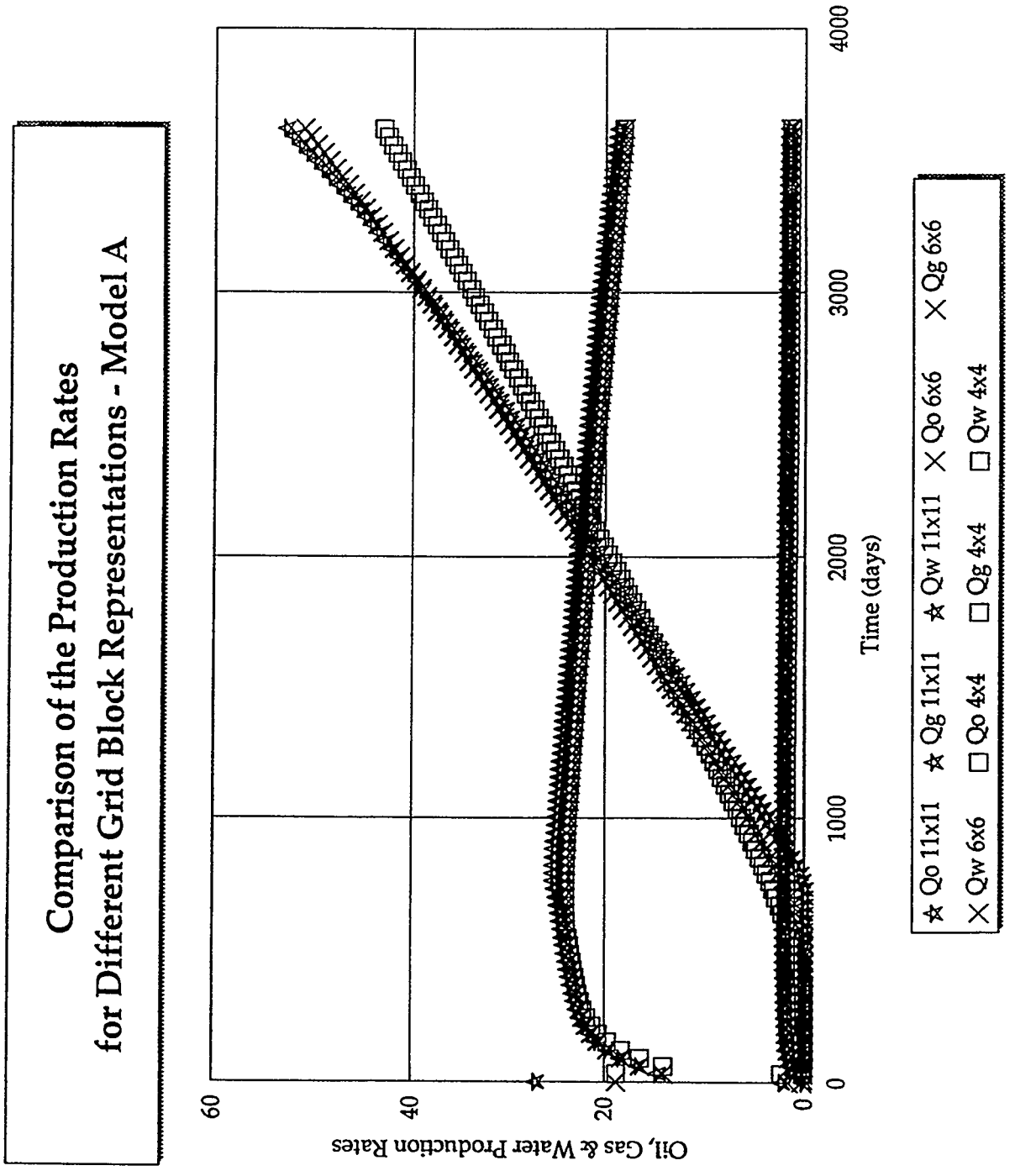

Figure 6.13 Comparison of the Production Rates for Different Grid Block Representations of Model A.

approximately 225% for the 6x6 model and 450% for the 4x4 model. Keeping the parameters constant the sum of square of errors increased as the dimensions of the grid block increased, due to numerical dispersion. Nevertheless the maximum error boundaries of the cumulative oil production rate were smaller as we increased the grid block dimensions. This was caused by averaging saturations over larger areas as we increase the grid block sizes. In fact the earlier breakthrough of the 4x4 model suggests that the bigger the grid block dimensions the less accurate the simulation is. This effect is called *numerical dispersion* and causes the displacement front to smear.

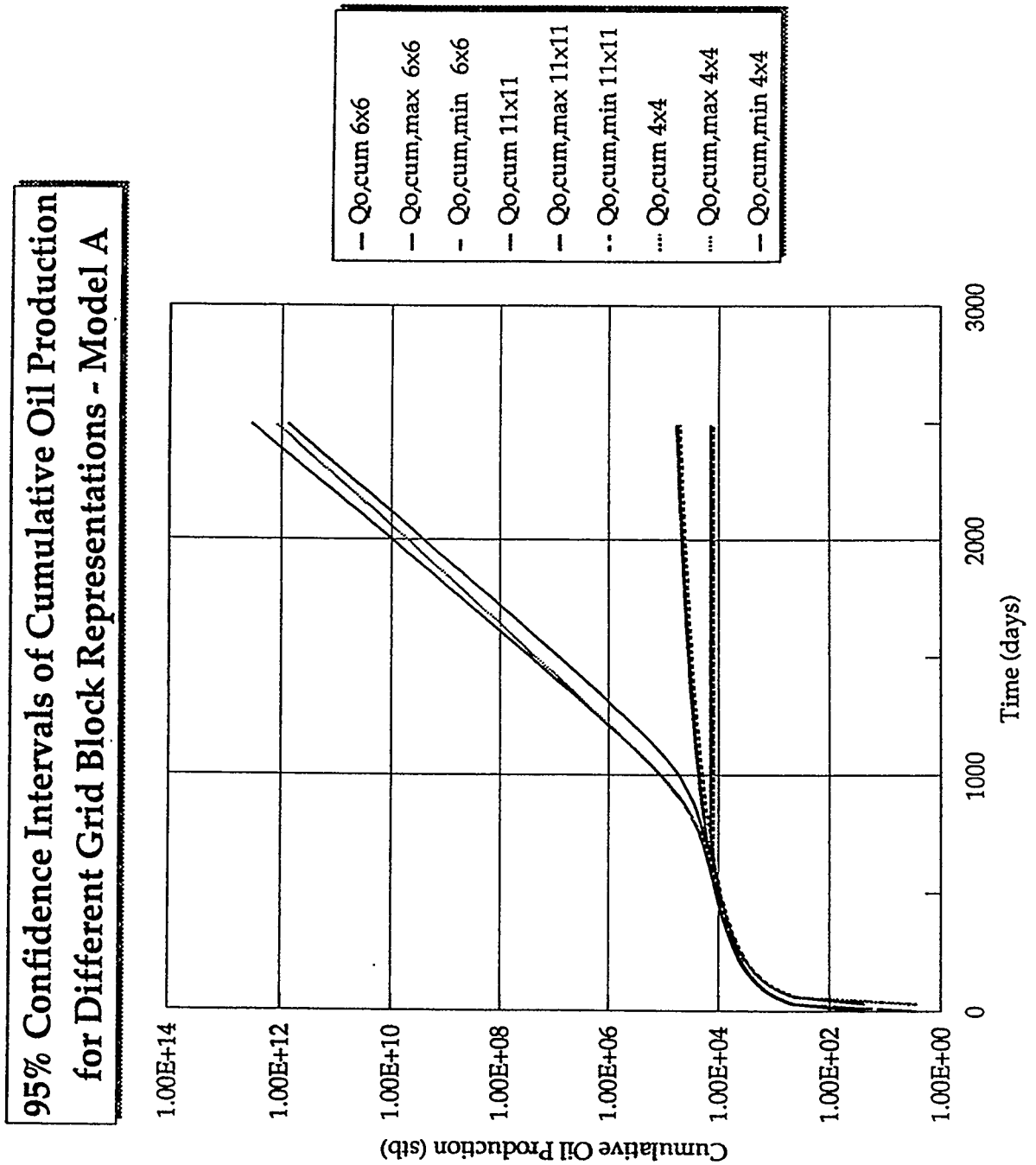

Figure 6.14 95% Confidence Intervals of the Cumulative Oil Production for Different Grid Block Representations of Model A

CHAPTER 7

APPLICATION TO HETEROGENEOUS RESERVOIRS

7.1 Reliability of horizontal well performance

For this case study we have adopted the model, used by Collins et al (1992), to examine the performance of horizontal wells in a thin reservoir where both gas cusping and water conning are important. In the following sections we first use a finer grid representation of the reservoir (the "actual model") in order to produce synthetic data (production rates and bottom hole pressures), which are subsequently used by the automatic history matching program to estimate the porosity and permeability distribution of the reservoir (postulated models) and eventually determine the 95% confidence intervals of the future production rates.

7.1.1 Overview of the Actual Model

The reservoir is comprised by a 10x12x8 grid system. A schematic diagram of the reservoir including grid block dimensions (x, y and z direction) is presented in Figure 7.1. The porosity and permeability distribution of the actual model are presented in Table 7.1 and Figure 7.2, The vertical permeabilities are taken equal to one tenth of the horizontal ones. As Brigham (1990) has shown this level of anisotropy does not necessitate the use of equivalent wellbore radius corrected for anisotropy ($r_{w,eq}$) and therefore the effective drainage radius is taken by the Peaceman's formula. Four injectors have been used at the corners of the reservoir in order to simulate production under an active water drive. All the injectors have been completed at the top 80 ft of the bottom layer.

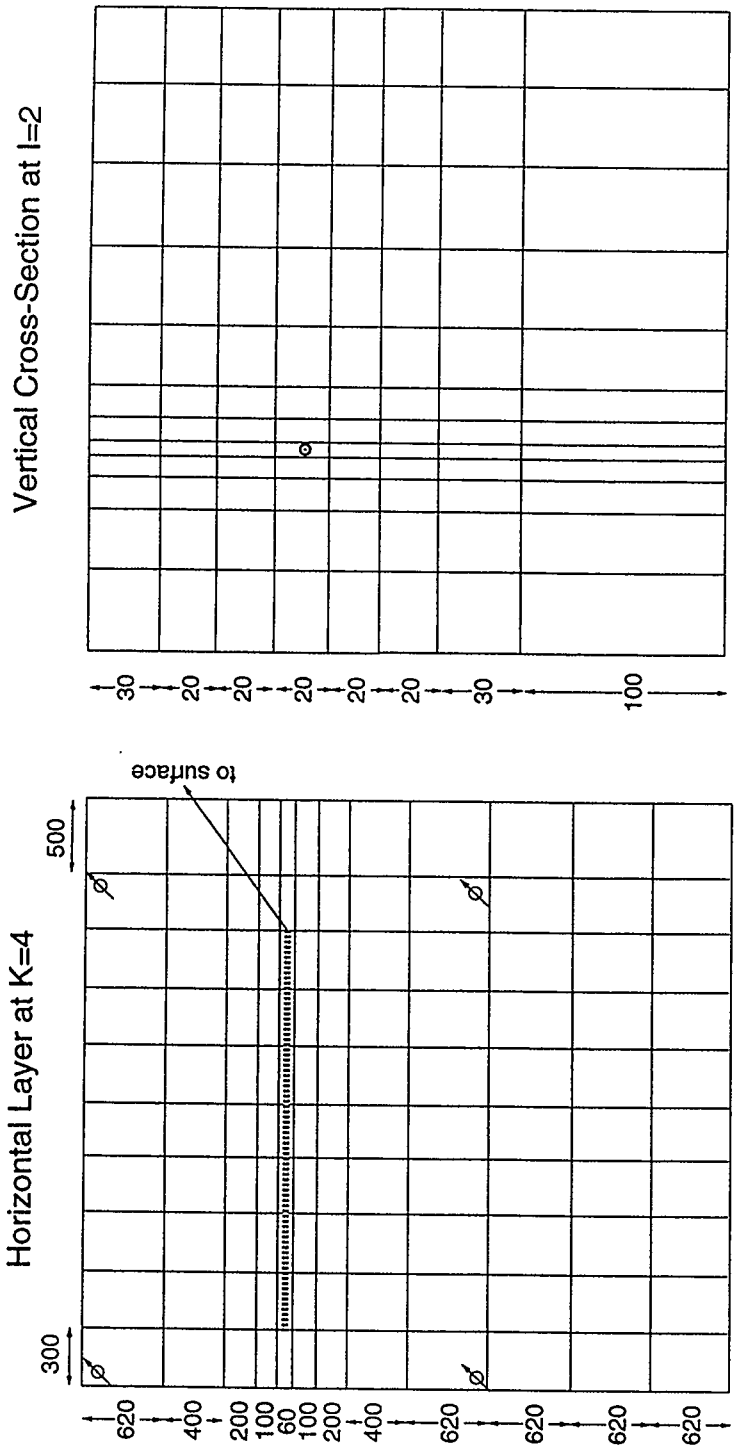

Figure 7.1 Grid Block Representation of the Actual Reservoir: (a)Producer Layer (b) Cross Section

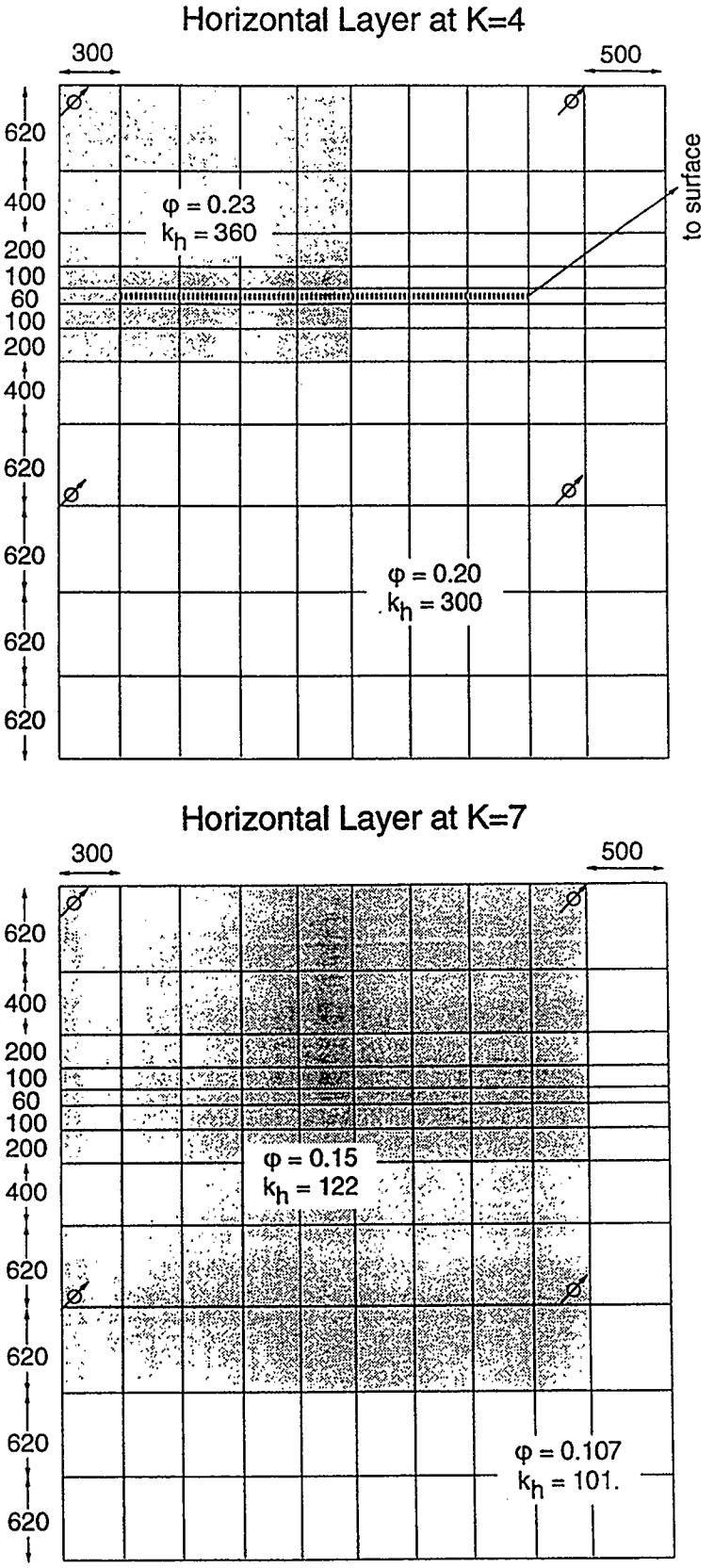

Figure 7.2 Permeability and Porosity Distribution of the Actual Reservoir: (a) Layer 4 and (b) Layer 7

The PVT data , the relative permeabilities and the capillary pressures are those reported by Collins *et al* (1992). Figure 7.3 presents the relative permeability curves assumed in the Actual Model.

Table 7.1: Porosity and Permeability Distribution of the Actual Model from Top to Bottom.

Layer	Thickness (ft)	Porosity*	Permeability (md)*
1	30	0.087 I=1 , J=1,2 0.100	60 I=1 , J=1,2 72
2	20	0.097 I=1,2 J=1,4 0.112	75 I=1,2 J=1,4 90
3	20	0.120 I=1,3 J=1,6 0.138	125 I=1,3 J=1,6 150
4	20	0.200 I=1,5 J=1,7 0.230	300 I=1,5 J=1,7 360
5	20	0.200 I=1,7 J=1,8 0.230	300 I=1,7 J=1,8 360
6	20	0.150 I=1,8 J=1,9 0.172	175 I=1,8 J=1,9 210
7	30	0.107 I=1,9 J=1,10 0.150	101 I=1,9 J=1,10 122
8	100	0.092 I=1,10 J=1,11 0.106	51 I=1,10 J=1,11 62

*The shown values apply to the whole layer expect at the specifies grid blocks for which a different value is provided

The history matching was based on the production and pressure data obtained over the first 1250 days of operation. Gaussian noise with zero mean and variance 1 (stb/d, scf/d and psia) was added to the artificial data, in order to generate more realistic observations. The production rate by the actual model during the next 4 year period was also computed to be compared with the prediction of the history matching models.

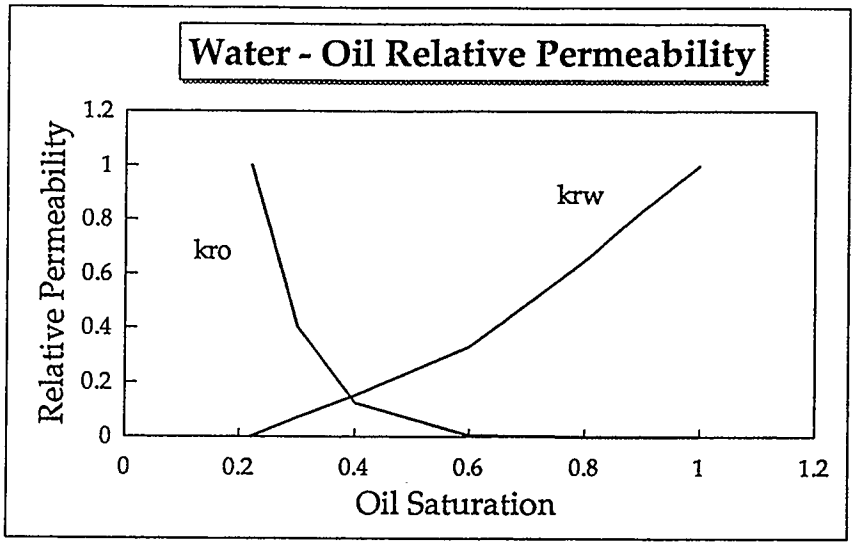

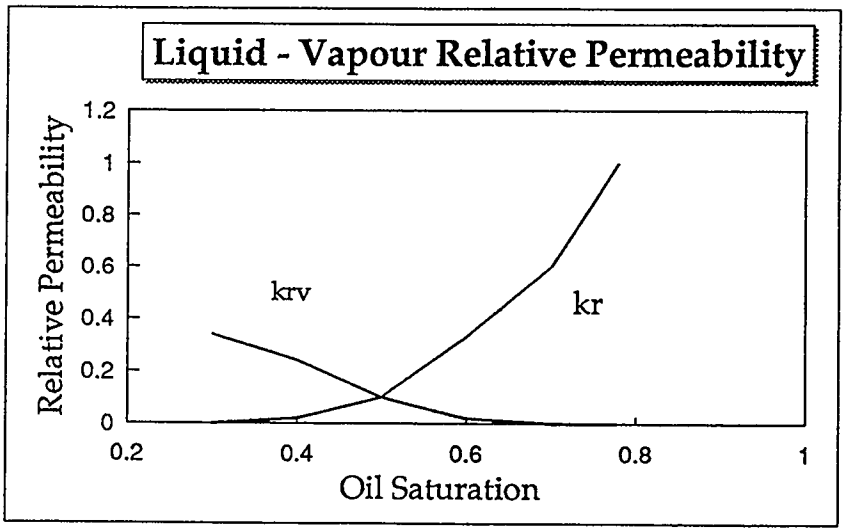

Figure 7.3 Relative Permeability Curves of the Actual Model

7.1.2 Postulated Models A, B and C

As postulated models A and B, we have considered a 6x9x6 reservoir shown in Figure 7.4. As shown the postulated models are considerably smaller than the actual model. This was done in an effort to simulate a more realistic situation. The vertical permeabilities are also taken equal to one tenth of the horizontal ones. Throughout this case study a zonation approach has been used, with respect to the porosity and permeability distribution of the postulated models.

The three postulated models considered, have the same grid block representation of the reservoir, however a different zonation for porosities and permeabilities is employed. In particular model A assumes a simple zonation for porosities and permeabilities, namely, it is comprised of three zones: the first corresponds to layer 1, the second zone corresponds to layers 2, 3 and 4 and, the third zone corresponds to layers 5 and 6. Hence in this case there are three porosities and three horizontal permeabilities, i.e., a total of six parameters to be estimated. Model B assumes six permeability and porosity zones, each corresponding to a layer of the postulated reservoir. Hence Model B requires a total of 12 parameters (six porosities and six permeabilities) to be estimated.

The major assumption in model C is that the reservoir rock is naturally fractured. The model is considered to be comprised of two superimposed continua, the matrix and the fracture system. The reservoir model lies within the validity of Kazemi's model. (Kazemi and Merril 1979, Gilman and Kazemi 1983). In the postulated reservoir model both fractures and matrix have non-zero permeability and porosity. Each matrix blocks is assumed to be completely surrounded by fractures and cannot communicate directly with adjacent grid block. The fracture system is assumed to be the only conduit of flow towards the producer. Flow also occurs between the matrix and the fracture system. Drainage and imbibition between the matrix and the fractures are the key factors for the estimation of the total recovery of the model. It is well known that such a model is not quite realistic since, the matrix blocks "float" and do not touch each other, whereas in reality the fractured media supports substantial

rock stresses. Nonetheless, these are typical assumptions used by the majority of dual porosity simulators. In this case, there are three unknown porosities and three permeabilities for the fracture system and another set of three porosities and permeabilities for the matrix system.

The whole study of the above models is composed by two steps. Initially we employ the automatic history matching capabilities of the simulator in order to arrive at the optimum values of the parameters. The estimated porosities and permeabilities for the postulated models are listed in Tables 7.2, 7.3 and 7.4. In all cases the algorithm converged to unrealisticlly high relative values of porosity. This was expected since all the postulated models lack pore volume compared to the actual model. Finally, using the values of the estimated parameters and their covariance matrix, we estimate the 95% confidence intervals of the history matched production rates as well as the future production rates. The results for the model A are shown in Figures 7.5 and 7.6, for the model B in Figures 7.7 and 7.8 and for the model C in Figures 7.9 and 7.10.

Table 7.2: Estimated Porosities and Permeabilities for Model A

Layer	Porosities		Permeabilities	
	Estimated ϕ	Standard Dev. (%) *	Estimated K_h (md)	Standard Dev. (%) *
1	0.663	4.92	35.8	2.61
2, 3 &4	0.217	5.27	115	0.38
5 & 6	0.114	23.2	40.0	0.89

* Prior Knowledge assumed: σ_ϕ=0.05 and σ_{kh}=50 (md)

As seen, for all the models the history matched period is practically the same. Of course the 95% confidence intervals are larger as the number of the unknown parameter increases. In addition in Table 7.3, it is shown the effect of the prior information on the estimated standard deviation of the parameters which in turn have a strong effect on the computed 95% confidence intervals (Figure 7.11).

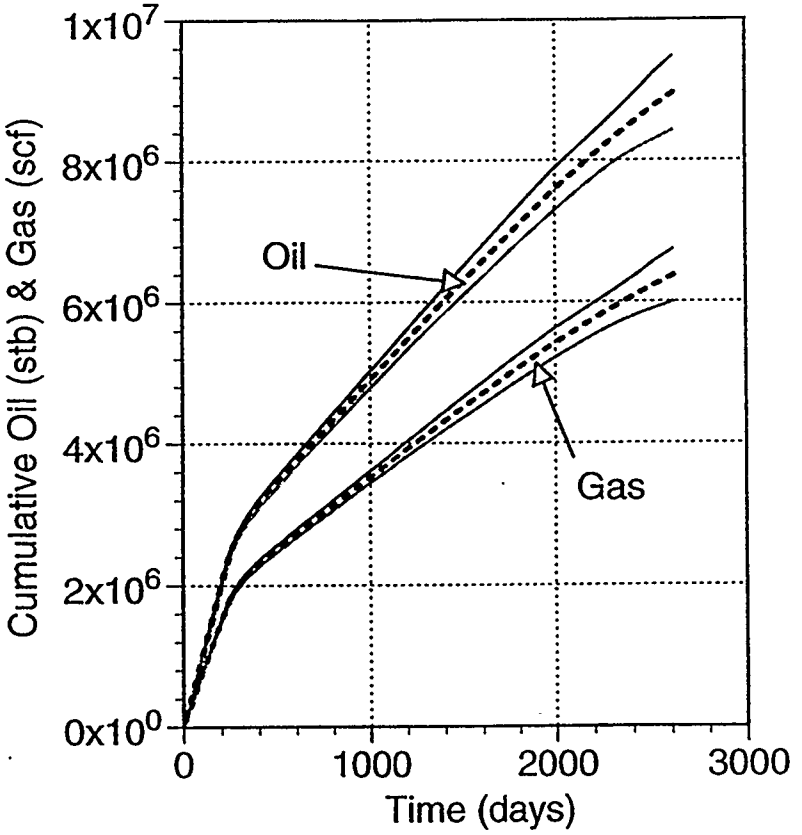

Figure 7.5 95% Confidence Intervals of Cumulative Oil and Gas Production Based on Model A

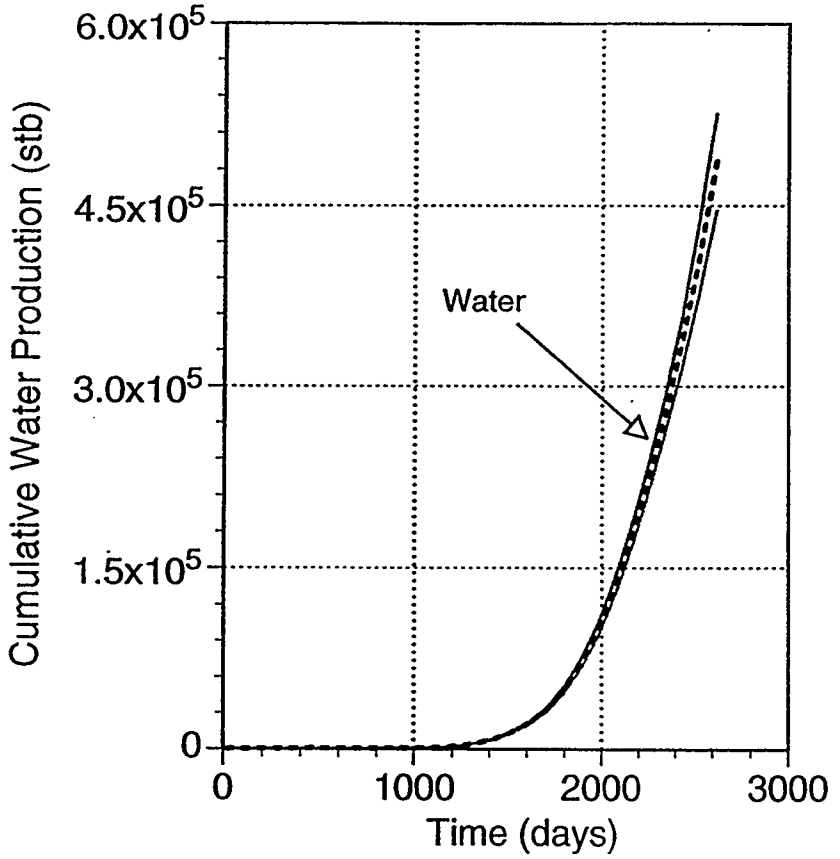

Figure 7.6 95% Confidence Intervals of Cumulative Water Production Based on Model A

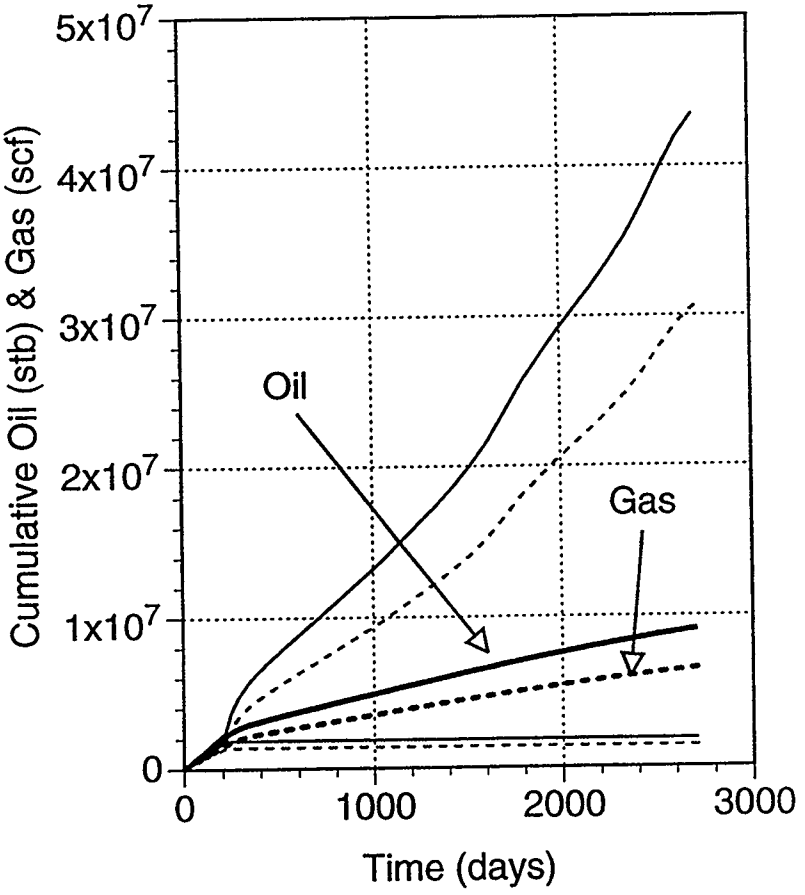

Figure 7.7 95% Confidence Intervals of Cumulative Oil and Gas Production Based on Model B.

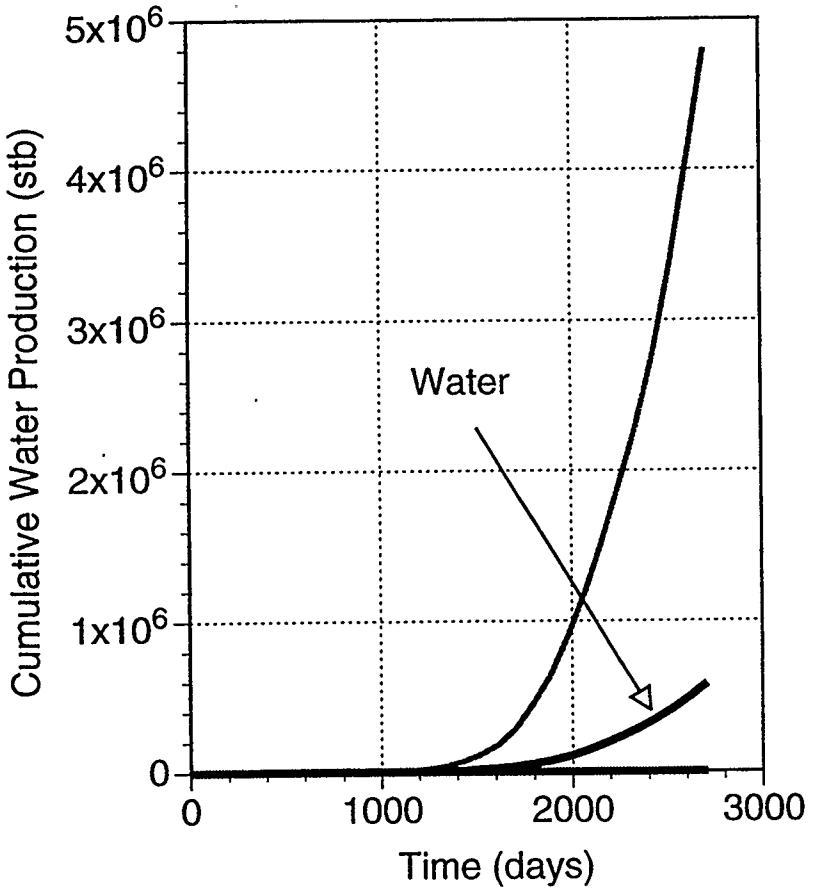

Figure 7.8 95% Confidence Intervals of Cumulative Water Production Based on Model B.

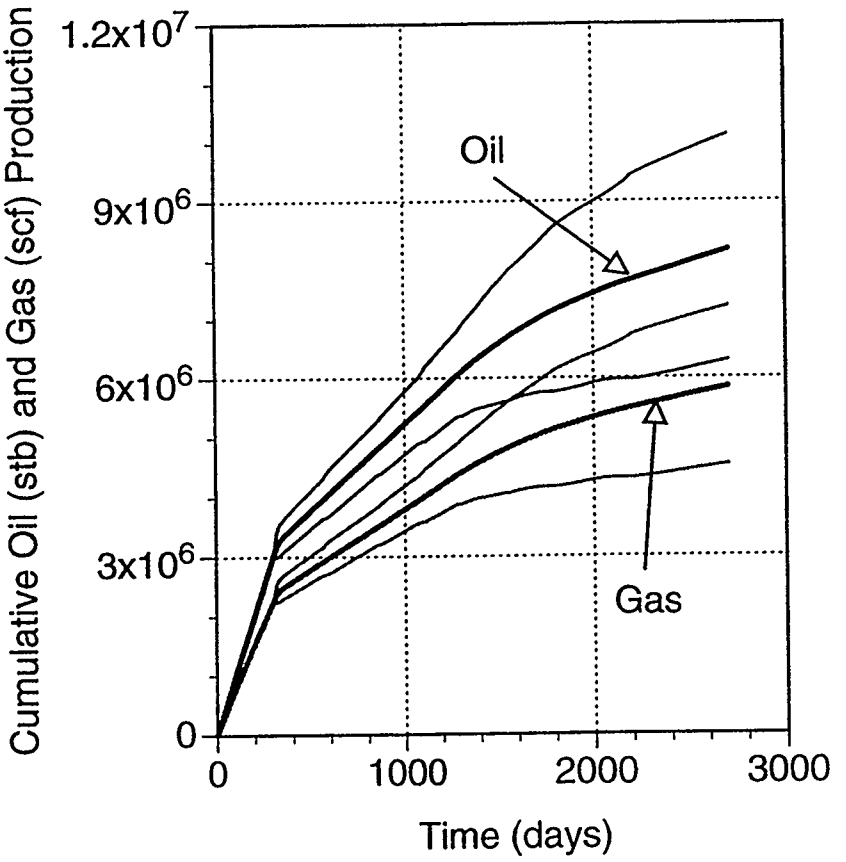

Figure 7.9 95% Confidence Intervals of Cumulative Oil and Gas Production Based on Model C

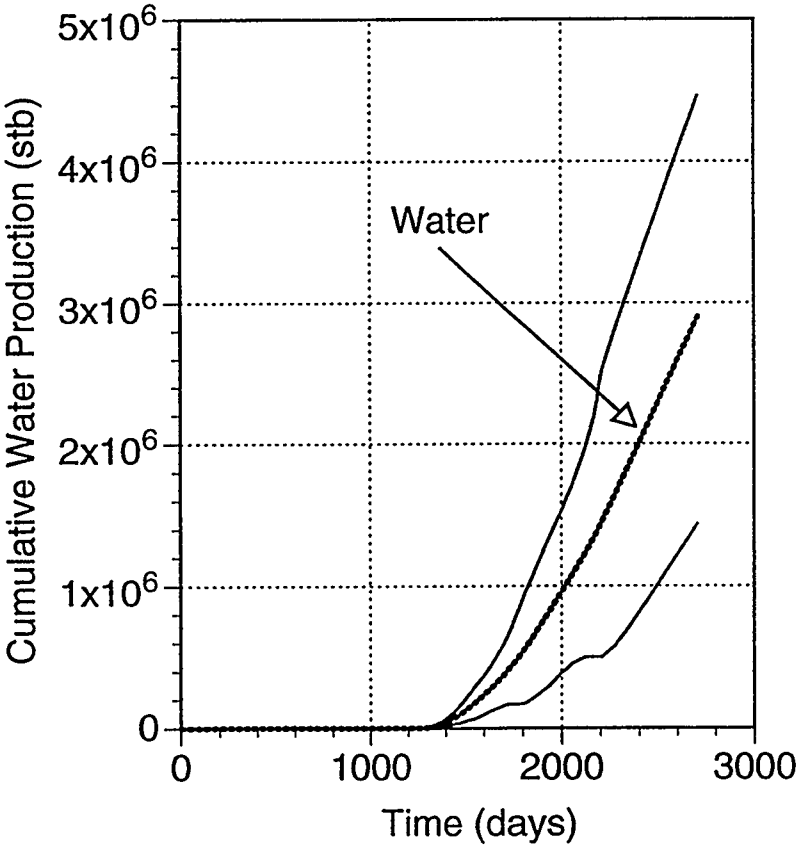

Figure 7.10 95% Confidence Intervals of the Cumulative Water Production Based on Model C

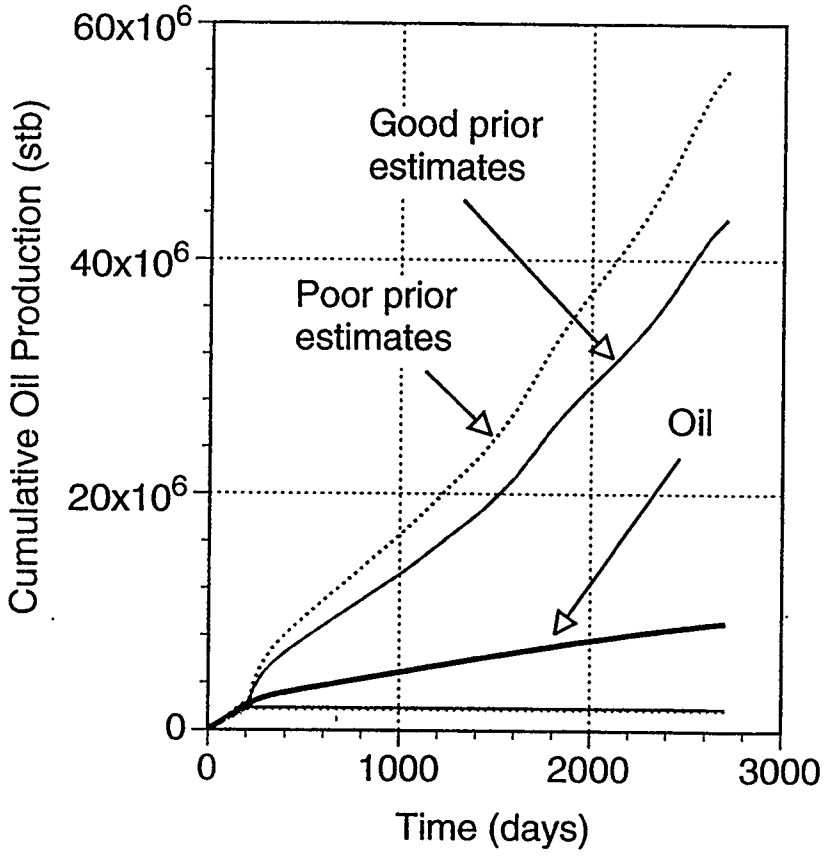

Figure 7.11 Comparison of 95% Confidence Intervals for Cumulative Oil Production Based on Model B with Good and Poor Prior Estimates.

Table 7.3: Estimated Porosities and Permeabilities for Model B

Layer	Porosities		Permeabilities	
	Estimated ϕ	Standard Dev. (%)	Estimated K_h (md)	Standard Dev. (%)
1	0.86	4.99 19.9	35.8	13.0† 16.1‡
2	0.186	15.1 60.1	115	4.01 5.12
3	0.186	11.5 18.1	116	1.2 1.41
4	0.177	14.2 55.6	115	7.5 8.87
5	0.0915	31.2 113	40.1	23.2 26.9
6	0.243	29.4 114	39.9	1.07 2.62

† Prior Knowledge assumed: σ_ϕ=0.05 and σ_{kh}=50 (md)
‡ Prior Knowledge assumed: σ_ϕ=0.2 and σ_{kh}=200 (md)

The quality of the obtained match for the models B and C is demonstrated in Figures 7.12 and 713. It can also be seen that as the forecasting time increases substantially, so does the uncertainty in the estimates. The fact of extrapolation is always risky and the deviation increases as we move further away from the history matched region.

Comparing the two postulated models B & C, one can see that even though, the estimated 95% error boundaries of the model C are tighter than the ones from model B, the deviation of the production as we move further from the history matched period is becoming significant for the model C, especially for the first 1750 days after the history matched region. It can also be seen that the water production rate exhibits the greater deviation. This is expected since naturally fractured reservoirs exhibit an earlier water breakthrough than a single porosity system. The forecasted production rates for the model C, eventually become similar to the ones of the actual model.

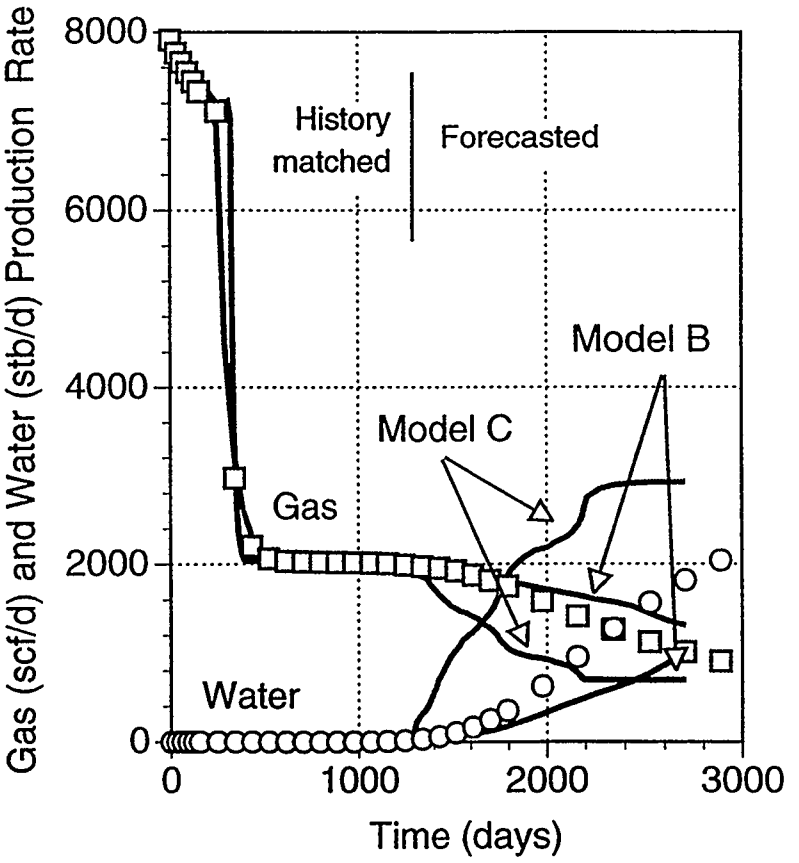

Figure 7.12 Comparison Between Gas (□) and Water (O) Production Rates of the Actual Reservoir and Postulated Models B, C.

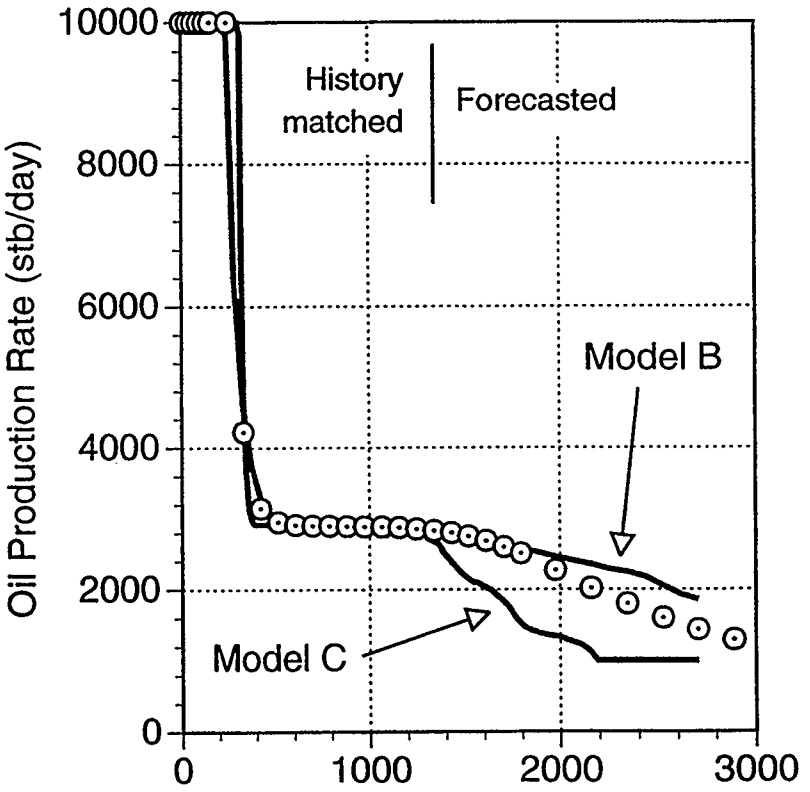

Figure 7.13 Comparison Between Oil (⊙) Production Rates of the Actual Reservoir and Postulated Models B, C.

Table 7.4: Estimated Porosities and Permeabilities for the Fractured System and Matrix System

Layer	Porosities		Permeabilities	
	Estimated ϕ	Standard Dev. (%) *	Estimated K_h (md)	Standard Dev. (%) *
Fractured System				
1	0.005	6.78	262	0.25
2, 3 &4	0.005	6.78	231	0.33
5 & 6	0.005	6.78	246	0.32
Matrix System				
1	0.759	19.5	1.5	1.49
2, 3 &4	0.196	40.4	1.5	1.49
5 & 6	0.116	36.1	1.5	1.49

* Prior Knowledge assumed: σ_ϕ=0.8 and σ_{kh}=300 (md)

Going one step further one can improve the characterization of the reservoir by estimating the geometrical attributes of the fractures in postulated model C. Finally the intrinsic permeability, the fracture width and the size of the matrix blocks can be regarded as independent parameters. The values of the preceding parameters are presented in Table 7.5, for different regions of the reservoir. Also, since a decrease of the capillary pressure, results in encouragement of imbibition between the matrix and the fracture blocks, one can adjust the water-oil ratios, by considering the capillary pressure as a parameter to the model.

Deciding, which of the above models is the best representation of the "true" reservoir is a function of incorporating all the available "soft" data into the postulated models. Data resulting from geological and geostatistical studies, log and seismic interpretation and well test analysis can be crucial in selecting the best production scenario. Comparison of the recovery estimates for the three postulated models is presented in Table 7.6

Table 7.5 Geometrical Attributes of the Fracture System for the Actual Model.

Layer	Grid Block Index (I, J)	MatrixBlock Dimensions (ft)	Fracture Width(m)	Intrinsic Permeability (D)
K=1, 5, 6	I=1,6 J=1 to 9	25x25x25	50	6975
K=1, 5, 6	I=2,3,4,5 J=1 to 9	44x44x44	88	21360
K=2, 3, 4	I=1,6 J=1 to 9	14x14x14	28	2282
K=2, 3, 4	I=2,3,4,5 J=1 to 9	25x25x25	50	6975

Table 7.6 Comparison of Recovery Estimates Between the Actual and the Three Postulated Models

Recovery Estimates after 2708 days of production				
	Actual Model	Model A	Model B	Model C
Predicted Recovery	32 %	31.00 %	31.3 %	25.0 %
Maximum Recovery	-	33.24 %	31.9 %	31.6 %
Minimum Recovery	-	29.39 %	30.7 %	19.0 %

Overall, as seen from Figures 7.7 to 7.12, we can only make "useful" predictions for a rather short horizon where all models perform well. Once the forecasting time increases substantially, so does the uncertainty in the estimates. The fact that extrapolation is always risky is demonstrated in Figures 7.14 and 7.15 where we compare the expected production rates from the" actual" reservoir with those predicted by Model B. As sees, the deviation increases as we move further from the history matched region (first 1250 days).

7.2 Case Study - Horizontal Shale Barriers

This case study involves a tilted waterflooded reservoir with shale barriers. The goal is to examine the effect of shales on the performance of horizontal wells. Again an actual model was used to produce synthetic data (production rates and bottom hole pressures), which are subsequently used by the automatic history matching program to estimate the porosity and permeability distribution of much simpler postulated reservoir models

7.2.1 Overview of the Actual Model

The actual model is an undersaturated reservoir, which is comprised by a 10 x 12 x 4 grid system. Figure 7.14 present a schematic diagram of the reservoir model including the grid block dimensions (x, y and z direction). Table 7.7 presents the porosity and the permeability distribution of the actual model, a schematic of which is shown in Figure 7.15, for the second and the forth layer. The vertical permeabilities are assumed to be equal to the one tenth of the horizontal ones. The reservoir exhibits a dip of 0.30%. In the upper part of the structure a horizontal well of 1500m has been completed, while in the lower part there are two injectors. This configuration has been adopted in order to simulate production under an active water drive and examine the effect of the shale barriers in the production scheme. The effect of the hydraulics of the horizontal well was assumed, to be negligible. The PVT data and the relative permeability curves have been taken from the second comparative problem of SPE. Figure 7.16 presents the assumed relative permeability curves. Shale layers of infinitely small thickness, have been assigned randomly to each of the layers of the reservoir, by modifying the vertical transmissibilities. The x and y dimensions of these barriers are identical to the ones of the grid blocks of the reservoir, while the thickness was assumed to be very small. Neither the producer nor the injectors have intercepted any of the preceding layers.

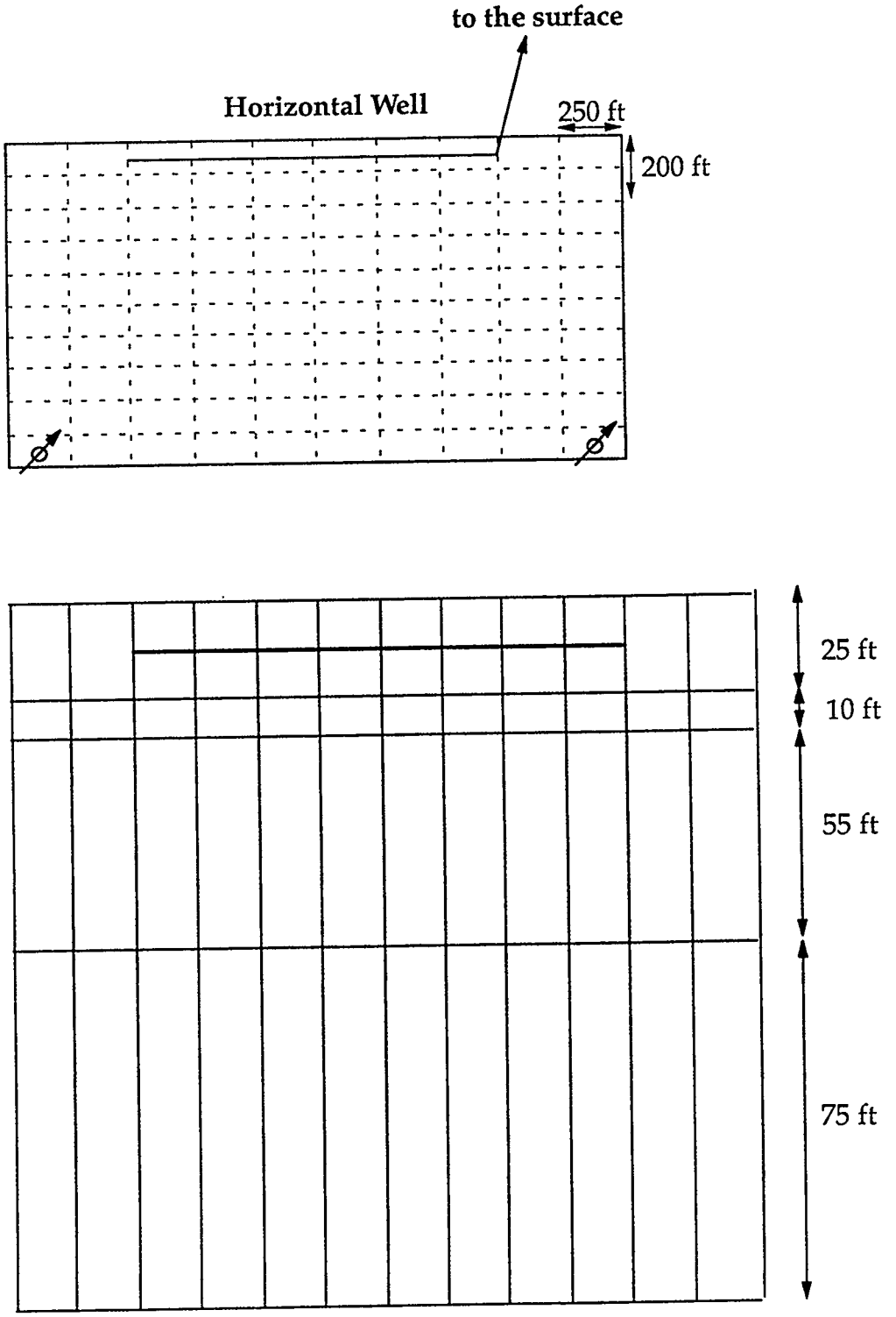

Figure 7.14 Grid Block Representation of the Actual Model: (a) First Layer and (b) Cross Section

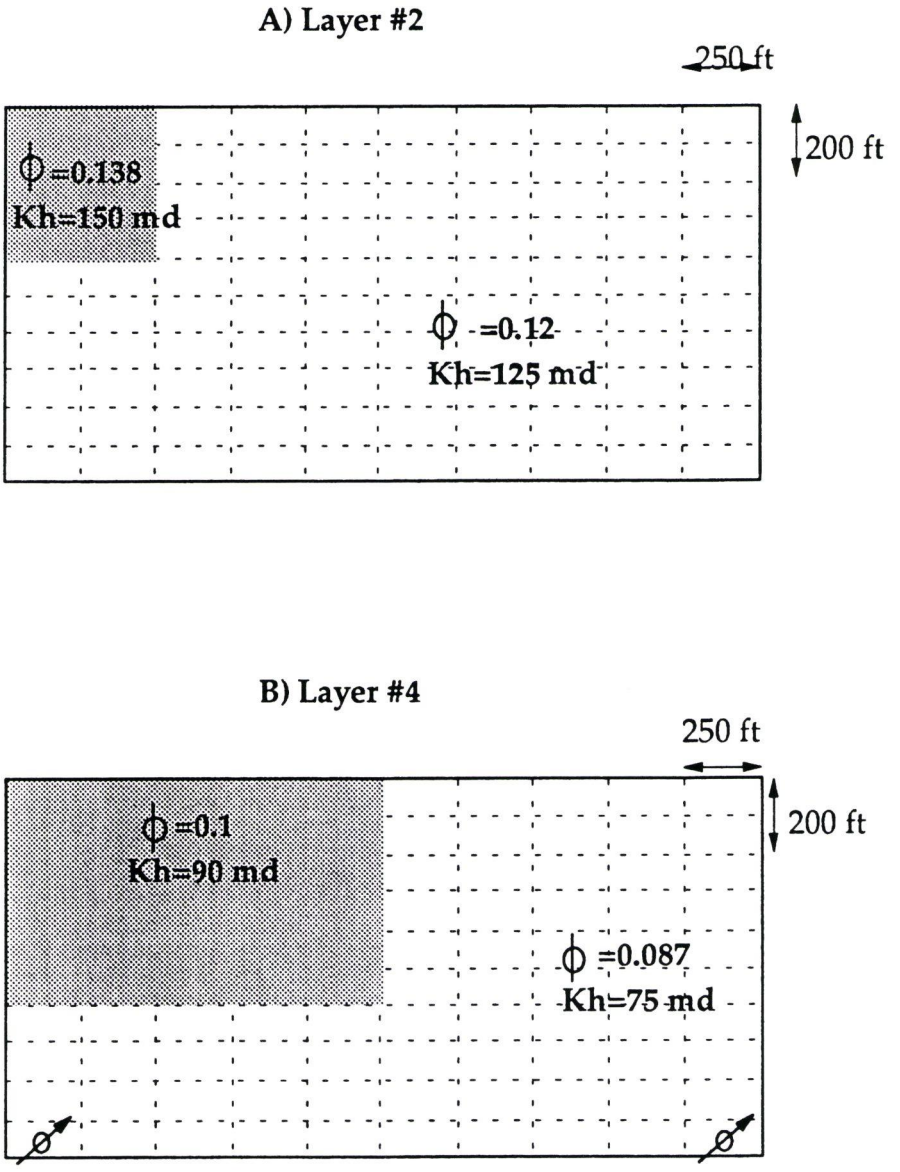

Figure 7.15 Schematic Representation of the Porosity and the Permeability Distribution of the Second and Forth Layer of the Actual Model.

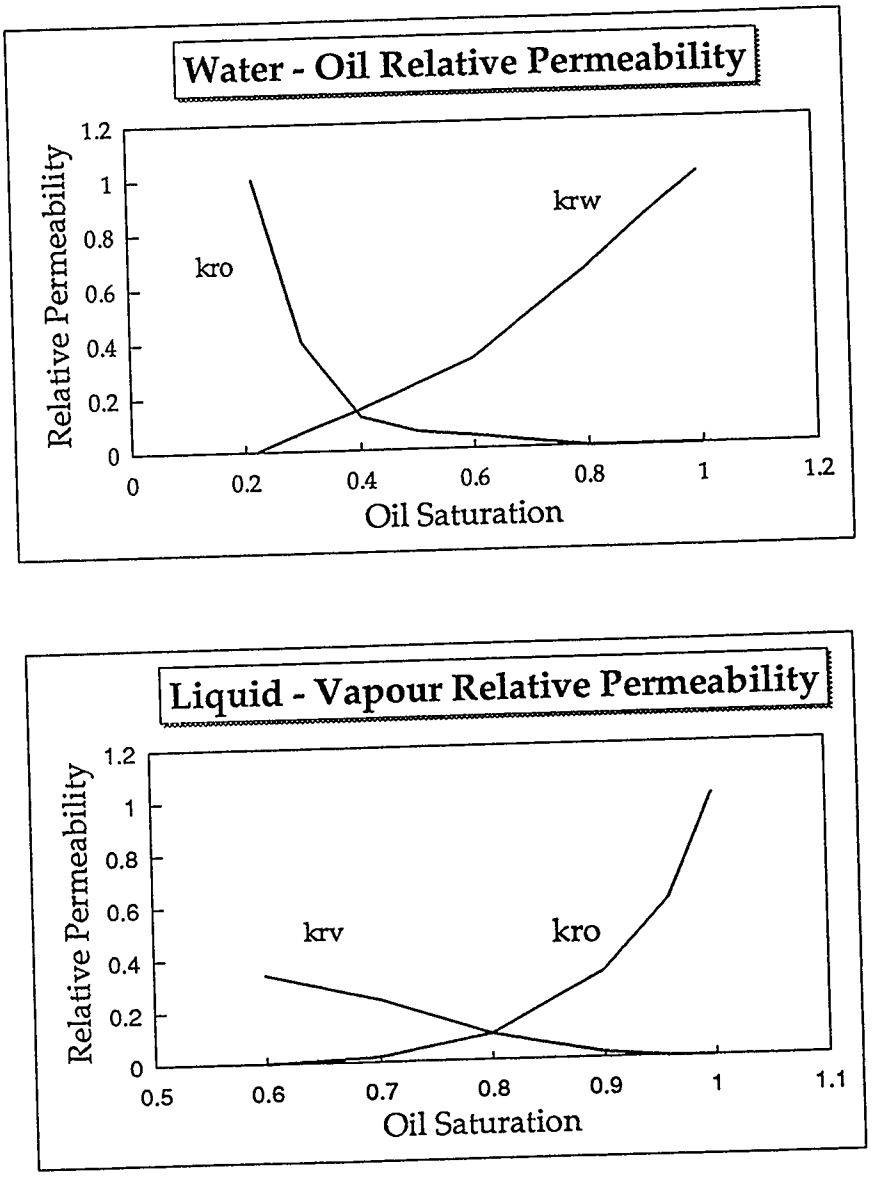

Figure 7.16 Relative Permeability Curves of the Actual Model.

The history matching has been based on the production and the pressure data obtained over the first 1096 days of operation. Again, Gaussian noise was added to the artificial data, in order to create more realistic observations. The frequency of the shale barriers for all the layers of the actual reservoir was assumed to be constant and equal to 36 per reservoir layer.. Figure 7.17 pictures the shale barriers (shaded areas), for the first two layers of the reservoir.

Table 7.7: Porosity and Permeability Distribution of the Actual Model - Horizontal shale barriers (from Top to Bottom).

Layer	Thickness (ft)	Porosity	Permeability (md)
1	25	0.2 I=1 , J=1,2 0.23	300 I=1 , J=1,2 360
2	10	0.12 I=1,2 J=1,4 0.138	125 I=1,2 J=1,4 150
3	55	0.097 I=1,3 J=1,6 0.12	60 I=1,3 J=1,6 72
4	75	0.087 I=1,5 J=1,7 0.10	75 I=1,5 J=1,7 90

7.2.2 Postulated Models A & B

In this case two postulated model have been considered. Their main difference is the assumed zonation. Model A has five zones and a total number of parameters 10, while Model B has only two zones and four parameters. Both models are represented by a 10 x 12 x 2 grid block system. The assumed zonation of the parameters for both models is shown in Figure 7.18. The first two layers of the actual model are combined in the first layer of the postulated model. The models are also inclined and it is assumed that are free of any impermeable barriers. The goal of this 3-D study is to investigate the sweep efficiency of water in a reservoir where there are no permeability barriers and thus determine the effect of the shale barriers on the performance of the horizontal well. The converged values of the parameters for model A and B are listed in Tables 7.8 and 7.9.

A) Shale Represantation of the first layer

to the surface

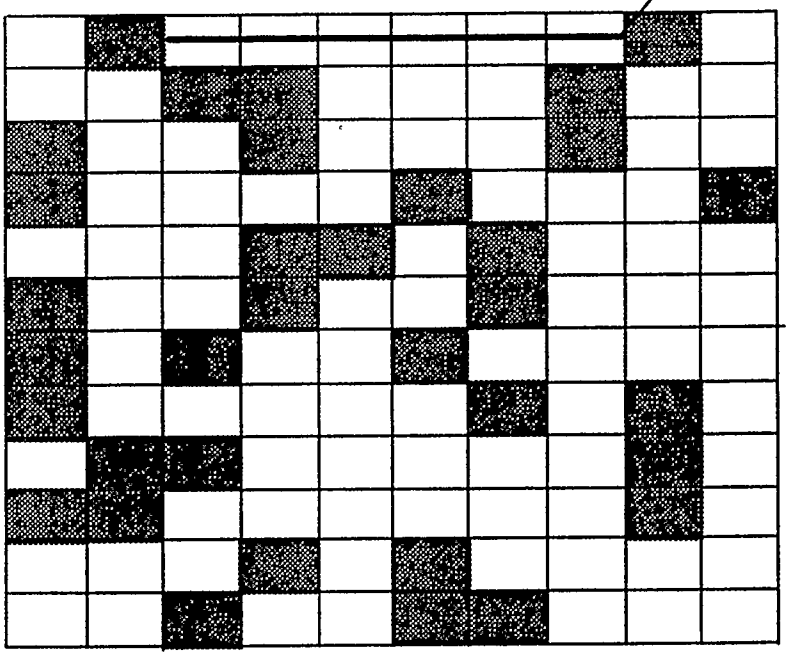

B) Shale Represantation of the second layer

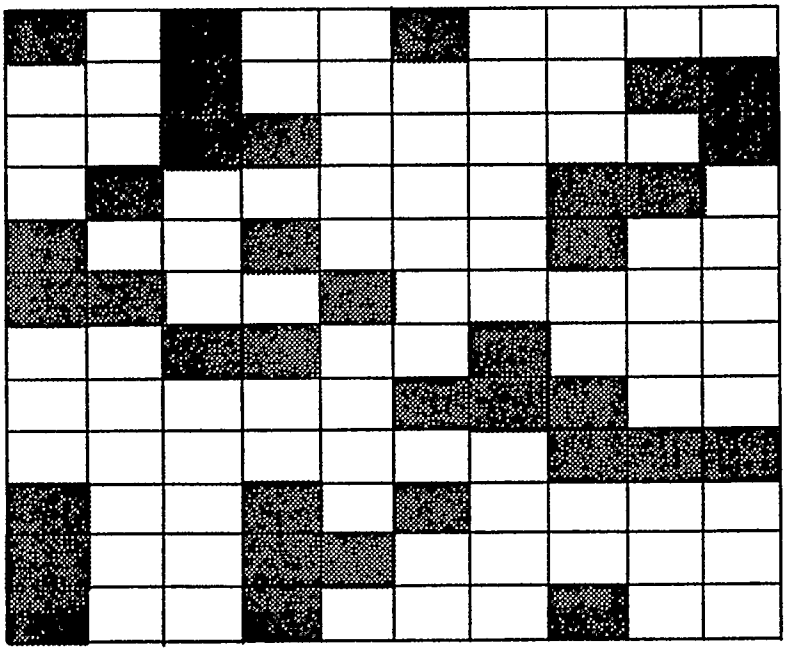

Figure 7.17 Frequency of the Shale Barriers for the First Two Layers of the Actual Reservoir - Plan View .

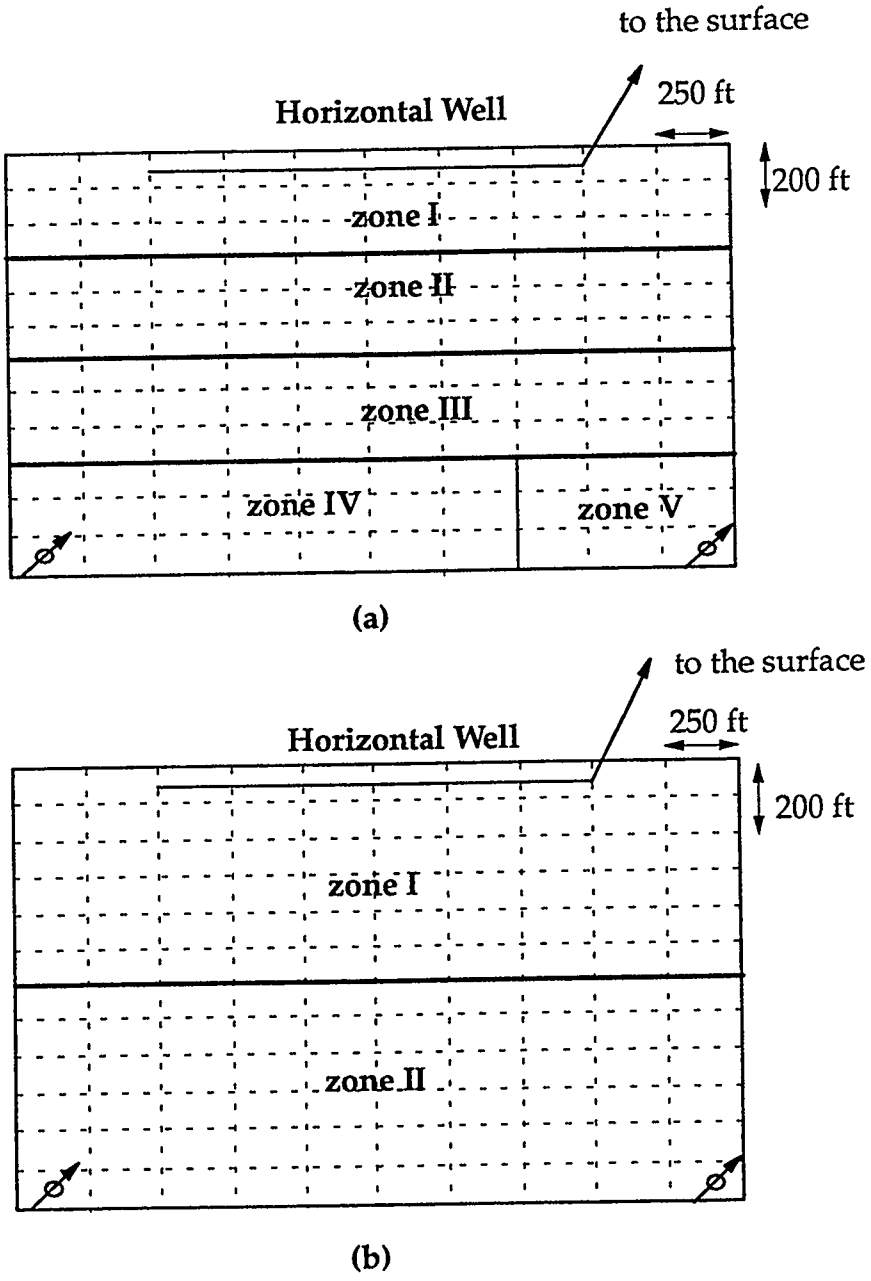

Figure 7.18 Grid Block Representation of the Postulated Models A (a) & B (b), Along with the Assumed Porosity and Permeability Zonation.

Table 7.8 Converged Values of the Parameters of the Postulated Model A.

Region	Estimated Porosity	Standard Dev.* (%)	Estimated Permeability (md)	Standard Dev (%)*
zone #1	0.229	9.3	174.78	0.20
zone #2	0.099	43.4	64.016	17.0
zone #3	0.012	109.0	58.733	17.4
zone #4	0.128	15.0	36.173	2.27
zone #5	0.127	44.15	33.431	11.6

* Prior knowledge assumed σ_ϕ=0.2 and σ_{kh}=200 md.

Table 7.9 Converged Values of the Parameters of the Postulated Model B.

Region	Estimated Porosity	Standard Dev.* (%)	Estimated Permeability (md)	Standard Dev (%)*
zone #1	0.229	1.58	100.00	0.024
zone #2	0.015	6.88	20.00	1.12

* Prior knowledge assumed σ_ϕ=0.2 and σ_{kh}=200 md.

Figure 7.19 and 7.20 show the quality of the obtained match for the above values of the parameters, for each postulated model. Figures 7.21 to 7.24 show the 95% confidence intervals of cumulative oil, gas and water production, for a prediction period of six years. From the preceding figures it is apparent that the greater the number of the parameters the greater the error boundaries of the cumulative oil, gas and water cumulative production.

It should be noted that the converged values of the permeabilities for the postulated models are considerably smaller than the ones of the actual model. During the automatic history matching procedure the algorithm converges to the relative values of porosity and permeability, taking into account the assumed zonation.

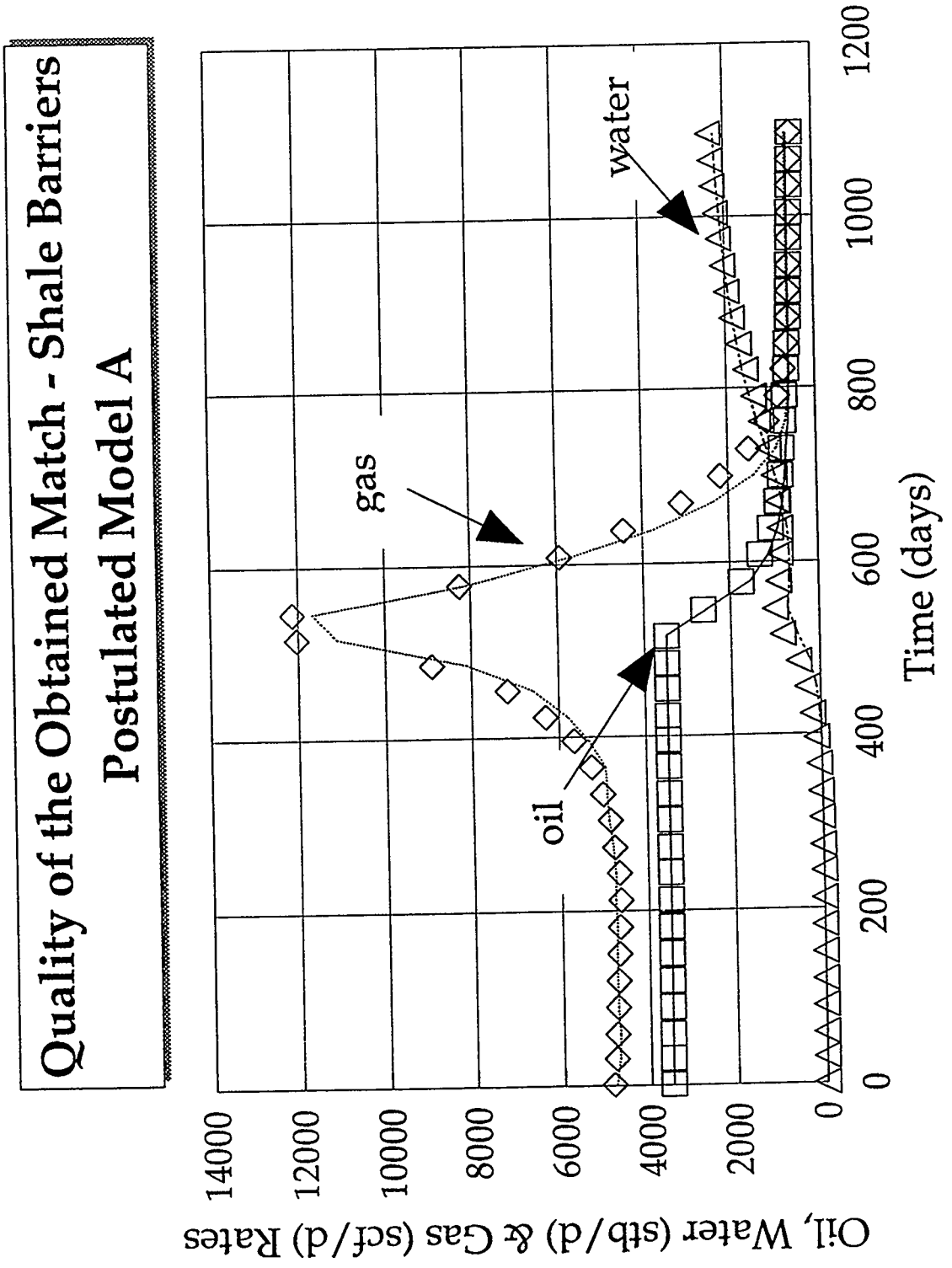

Figure 7.19 Quality of the Obtained Match of the Postulated Model A.

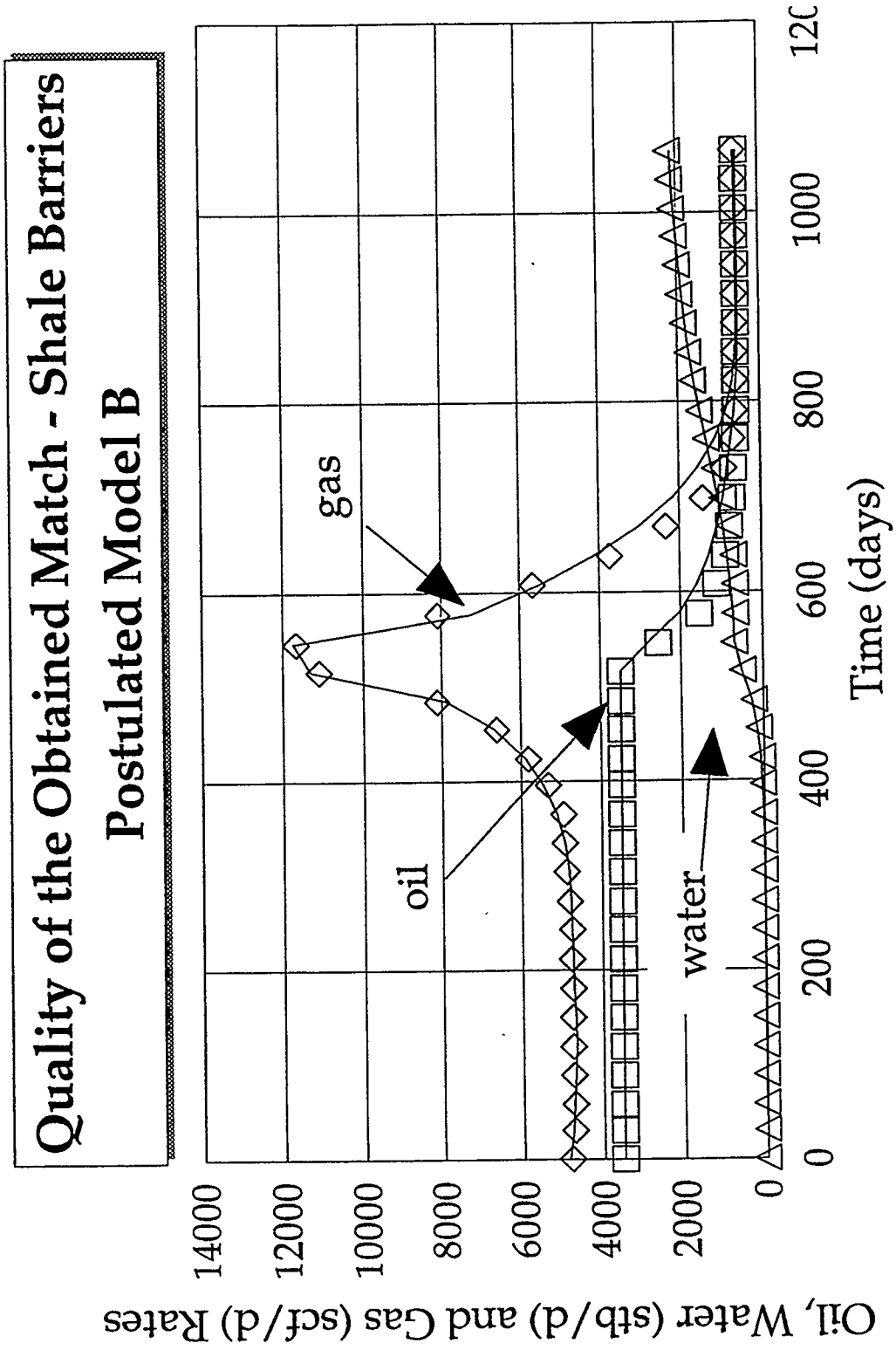

Figure 7.20 Quality of the Obtained Match of the Postulated Model B.

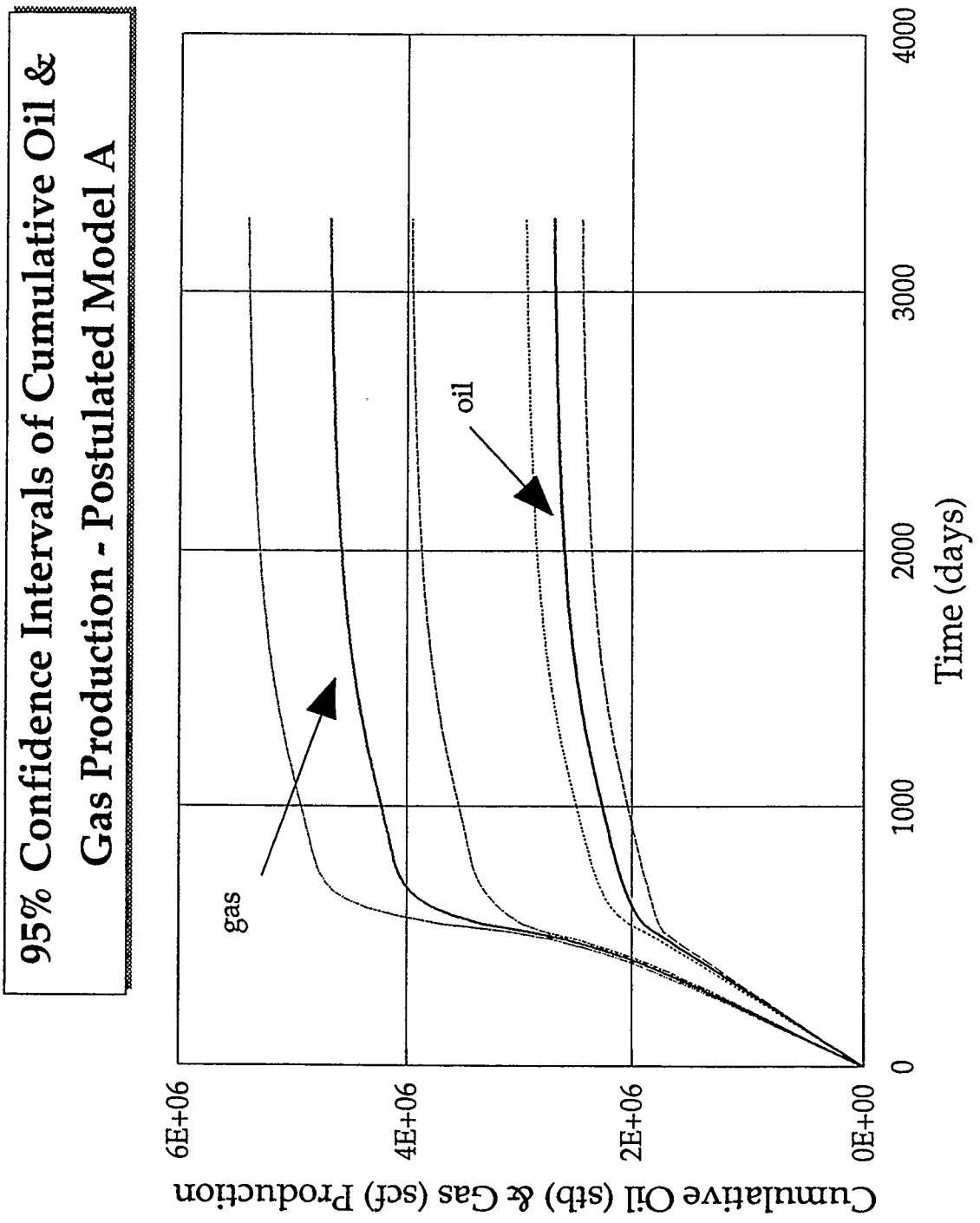

Figure 7.21 95% Confidence Intervals of the Cumulative Oil and Gas Production for the Postulated Model A.

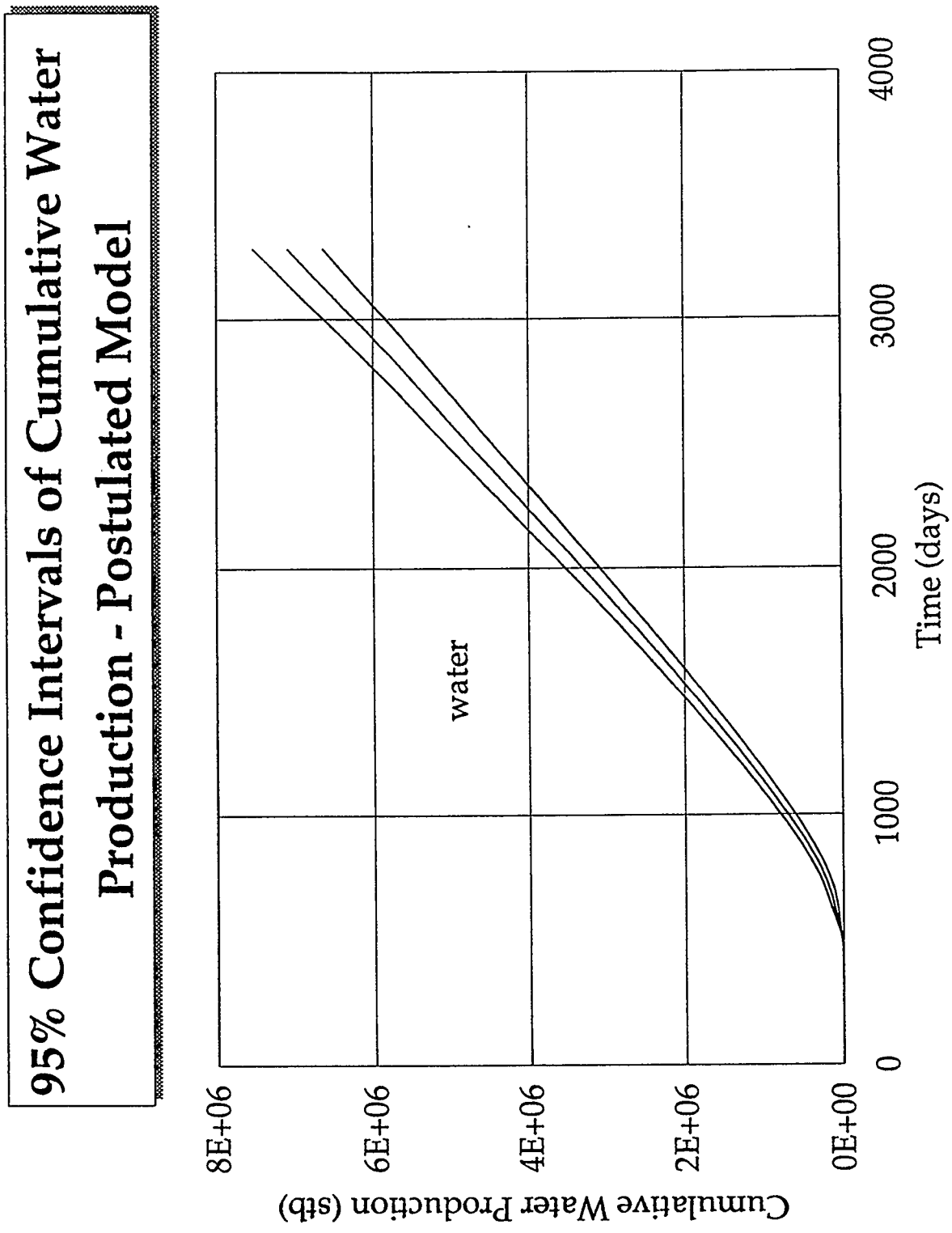

Figure 7.22 95% Confidence Intervals of the Cumulative Water Production of the Postulated Model A.

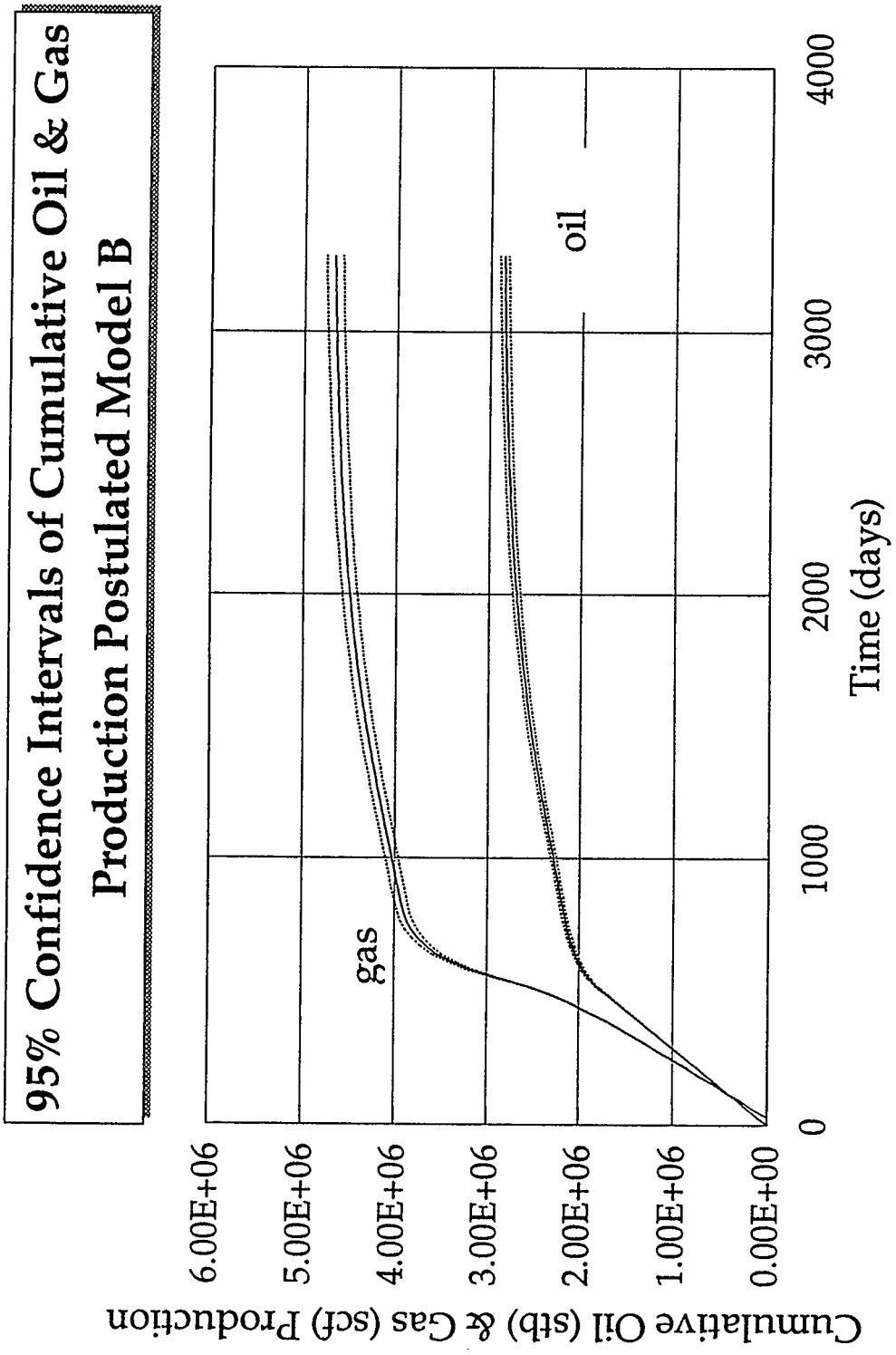

Figure 7.23 95% Confidence Intervals of the Cumulative Oil and Gas Production for thePostulated Model B.

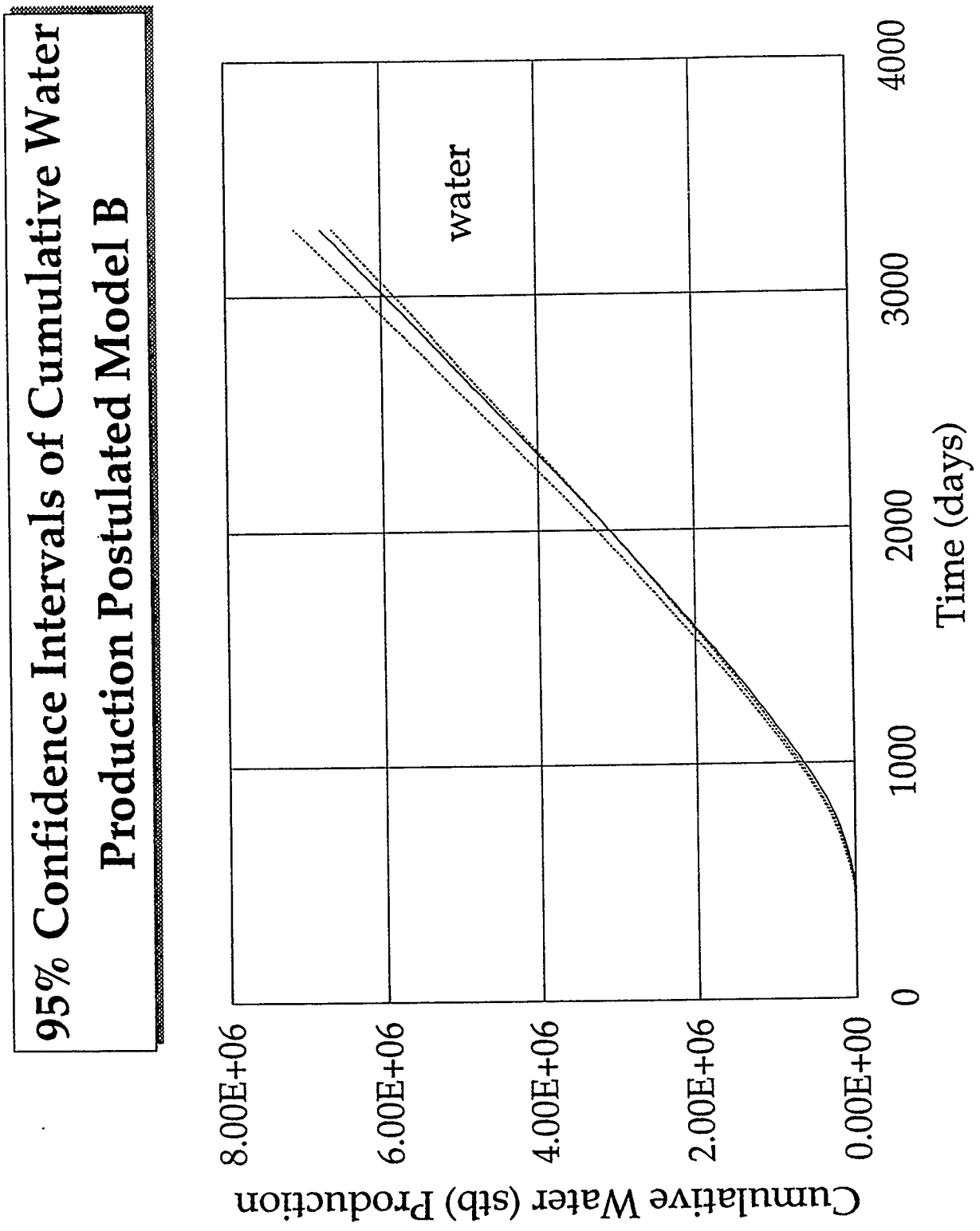

Figure 7.24 95% Confidence Intervals of the Cumulative Water Production of the Postulated Model B.

7.3 Application to a reservoir with a sealing fault.

One of the most common type of heterogeneity in hydrocarbon reservoirs is sealing faults. They play a dominant role in the overall production scenario since, they isolate different regions of the reservoir, or act as an impediment that retards the fluid flow in certain directions. Sealing faults can be detected by well testing, seismic exploration and geological surveying. When faults are non-sealing, they can be an important conduit for fluid flow. In reservoir simulation no flow boundaries can be modeled by either modifying the permeability between two adjacent grid blocks, or by using transmissibility multipliers to control the flow from one block to another.

In this section the effect of a no flow boundary on the reservoir performance is examined, using the automatic history matching procedure. Again an actual model was used to generate synthetic data, which was subsequently history matched by several postulated models. The postulated models were based on different assumptions regarding the shape of the faults. This approach was followed, in an effort to examine the sensitivity on the shape and the extension of the fault on the predicted production by these models .

7.3.1 Overview of the Actual Model

The schematic diagram of the actual reservoir, including grid block dimensions, is shown in Figure 7.25. The reservoir is represented by a 26x14x2 grid system and an impermeable boundary extends halfway across the reservoir partially separating the producer one (Prod #1) from the water injector (Inj #1). The effect of the impermeable boundary is to delay the water breakthrough of the first producer (Prod #1), which is located closer to the injector than Prod #2. The model is comprised of two layers. The first layer has a thickness of 40 ft, while the second 20 ft. In Figure 7.23 is also shown the path of the injected water towards the Prod #1. The porosity and the permeability distribution is shown in Figure 7.26. The porosity is assumed to be the same for the two layers, while the decrease of the horizontal permeability

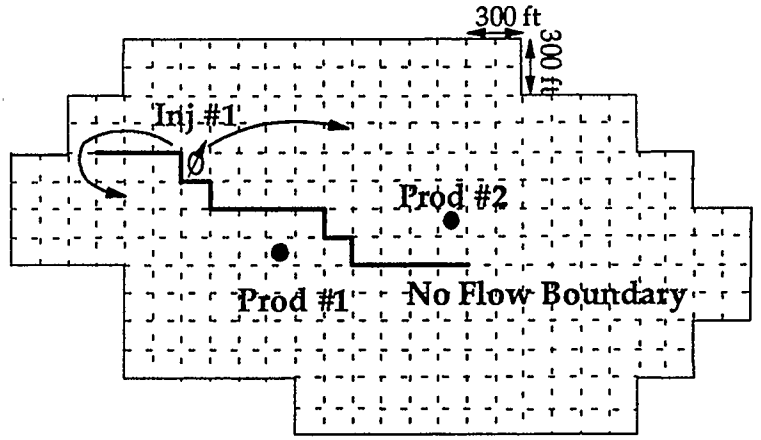

Figure 7.25 Grid block representation of the Actual model.

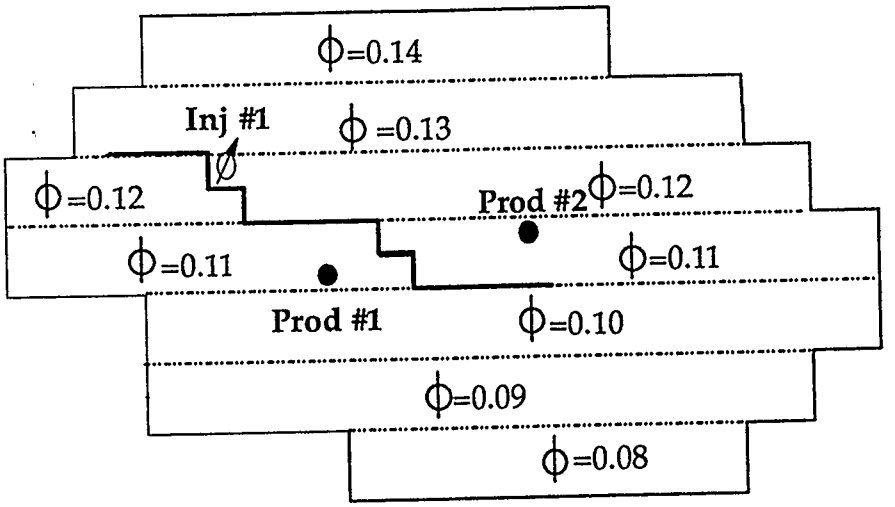

(a)

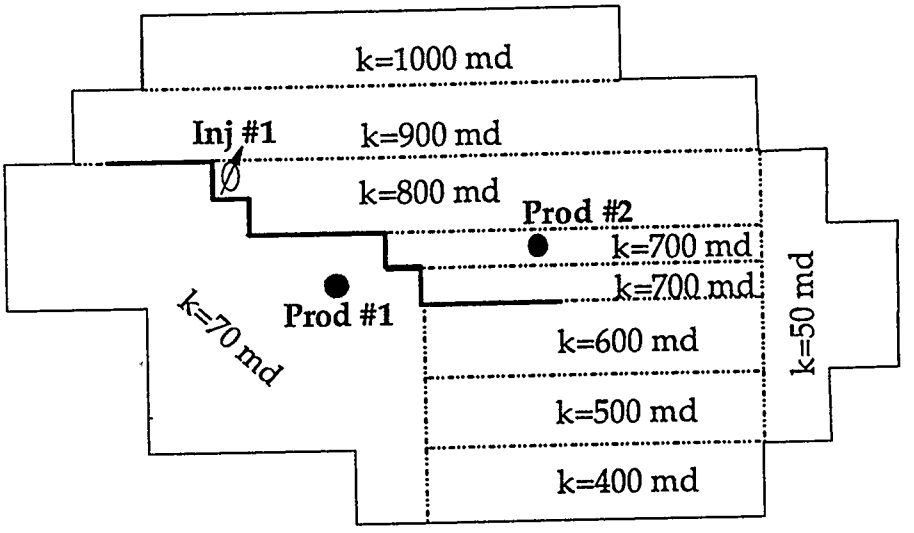

(b)

Figure 7.26 Porosity and Permeability Distribution of the Actual Model.

between the first and the second layer is approximately 10%. The vertical to horizontal permeability ratio was assumed constant and equal to 0.1. The modelling of the impermeable boundary was accomplished by using transmissibility multipliers between adjacent grid blocks. The reservoir is initially undersaturated with a connate water saturation. The reservoir fluid properties are identical to those used in the Second SPE Comparative Solution , Chappelear et al (1986). The relative permeability curves are identical to the ones in Figure 7.16

Grid refinement techniques where used in all the wells. The producers were completed in the first layer and the operating constraints were variable, depending on gas-oil ratios, bottom hole pressures and oil production. Prod #2 was shut-in, when the watercut exceeded the limit of 95%. This occurred after one year of production. However the operating constraints of that well were such, that it would come on line again, when its watercut would be smaller than the maximum value. The injector was completed in the second layer and was operated under a constant injection rate, subjected to maximum injection pressure.

For history matching purposes, we assumed that the production data were available for the first 1430 days (4 years). Figure 7.27 shows the production performance of the two wells of the actual model.

7.3.2 Postulated Models A, B and C

Numerous postulated models without any impermeable barriers were tested, without being able to obtaining an acceptable history match. The reason was that both producers were exhibiting early water breakthrough. Postponement of the water breakthourgh was achievable either by altering the permeability and the porosity in the inter-well zones, or by modifying the oil-water relative permeability data. Changing the values of the permeability and the porosity resulted in very small values of porosity and permeability, even in the zones where wells exist, and hypothetically we have a better knowledge of the distribution of the parameters (core samples, log

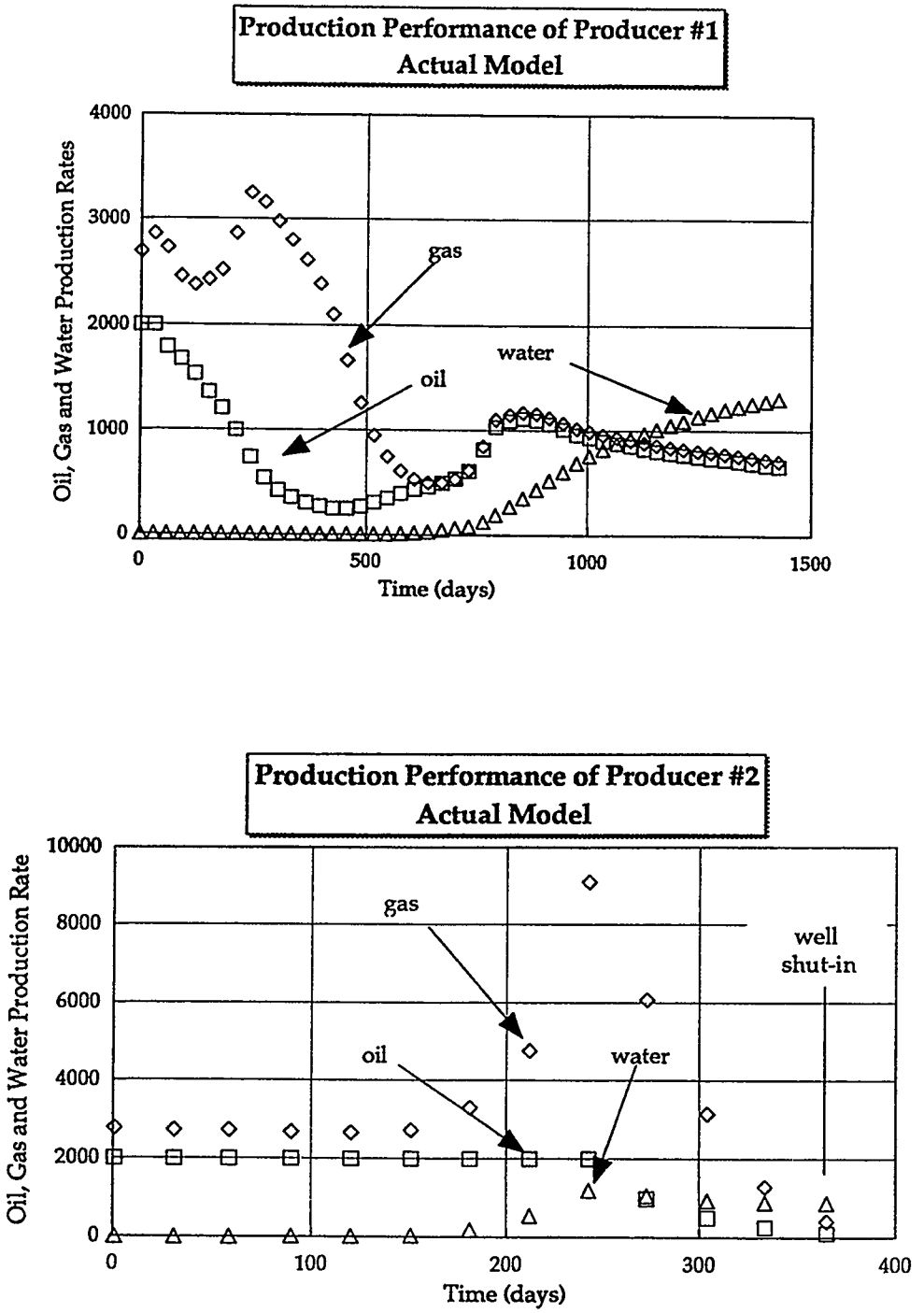

Figure 7.27 Production Performance of Prod #1 & #2 - Actual Model.

analysis, pressure transient tests). Figures 7.27 shows that Prod #1 does not produce any water for the first 550 days, even though it is located closer to the injector, compared to prod #2. Prod #2 was shut in after 365 days of production due to high watercut (95%). Therefore one has to assume that there has to be some sort of impediment to flow between Prod#1 and Inj#1 which makes water to follow a more tortuous path. All the postulated models considered in this section are based on different assumptions on the shape and the extend of the impermeable barriers, which are implemented in these models.

Breakthrough times, watercuts and whether the producer #2 will come back on line were considered to be the most crucial parameters in accepting a postulated model. The operating constraints of the producers, for all the postulated models, consisted of constant monitoring of the watercut and production under maximum oil rate and minimum bottom hole pressure.

The postulated model A was represented by a 7x4x1 grid block model. A comparison of the postulated model A with the actual reservoir is shown in Figure 7.28, where the first is superimposed on the second. As seen the postulated model is significantly smaller then the actual reservoir. This was done in an effort to simulate a more realistic situation. In the preceding figure it is also shown the four zones of porosity and permeability and the shape and extension of the presumed fault. Hence, there are eight parameters to be estimated and their converged values are presented in Table 7.10. The vertical permeabilities of each zone, were also taken as one tenth of the horizontal ones.

Table 7.10 Estimated Porosities and Permeabilities for Postulated Model A.

Zone	Estimated Porosity	Standard Dev. (%)	Estimated Permeability (md)	Standard Dev (%)
zone #1	0.047	26.90	1360.00	0.11
zone #2	0.292	5.90	9950.00	0.09
zone #3	0.035	12.70	95.00	0.50
zone #4	0.935	2.50	450.00	0.41

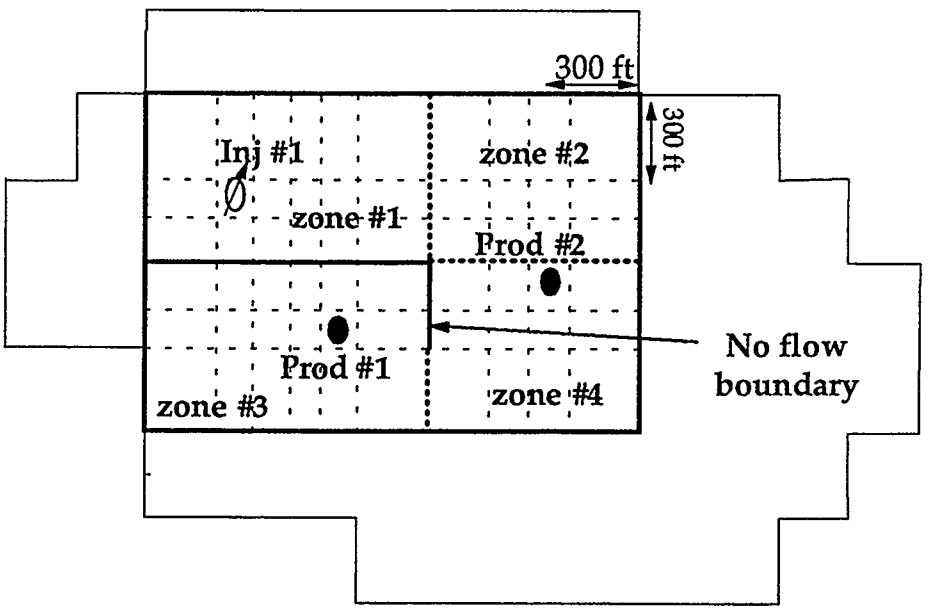

Figure 7.28 Comparison of the Postulated Model A with the Actual Reservoir, where the First is Superimposed on the Second.

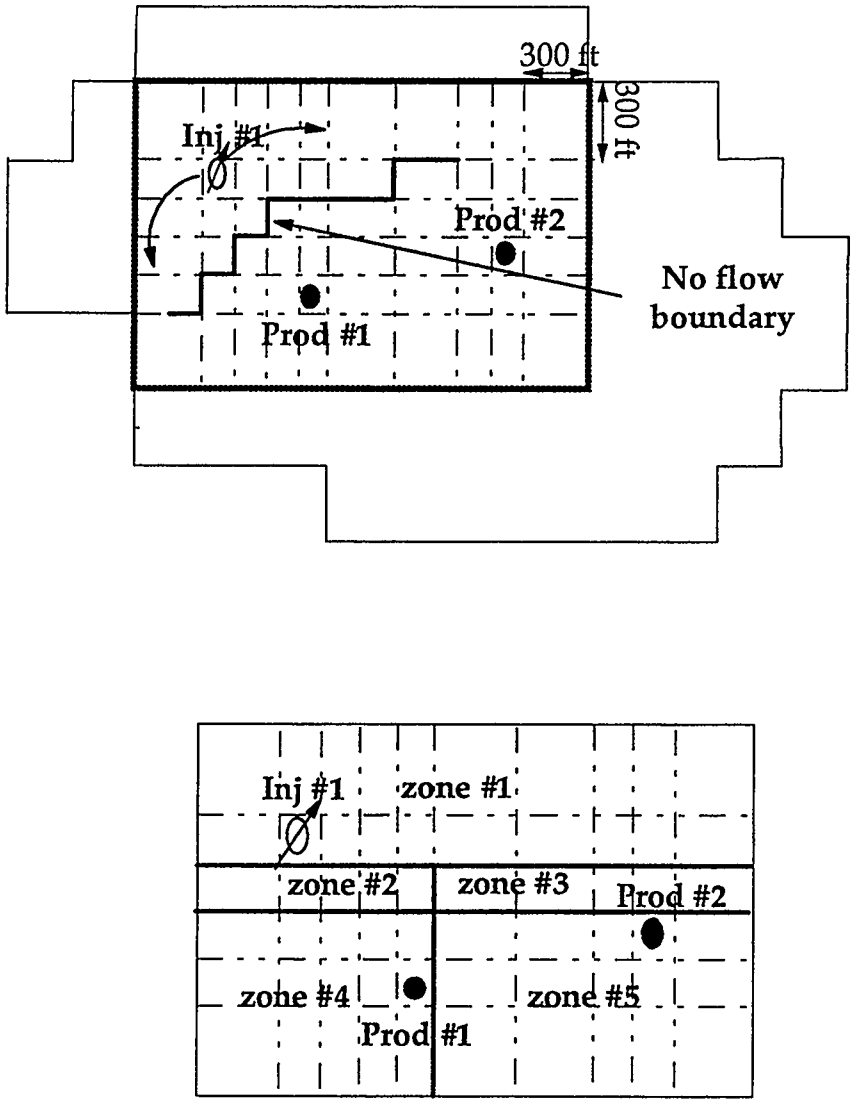

Figure 7.29 Comparison of the Postulated Model B with the Actual Model, Where the First is Superimposed on the Second. The Arrows Indicate the Path of the Injected Water.

In postulated model B we have assumed the same grid block representation but different zonation, shape and extension of the impermeable barrier as that of postulated model A. Figure 7.29 shows the model B superimposed on the actual model and the zonation used. Each zone has two parameters, one porosity and one permeability and thus model B has ten parameters totally. Table 7.11 lists the converged values of the parameters in this model.

Table 7.11 Estimated Porosities and Permeabilities for Postulated Model B.

Zone	Estimated Porosity	Standard Dev. (%)	Estimated Permeability (md)	Standard Dev (%)
zone #1	0.073	23.80	2000.00	0.05
zone #2	0.047	28.90	19.00	0.38
zone #3	0.913	5.67	622.00	1.37
zone #4	0.226	46.32	350.00	2.26
zone #5	0.294	13.77	47.00	1.11

Model C is based on the Model B. The only difference is that the fault seals the upper left part of the reservoir from the lower left one. A grid block representation of model C is shown in Figure 7.30. The converged values of the parameter of this model are listed in Table 7.12.

Table 7.12 Estimated Porosities and Permeabilities for Postulated Model C.

Zone	Estimated Porosity	Standard Dev. (%)	Estimated Permeability (md)	Standard Dev (%)
zone #1	0.074	13.35	700.00	0.31
zone #2	0.046	22.37	25.00	0.44
zone #3	0.938	5.24	618.00	0.98
zone #4	0.241	46.96	9000.00	0.21
zone #5	0.303	19.89	47.212	1.18

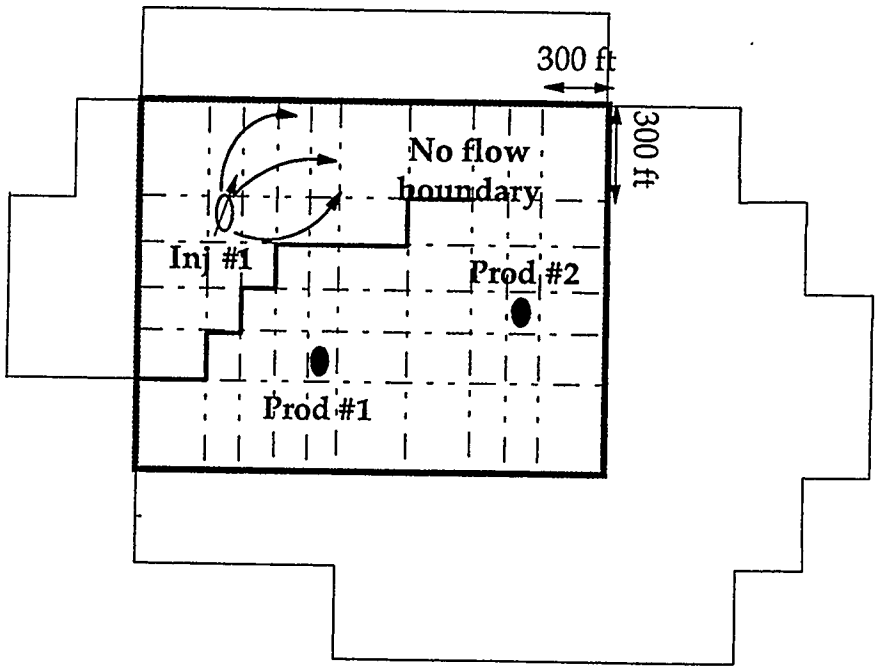

Figure 7.30 Comparison of the Postulated Model C Superimposed on the Actual Model. The Arrows Indicated the Flow Path of the Injected Water.

As seen from the tables 7.10 to 7.12, porosity and permeability values vary significantly for all the models. High values of porosity are expected, since all the postulated models lack in pore volume compared to the actual model. The high values of permeability are mostly related to the assumed shape of the fault in each postulated model. Thus the injected water in model A has to follow a longer path compared to the actual model and in order to arrive to Prod #1 after 600 days of production the permeability of the zones #1 and #2 has to be high. If reservoir characterization was the primary objective, the first step would be the match of the original oil in place (OOIP) between the actual and the postulated models. All the converged values of the parameters are relative values and they incorporate information regarding the assumed complexity of the postulated models.

The quality of the obtained match for the preceding models is presented in Figures 7.31 to 7.33. As seen, the behaviour of all postulated models for the history matching period is practically the same, regardless of the assumptions made about the extension and the shape of the sealing fault.

The 95% confidence intervals of the total cumulative production of oil, gas and water are shown in Figures 7.34 to 7.36. The predictions were made for six years after the end of the history matching period (four years). From the preceding figures, it is obvious that the maximum boundary of the cumulative oil, gas and water production for model C appears to exhibit the greatest deviation from the cumulative production of the actual model. This was considered be an indication that the producer #1 is not completely isolated from the injector, by the impermeable barrier. Nevertheless the confidence intervals of all the models are fairly tight for a short period of time after the history matching (approximately two years). Figures 7.37 to 7.39 present a comparison of the forecasted oil, gas and water production rates of the postulated models, with the ones of the actual model. All the models predicted perfectly the actual performance of the producer #1 and producer #2 never came back on line.

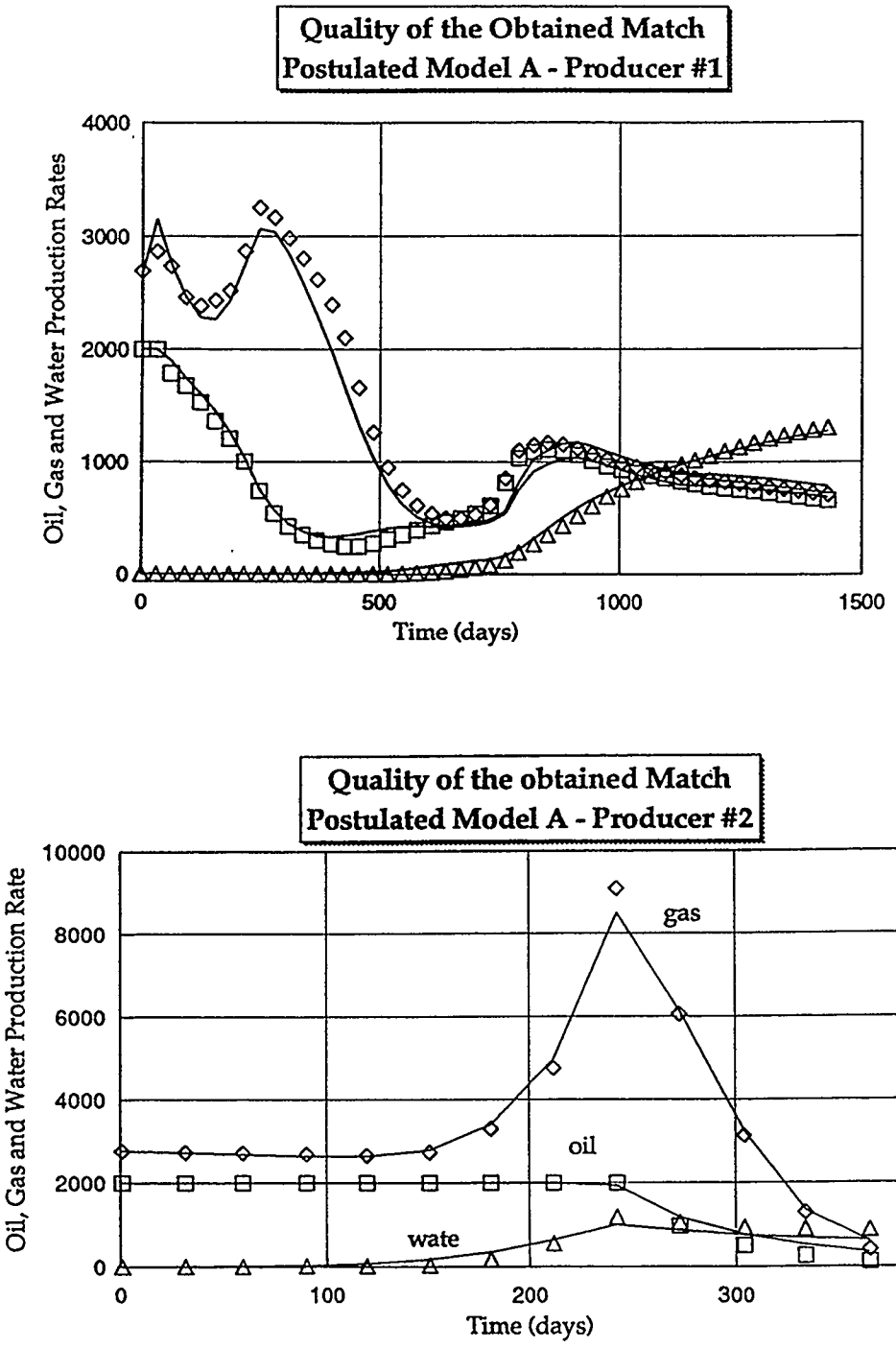

Figure 7.31 Quality of the Obtained Match for the Model A - (a) Producer #1, (b) Producer #2

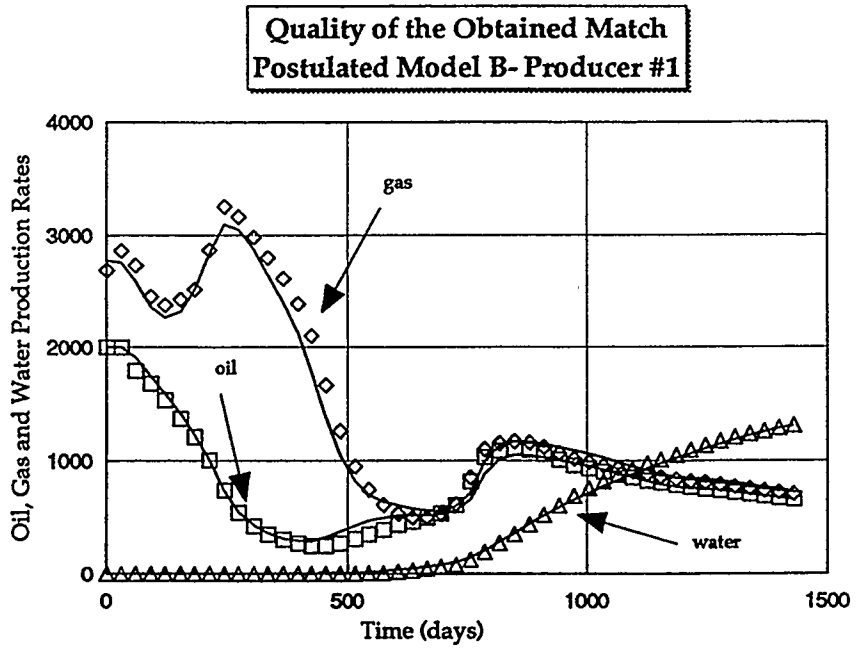

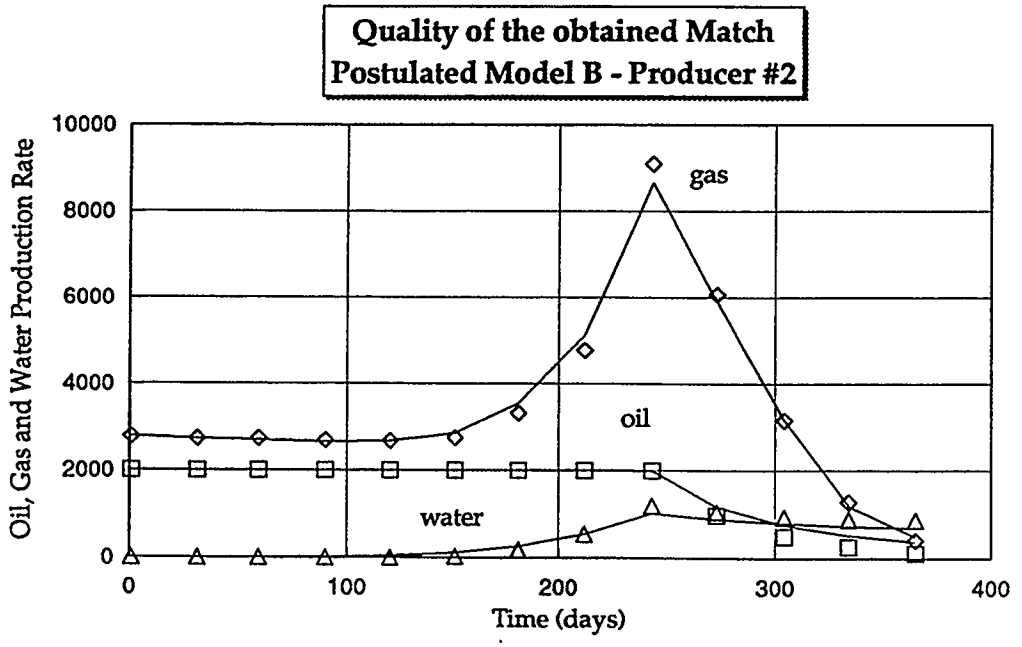

Figure 7.32 Quality of the Obtained Match for the Model B - (a) Producer #1, (b) Producer #2

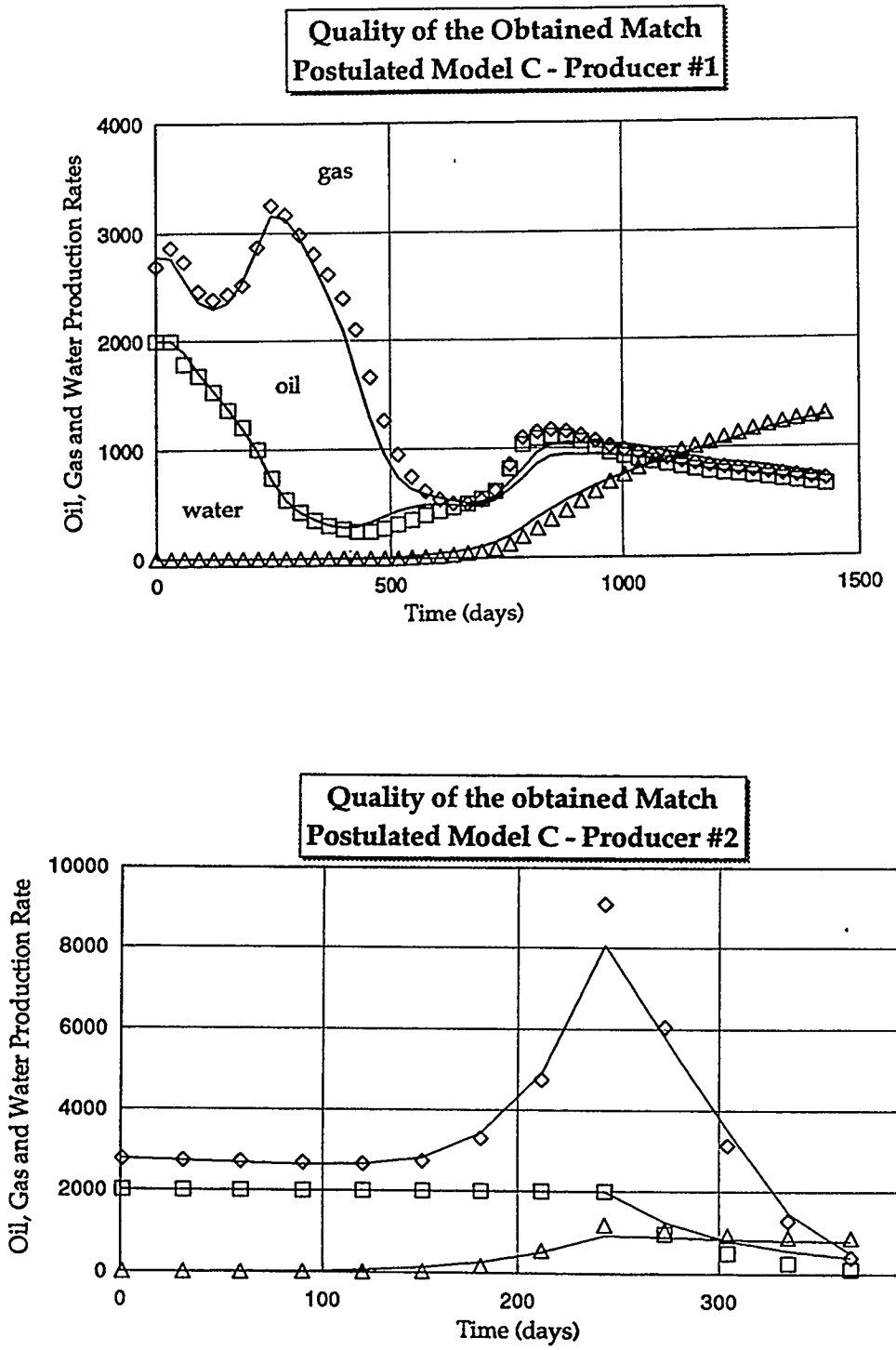

Figure 7.33 Quality of the Obtained match for the Model C - (a) Producer #1, (b) Producer #2

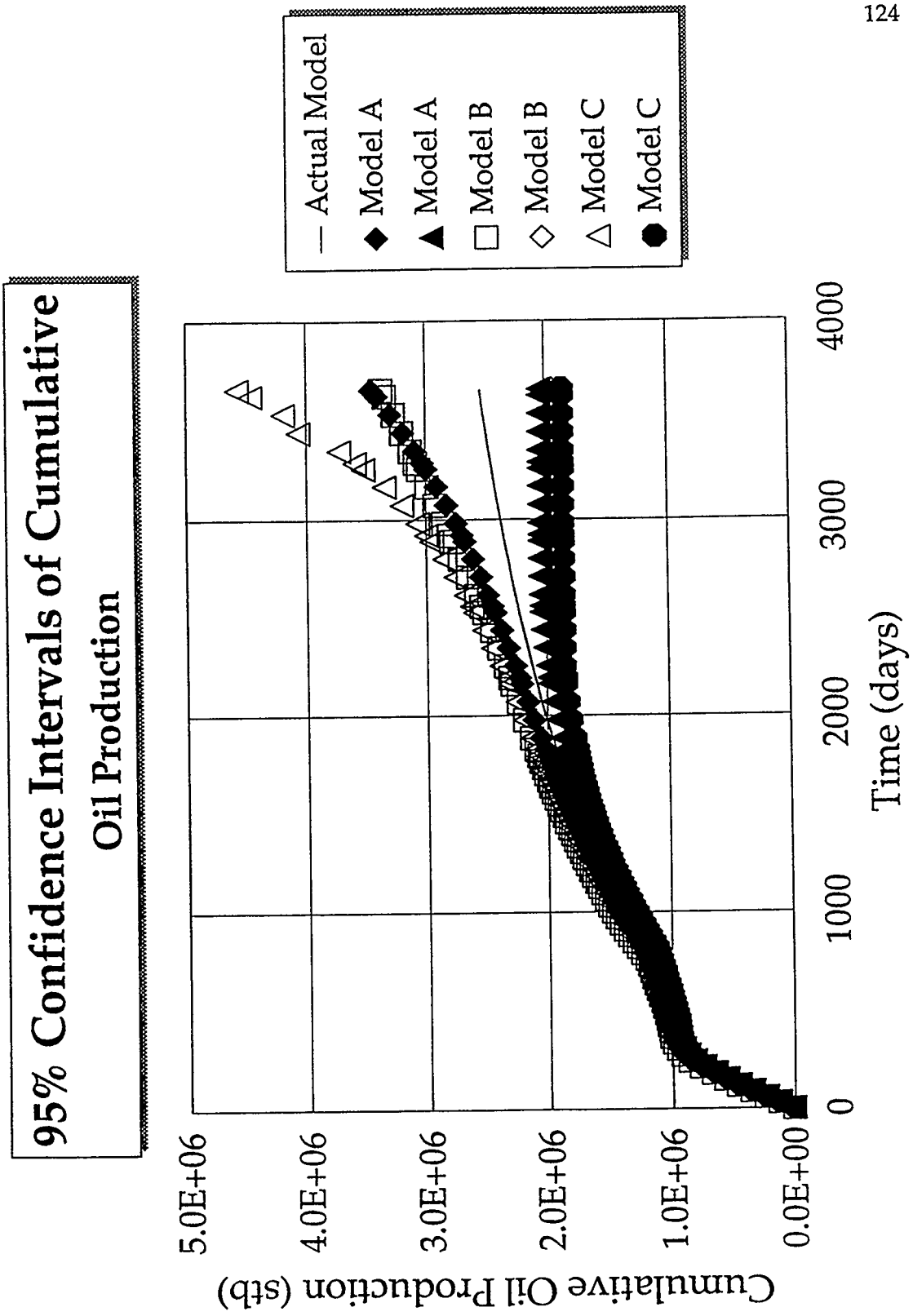

Figure 7.34 95% Confidence Intervals of the Cumulative Field Oil Production of Models A, B and C.

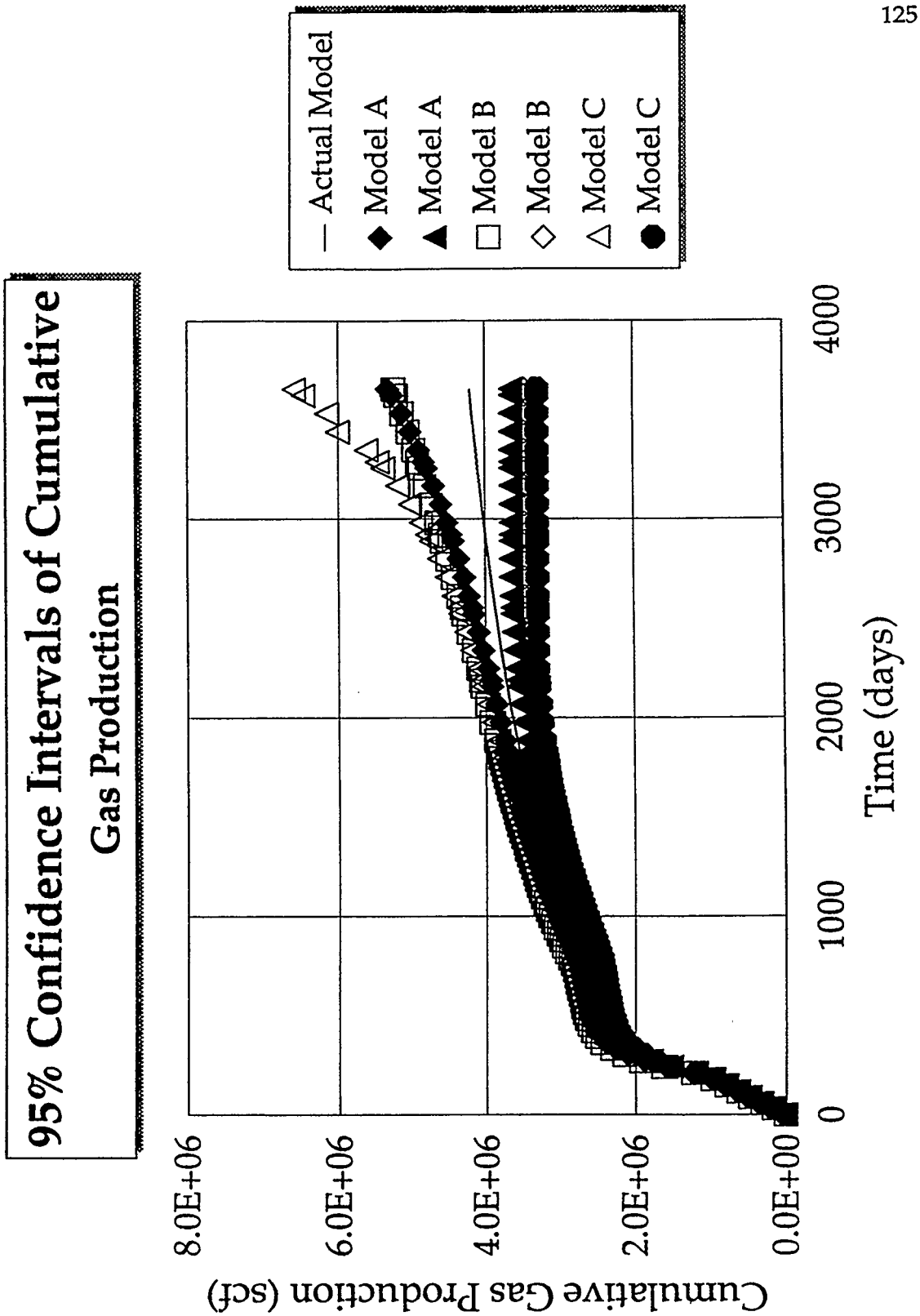

Figure 7.35 95% Confidence Intervals of the Cumulative Field Gas Production of Models A, B and C.

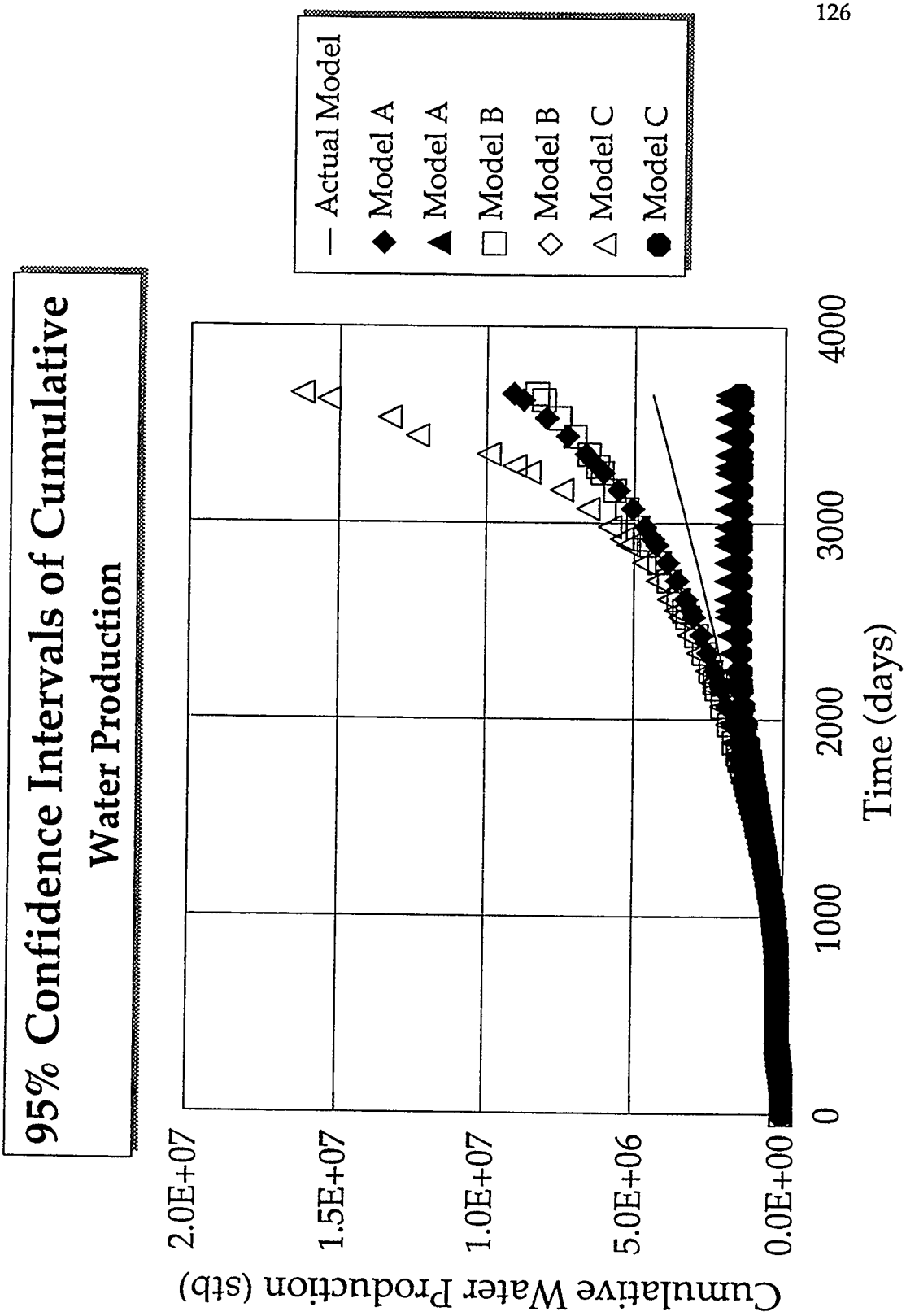

Figure 7.36 95% Confidence Intervals of the Cumulative Field Water Production of Models A, B and C.

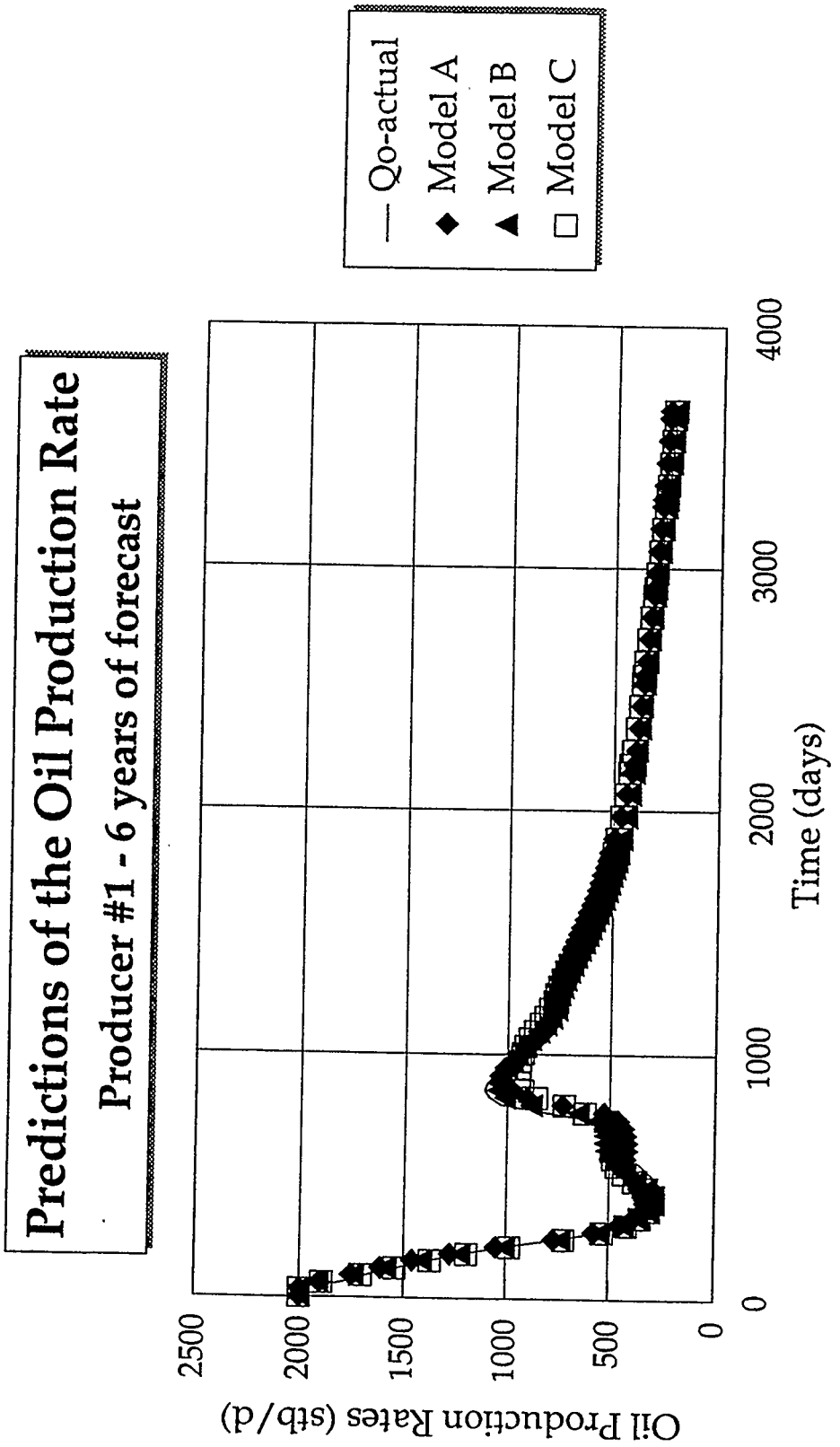

Figure 7.37 Predictions of the Oil Production Rates of the Postulated Models

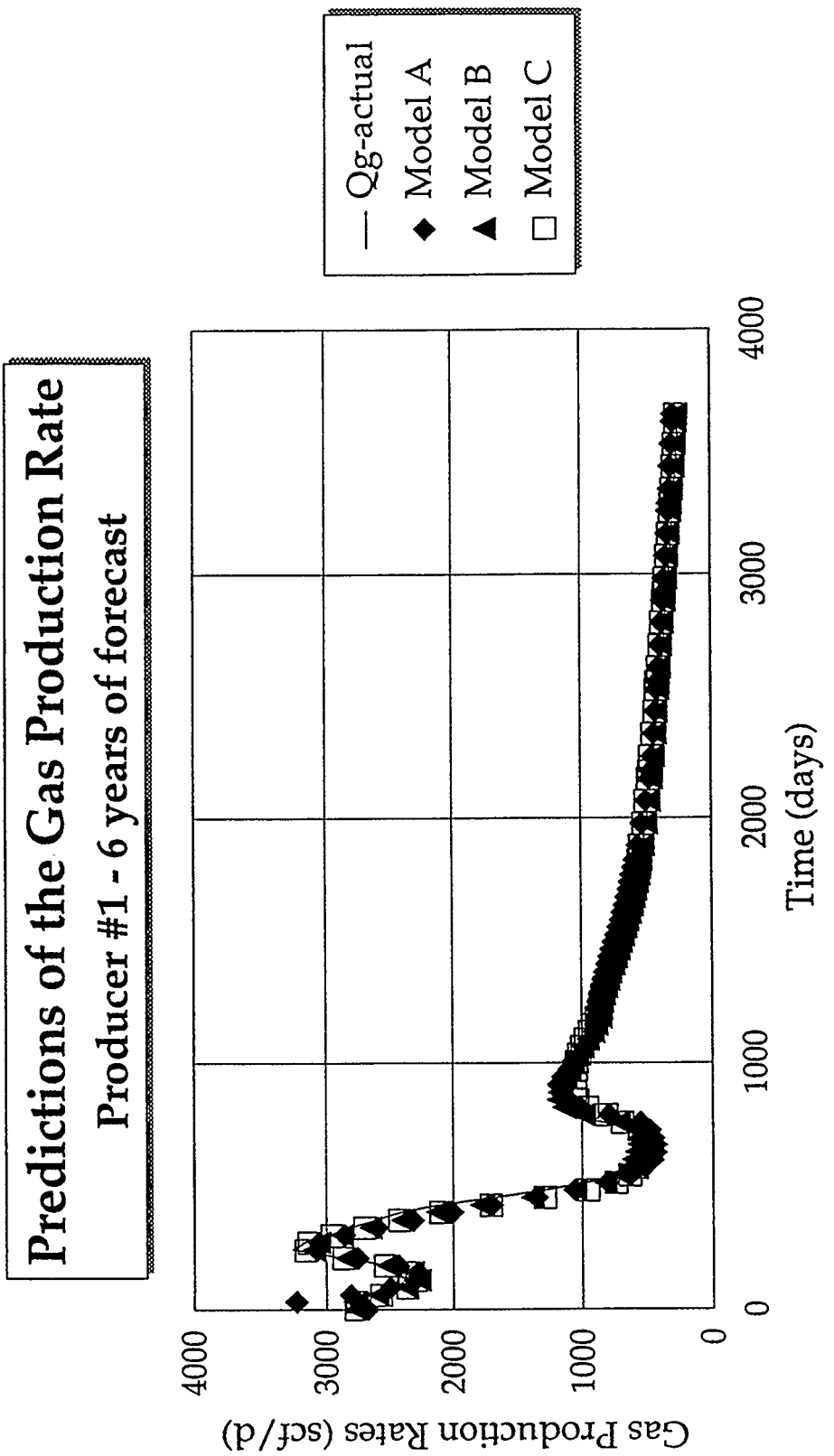

Figure 7.38 Predictions of the Gas Production Rates of the Postulated Models

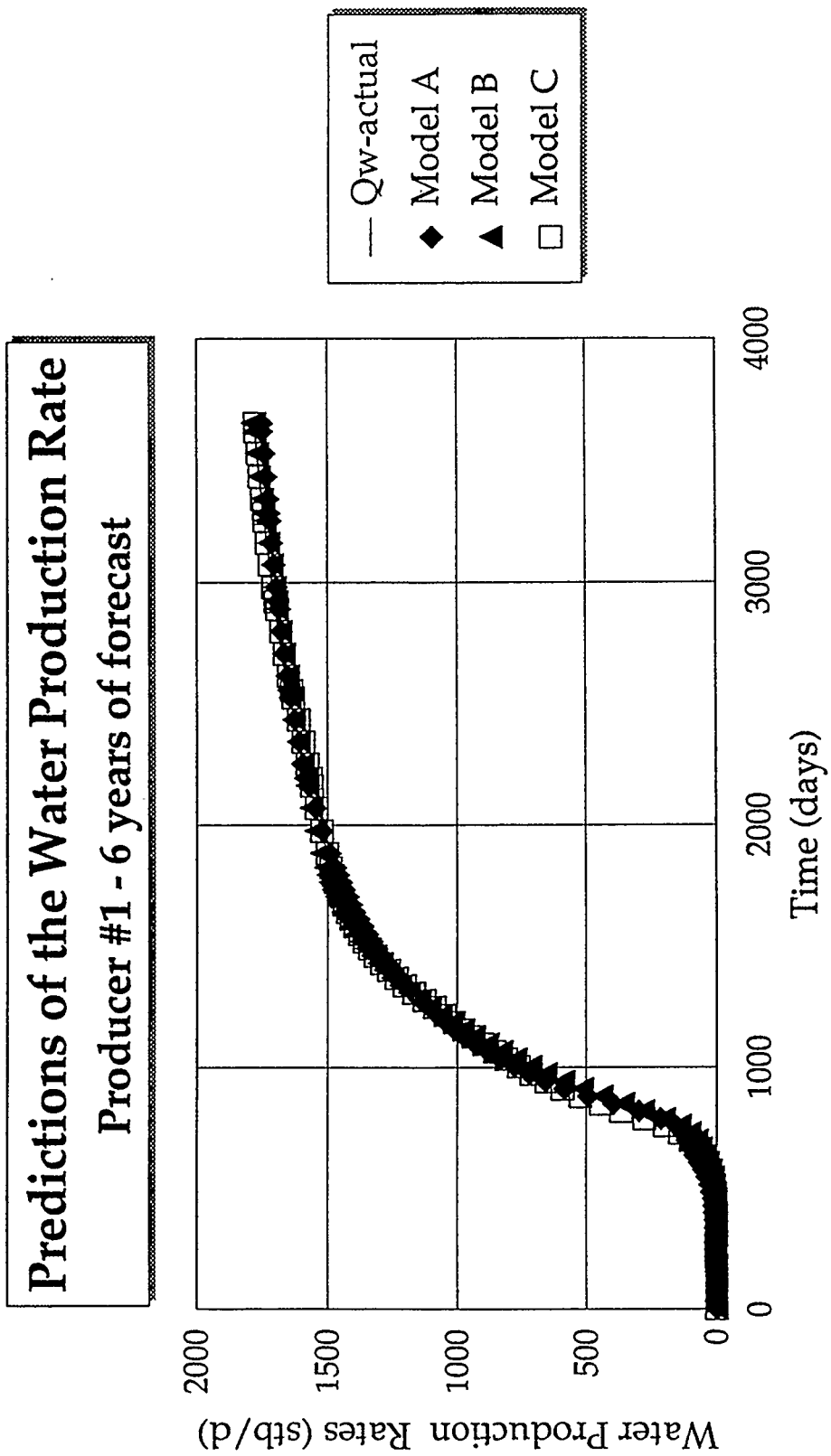

Figure 7.39 Predictions of the Water ProductionRates of the Postulated Models

CHAPTER 8

CONCLUSIONS

A new extrapolation model has been developed, in reservoir characterization, using the Gauss-Newton method. A reservoir simulator (DRS)[3] has been modified to account for automatic history matching, and prediction of future reservoir performance within certain confidence intervals (95%). The following conclusions can be drawn when using this procedure:

1. The Gauss-Newton and the simulated Annealing method were tested on chemical kinetic models. Both algorithms converged to the global minimum. Simulated Annealing was found to be insensitive on the initial estimates of the parameters and their maximum number and finally ideal when there is no reliable prior information regarding the parameter distribution, since it is a global optimization method. Also adapting the simulating Annealing method into a reservoir simulator is an easy task, since it does not require the computation of the sensitivity coefficients. The major drawback of the method was found to be the tremendous CPU requirements, which probably makes is intractable for most practical cases. Combining the two methods, simulated Annealing for investigating the whole range of the parameters and suggesting their best values as initial estimates to the Gauss-Newton method, seems to be a promising alternative.
2. The selection of the initial estimates of the parameters and the reservoir zonation is very important and rests solely at the engineer's discretion. Intuition and experience seem to be the only weapons that one has.
3. In some cases the algorithm converged in unrealistic values of porosity and permeability. This is expected, since all the postulated models were purposely chosen to be considerably smaller than the actual ones. On the other hand, the high values of permeability, are mostly related on the assumed complexity of the postulated

[3]DRS is a commercial black oil, three phase, three dimensional reservoir simulator (SIMTECH Consulting Services Ltd.)

models. It was not our intention to improve the reservoir characterization of the postulated models. We simply refer to the problem of non-uniqueness of the reservoir simulation. Even if the actual model varies considerably from the postulated ones, we can often obtain a perfectly acceptable history match and examine the future behaviour of these models under different depletion scenarios. Using a zonation approach we can arrive to simple reservoir descriptions that duplicate the actual reservoir performance. Of course the number of the parameters in a real test case would be greater and therefore the uncertainty of the forecast would increase. In such cases the importance of any prior information is becoming significant for "conditioning" the matrix A of the Equation (4.11). Additionally the sweep efficiency varies for each model since it strongly depends on the reservoir heterogeneity, anisotropy, the mobility of the displaced fluids, the physical arrangement of the injection and the production wells, the type of the rock matrix in which oil, gas and water exists.

4. It was found that the error boundaries, for the same set of porosities and permeabilities were gradually increased as the level of implicitness was decreased. Thus, using the IMPES formulation the maximum confidence interval of the cumulative production exhibits the greatest deviation due to instabilities in estimating the sensitivity coefficients

5. In all the test cases the algorithm converged to the "effective" values of the parameters. The converged values strongly depend on the presumed zonation.

6. The calculated confidence intervals, around the expected reservoir behaviour, incorporate all the uncertainty of the estimated parameters. As a rule of thump, one can say that the larger the number of the estimated parameters the greater the estimated confidence intervals. Overall future predictions can be made for a rather short horizon, where the postulated models perform equally well. Once the forecasted period increases substantially, so does the uncertainty in the estimates. After all, extrapolation is always risky.

7. The time required for the engineer to obtain an acceptable match and the predictions of the future performance of a model, is relatively short. Thus, one can spend more time evaluating the performance of the reservoir under different depletion strategies, instead of struggling to get one match and eventually only one forecast.

REFERENCE

Aziz, K. and Settari A.: *Petroleum Reservoir Simulation*, Elsevier Applied Science Publishers Ltd., London, 1979

Baker R,:"Effect of Reservoir Heterogeneities and Flow Mechanisms on Numerical Simulation Requirements", M.Sc. Dissertation Thesis, The University of Calgary, (Jul. 1993).

Brigham, D.E.: "Discussion of Productivity of a Horizontal Well", SPE, Reservoir Engineering (May 1990) 254-255.

Carter R.D., Kemp, L.F., Pierce, A.C. and Williams D.L.:"Performance Matching with Constraints," *SPE J* (April 1974), 187-196.

Chappelear, J.E. and Nolen, J.S.: "Second Comparative Project: A Three Phase Conning Study", *JPT*, (Mar. 1986), 345-353.

Chavent G., Dupuy M., and Lemonnier P.:"History Matching by Use of Optimal Theory ", *SPEJ* , (Feb 1975) 74-86; *Trans.;* AIME, 259.

Chen, W.H., Gavalas G.R., Seinfeld J.H. and Wasserman M.L.:"A New Algorithm for Automatic History Matching", *SPEJ*, (Dec 1974) 593-608; *Trans.*, AIME, 257.

Chrichlow, H. B.: *Modern Reservoir Engineering - A Simulation Approach*, Prentice - Hall Inc., New Jersey, (1977).

Coats, K.H., Demsey, J.R. and Henderson, J.H.: "A New Technique for Determining Reservoir Description from Field Performance Data," *SPEJ*. (March 1970) 66-74.

Collins, D., Ngheim, L., Sharma, R., Li, Y.K. and Jha, K.:"Field Simulation of Horizontal Wells", *JCPT* (January 1992), 31, 14-21.

Cooley, R.L.: "Incorporation of Prior Information on Parameters into Nonlinear regression groundwater flow models: 1.Theory," *Water Resources Res.*,18 965-76, 1982.

Dogru, A.H. et al:"Confidence Limits on the Parameters and Predictions of Slightly Compressible, Single-Phase Reservoirs." *SPEJ*, (Feb 1977) 42-56

Elsayed, S.A. et al:"Multidisciplinary Reservoir Characterization and Simulation Study of the Weyburn Unit",*JPT*, (Oct 1993) 930-973.

Farouq Ali ,S.M. and Berkowitz, B.S.:"Limiting Aspects of Automatic History Matching," paper 88-36-03 presented at the CIM 39th Annual Technical Meeting, Calgary, June 1988.

Gavalas, G.R., Shah, P.C. and Seinfeld, J.H.:" Reservoir History Matching by Bauesian Estimation", *SPEJ*, (Dec 1976) 337-350

Ghori D.G. et al:" The Effect of Four Geostatistical Methods on Reservoir Description and Flow Mechanism", *Proc.*, 76th Annual Technical Conference and Exhibition of the Society of Petroleum Engineers, Washington, DC, Oct 4-7, 1992.

Glover, F,:"Future Paths for Integer Programming and Links to Artificial Intelligence", *Computers and Operations Research*, 13, 533-549.

Glover, F,:"Heuristics for Integer Programming Using Surrogate Constraints", *Decision Sciences*, 8, 156-166.

Heinemann, Z.E., Brand, C., Munka, M and Chen, Y.M.:"Modeling Reservoir Geometry with Irregular Grids" *SPERE* (May 1991), pp225-232.

Hirasaki, G,J: " Sensitivity Coefficients for History Matching Oil Displacement Processes," *SPEJ*, (Sept. 1975), 295-305; *Trans.*, AIME, 251.

Hird K.B. et al.:"Conditional Simulation for Reservoir Description Using Spatial and Well Performance Constraints,"*Proc.*, 76th Annual Technical Conference and Exhibition of the Society of Petroleum Engineers, Washington, DC, Oct 4-7, 1992.

Holland, J.H.:"Adaptation in Natural and Artificial Systems", University of Michigan Press, Ann Arbor,MI.

Hougen, O. and Watson, K. M.,:"Chemical Process Principles," Vol. 3. Wiley, New York (1948).

Jacquard, P. and Jain, C.: " Permeability Distribution from Field Pressure Data,." *SPEJ* (Dec. 1965) 281-294

Kalogerakis, N. and Rein L.: "Simplification of Quasilinearization Method for Parameter Estimation", I & EC Fundamentals, (Sept. 1983), Vol 29, pp.858-864.

Kalogerakis, N. and Rein L.:" Improvement of Gauss - Newton method for Parameter Estimation through the Use of Information Index", I & EC Fundamentals, (Nov 1983), Vol 22, pp.436-445.

Kravaris, C. and Seinfeld. J. H.:"Identification of Parameters in Distributed Parameter Systems by Regularization," *SIAM J. Control and Optimization*, 23, No.2, 217-41.

Kravaris, C. and Seinfeld. J. H.:"Identification of Spatially-Varying Parameters in Distributed Parameter Systems by Discrete Regularization," *J. Mathematical Analysis and Appl.* (1986), 118, No. 9.

Lapidus L. and Luus R.:" *Optimal Control of Engineering Processes*", Blaisdell, Boston, 1967.

Mattax C. C. and Dalton R.L.: *Reservoir Simulation* ,Monograph Volume 13, SPE, Richardson, TX, (1986), 7.

McCulloch, W. S. and Pitts,W.:"A Logical Calculus of the Ideas Immanent in Nervous Activity", *Bulletin of Mathematical Biophysics*, 5, 115-133

Neuman, S.P. and Yakowitz, S.:" A Statistical Approach to the Inverse Problem of aquifer Hydrology: Theory," *Water Resources Res.*,15 845-60, 1979

Numerical Simulation II, Reprint Series, SPE, Richardson, TX, (1986), 7.

Ouenes, A., Bahralolom,I. Gutjahr, A. and Lee, R.:"A New Method for Predicting Field Permeability Distribution," *Proc.*, 1992 Mediterranean Petroleum Conference and Exhibition, Tripoli, Libya, Jan. 19-22, 468-477. (1992 B).

Ouenes A. et al :"A New Fast Parallel Simulated Annealing Algorithm for Reservoir Characterization",*Proc.*, 68th Annual Technical Conference and Exhibition of the Society of Petroleum Engineers, Houston, Texas, Oct 3-6, 1993.

Ouenes, A., Bahralolom,I. Gutjahr, A. and Lee, R.:"Conditioning Permeability Fields by Simulated Annealing,"*Proc.*, Third European Conference on the Mathematics of Oil Recovery, Deft, Netherlands, (1992, D), June 17-19, 41-50.

Ouenes, A., Guy, Fasanino, Lee, R.L.:"Simulated Annealing for Interpreting Gas/Water Laboratory Corefloods" *Proc.*, 76th Annual Technical Conference and Exhibition of the Society of Petroleum Engineers, Washington, DC, Oct 4-7, (1992 F).

Ouenes, A., Bahralolom,I. Gutjahr, A. and Lee, R.:"Application of Simulated Annealing Method (SAM) to Laboratory an Field Anisotropic Porosity," *Proc.*, 1992 Lerkendal Petroleun Engineering Workshop, Norwegian Institute of Technology, Trondheim, Norway, Feb. 5-6, 107-118 (1992 C).

Ouenes, A.:"Application of Simulated Annealing to Reservoir Characterization and Petrophysics Inverse Problems", PhD Dissertation Thesis, New Mexico Institute of Technology, (Oct. 1992, A).

Ouenes, A., Brefort, B. Meunier G. and Dupere, S.:"A New Algorithm for Automatic History Matching: Application of Simulated Annealing Method (SAM) to Reservoir Inverse Modeling", *Proc.*,(1992 E).

Palatnik B., Zakirov, I. and Agaev G.:"History Matching Problems of Filtration Theory. Complex Adaptive Geological Models of Fields," 2nd European Conference on the Mathematics of Oil Recovery, Paris, 1990.

Parish R.G. et al.:" Effective History Matching: The Application of Advanced Software Techniques to the History-Matching Process,"*Proc.*, 12th SPE Symposium on Reservoir Simulation, New Orleans, LA, U.S.A, Feb 28-March 3, 1993.

Peaceman, D.W.: "Interpretation of Well-Block Pressures in Numerical Reservoir Simulation with Non-Square Grid Blocks and Anisotropic Permeability", *SREJ*, (June, 1983), pp531-543.

Peaceman, D.W.: " Interpretation of Well - Block Pressures in Numerical Reservoir Simulation", *SPEJ*, (1978) pp183-194.

Peaceman, D.W., *Fundamentals of Numerical Reservoir Simulation*, Elsevier , 6, (1977).

Rao, S. N. et al:"Evaluation and Improvement of Control Vector Iteration Procedures for Optimal Control",*Can. J. Chem.Eng.* 1972, 50, 777.

Rosenblatt, F., *Principles of Newrodynamics*, Spartan, Washington D.C., 1962.

Savioly, G.B., C.A. Grattoni, Bidner M. S.: "On the Inverse Problem Application to Reservoir Characterization," *Proc.*, 6th European IOR-Symposium, Stavanger, Norway, May 21-23, 1991.

Seinfeld, J.H., and Gavalas G.R.:" Analysis of Kinetic Parameters from Batch and Integral Reactor Experiments: *AIChE J.*, 16, 644, (1970).

Seinfeld, J.H., and Lapidus L.:"*Mathematical Methods in Chemical Engineering*", 3, Prentice Hall, Englewood Cliffs, NJ (1974).

Settari A.: *"Topics in Reservoir Simulation"*, Simtech Consulting Services Ltd.., Calgary, Alberta, Canada, 1993.

Shah P.C., Gavalas, G.R. , Seinfeld, J.H.: "Error Analysis in History Matching : The Optimum Level of Parametization," *SPEJ*. (June 1977) 219-228.

Slater, G.E. and Durrer, E.J.:" Adjustment of Reservoir Simulation Models to Match Field Performance,"*SPEJ* (Sep 1971) 295 - 305.

Smith R.A.W. et al.:"Reservoir Characterization of a Fractured Reservoir Using Automatic History Matching,"*Proc.*, 12th SPE Symposium on Reservoir Simulation, New Orleans, LA, U.S.A, Feb 28-March 3, 1993.

Stone, H.L., and Garder, A.O.:"Analysis of Gas-Cap or Dissolved-Gas Drive Reservoirs," *SPEJ*, (June 1961) 91-102.

Sultan A.J. et al :"Reservoir Description by Inverse Modelling: Application to EVGSAU Field",*Proc.*, 68th Annual Technical Conference and Exhibition of the Society of Petroleum Engineers, Houston, Texas, Oct 3-6, 1993.

Tai-Yong Lee et al,: "History Matching by Spline Approximation and Regularization in Single-Phase Areal Reservoirs", *SPEJ*, (Sept 1986) 521-534.

Tan, T.B. and Kalogerakis, N.,"Improved Reservoir Characterization Using Automatic History Matching Procedures", JCPT, (June 1993), Vol 32, No. 6, pp.26-33.

Tan, T.B. and Kalogerakis, N., "A Fully Implicit Three - Dimensional Three-Phase Simulator With Automatic History Matching Capability", paper SPE #21205 presented at the Eleventh SPE Symposium on Reservoir Simulation, Anaheim, Feb 17-20 (1991).

Tan, T.B. and Kalogerakis, N: "A Three - Dimensional Three - Phase Automatic History Matching Model: Reliability of Parameter Estimates", JCPT (March 1992), Vol 31, No3, pp.34 - 44.

Tan, T.B.,: "Parameter Estimation for Reservoirs", PhD Dissertation Thesis, The University of Calgary, (Sept, 1991).

Thomas, L.K. and Hellums, L.J.:"A Nonlinear Automatic History Matching Technique for Reservoir Simulation Models", *SPEJ* (Dec. 1972) 508 - 514

Thomas, G.W. and Thurnau, D. H.:"Reservoir Simulation Using an Adaptive Implicit Method", *SPEJ*, (Oct. 1983), 759-68

Wasserman, M.L., Emanuel, A.S. and Seinfeld, J.H.:"Practical Application of Optimal Control Theory to History Matching Multiphase Simulator Models", *SPEJ*, (Aug 1975) 347-355.

Watson A.T. et al.:"An Analytical Model for History Matching Naturally Fractured Reservoir Production Data," *SPE Reservoir Engineering*, (Aug 1990) 384-388.

Watson, A.T., Gavalas G.R., Seinfeld J.H and Woo, P.T.:"History Matching in Two-Phase Petroleum Reservoirs", *SPEJ*, (Dec 1980) 521-532.

Williamson, A. S. and Chappelear, J.E.:"Representing Well in Numerical Reservoir Simulation: Part1 - Theory", *SPEJ*, (1981).

Yang, P.H. and Watson A.T.:"A Bayesian Methology for Estimating Relative Permeability Curves," *SPE Reservoir Engineering*,(May, 1991) 259-265.

Yang, P, Armasu, R.V. and Watson, A.T.: "Automatic History Matching with Variable Metric Methods" paper SPE #16977 presented at the 62nd SPE Annual Technical Conference, Dallas, Sep.27-30, 1987.

APPENDIX A'

A.1 Detailed Description of the Dual Porosity Model Used.

In order to determine whether Kazemi's model is valid for the reservoir examined in this part, one has to check the validity range of the above model using the following equations:

$$\lambda = \sigma \frac{k_m r_w^2}{K_f} > 1.0 \times 10^{-6}, \qquad k_m > 0.1 \text{ md} \tag{A.4}$$

where: σ: the shape factor (eq A.5)

k_m: permeability of the matrix

r_w: the wellbore radius

K_f: effective permeability

According to the above equations, one can conclude that the considered reservoir lies within the validity range of the Kazemi's model (worst case scenario $\lambda=3.666 \times 10^{-6}$ and the converged value of $k_m=1.5$ md).

The expressions used in this part for the calculation of the fracture and matrix parameters are based on a common assumption that the density of fracturing is sufficient such that average "continuum" properties exist for volume elements, which are large compared to discrete fracture features. Then the system is represented by two superimposed continuous media, fractures and matrix. In the model that was considered in this study both fractures and matrix have non-zero porosity and permeability. Flow takes place in the fracture network, and between fracture and matrix. Each matrix block is assumed to be completely surrounded by fractures and cannot communicate directly with adjacent matrix blocks. Obviously, such a model is not quite realistic because the matrix blocks "float" and do not touch, while in reality the frac-

tured media supports substantial rock stresses. However, such kind of model has been the basis for majority of dual porosity simulators.

Kazemi's model was derived from Warren Root theory. The waterflood behavior is analogous to Warren - Root pressure transient theory. That is, as the matrix and the fracture permeability approach each other the waterflood behaviour became similar to a single porosity system. This is similar to a pressure build up or drawdown test in Warren and Root theory.

The total effective permeability of a fractured reservoir is calculated from the following equation:

$$K_T = \frac{K_M L + K_F \omega}{L} \qquad \text{(A.5)}$$

where: K_T is the total effective permeability of the system

K_M is the permeability of the matrix (md)

K_F is the permeability of the fracture (md)

ω is the width of the fracture (microns)and

L is the size of the matrix cubic blocks (ft)

From the equation (A.2) one can calculate the product of the permeability of the fracture times the width of the fracture. At the same time assuming parallel smooth plates and neglecting turbulence and roughness of the fracture walls we can use Poiselle's law:

$$K_F\ \omega = 54 * 10^9\ \omega^2 \qquad \text{(A.6)}$$

The fracture porosity ($\varnothing_F$) is calculated from the following equation:

$$\varnothing_F = \frac{1}{100}\left(\frac{3\ \omega}{L}\right) \qquad \text{(A.7)}$$

where: $\varnothing_F$: porosity of the fracture (%)

ω : width of the fracture (microns)

L: length of the matrix blocks (in)

The shape factor based on Kazemi's model is given from the following equation:

$$\sigma = 4\left(\frac{1}{L_x^2} + \frac{1}{L_y^2} + \frac{1}{L_z^2}\right) \qquad \text{(A.8)}$$

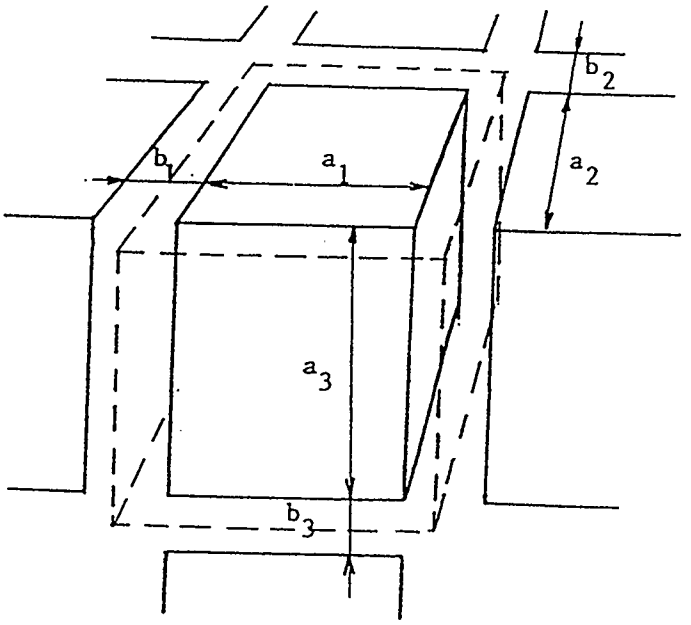

Figure A.1 Schematic Representation of the Matrix and theFracture Continuum.

where: L_x, L_y, L_z are the dimensions of the matrix blocks according to Fig. A.1

The existing Black Oil Model simulator (DRS) can be set up to account for dual porosity model in two ways:

- Using the available special connection option. Special Connections are responsible for "superimposing" the grid-blocks of the matrix system with the equivalent grid-blocks of the fracture network, by specifying non-standard transmissibility multipliers.

- By placing the fracture system on top of the matrix system and trying to get rid of the gravitational effects, that come from a total height difference of 420ft.

In the special connection case the model consisted of two different regions, fractures and matrix. Each region had 12x9x6 grid blocks and they were placed side by side. Therefore the total number of grid blocks of the whole reservoir was 24x18x6. The wells were placed at the fracture system in order to gain a higher productivity index, due to the high permeability of this region. The non-standard transmissibility multipliers for the x-direction are calculated by the following equation:

$$T_{MULT} = \frac{T_{fm}}{T_X} = \frac{\sigma\ (\Delta x\ \Delta y\ \Delta z\ )\ \dfrac{k\ k_{rl}}{\mu_l\ B_l}}{\dfrac{\Delta y\ \Delta z}{\Delta x}\ \dfrac{k\ k_{rl}}{\mu_l\ B_l}} = \sigma \Delta x^2 \qquad \text{(A.9)}$$

In the layered reservoir case the two different regions were connected vertically. No fluid flow was permitted inside the matrix layer and the transmissibility multiplier for transfer of fluid among the fracture-matrix system is calculated by the following equation:

$$T_Z = \sigma\ \Delta z^2 \qquad \text{(A.10)}$$

It should also be noted that the relative permeability to oil and water curves in the fractures cover the full spectrum of saturations from 0 to 1, and they are straight lines. The matrix capillary pressure is always much greater than the fracture capillary pressure, which is always zero.